Department of AERONAUTICS and ASTRONAUTICS
STANFORD UNIVERSITY

MARSHALL H. KAPLAN
HOWARD S. SEIFERT

INVESTIGATION OF A HOPPING TRANSPORTER CONCEPT FOR LUNAR EXPLORATION

JUNE
1968

The printing of this report was made possible
by the National Aeronautics and Space Administration
under Grant NASA NGR 05-020-258

SUDAAR
NO. 348

Department of Aeronautics and Astronautics
Stanford University
Stanford, California

INVESTIGATION OF A HOPPING TRANSPORTER CONCEPT FOR LUNAR EXPLORATION

by

Marshall H. Kaplan

and

Howard S. Seifert

SUDAAR No. 348

June 1968

The printing of this report was made possible by the
National Aeronautics and Space Administration under grant
NASA NGR 05-020-258

ABSTRACT

Currently proposed manned lunar mobility systems are severely limited in speed and payload capabilities. Roving vehicles are massive and move slowly over the rough lunar terrain, at high cost of energy and life support supplies. Flying units, powered by chemical rockets, are fast, but the price of speed is payload and range. Recently, a hopping transporter concept was conceived which incorporates both a conservative use of fuel and a high average speed. As a first-step toward the practical application of such devices, an investigation of feasibility, with respect to performance capabilities, was carried out.

This objective was achieved by studying the dynamic characteristics of somewhat idealized hopping vehicle configurations which are, however, based on actual conditions and mission requirements. Two schematic designs were investigated. One is a single-man device assumed to be of minimum complexity and mass, transportable with Apollo crews. This device is intended to extend the operating range of lunar astronauts. The other design is a multi-man transporter capable of making long range and duration explorations of the lunar surface. Both vehicles employ the technique of accelerating up a thrust-leg, locking this leg to the main body at the end of acceleration, executing a classic ballistic parabola, and finally, decelerating down this leg to complete each hop. Energy is essentially conserved in this process, thus providing for substantial payload capability, in addition to other performance advantages. Since lunar irregularities do not impede hopping motion, these devices can maintain a high average speed and visit almost any topographic feature of interest within vehicle range. Specific tasks addressed in

this study include investigation of influencing factors which affect transporter design and operation, definition of performance limiting phenomena, development of general operating constraints and functions, derivation and solution of equations of motion for each vehicle design studied, and calculation of hop performance data based on digital computer simulations of vehicle dynamics.

Results of hop simulations of both transporter models indicate a significant improvement in performance over roving and flying vehicles. The smaller device offers extended range to Apollo astronauts, up to and exceeding an operating radius of 10 km. The larger vehicle has an average speed of the order of 30 km/hr, very high compared to roving unit designs. A unique hop plane changing technique used by this transporter permits these high values of average speed. Therefore, within the accuracies of assumptions applied in this study, hopping vehicles offer superior performance capabilities for lunar surface mobility.

ACKNOWLEDGMENT

The authors wish to express their gratitude to the Stanford Computation Center for supplying the required computing facilities to complete the work presented. This work was made possible through NASA and NSF Traineeships.

TABLE OF CONTENTS

LIST OF TABLES

LIST OF ILLUSTRATIONS

LIST OF SYMBOLS

a_{ij} = coefficient in kinetic energy expression (B-1), i,j = 1,2, . . .,n

A = piston area

A = transformation matrix used for rotating coordinates and vectors

$\mathbf{A}^T$ = transpose of **A**

C_i = constant with respect to the $\dot{u}_j$'s in equations (B-10), i = 1,2,...,n

d = propulsion cylinder displacement

$\vec{e}_x, \vec{e}_y, \vec{e}_z$ = unit vectors in the x, y and z directions, respectively

F = force exerted on piston by the working fluid

$\mathfrak{F}$ = propulsive force on main body

g = gravitational constant

h = pod center of mass offset from leg axis measured in the x-direction

H = Hamiltonian

H_F = elevation of point F in Appendix A

$\overleftrightarrow{I}$ = moment of inertia tensor

K = isentropic constant

ℓ = half length of HOLAB thrust leg (length of rod in the example of Appendix B)

ℓ_M = leg displacement of SHOT measured between foot and main-body-plus-crew center of mass

L = Lagrangian (kinetic potential)

m = mass of thrust leg plus foot (mass of bar in the example of Appendix B)

M = mass of main body plus crew

n = number of degrees of freedom for a system under study

N = number of first order ordinary differential equations used in Appendix B

p = pressure in propulsion cylinder

p_i = conjugate momentum, $i = 1,2, \ldots,n$

q_i = generalized coordinate, $i = 1,2, \ldots,n$

Q_i = applied force associated with q_i, $i = 1,2, \ldots,n$

r = gear ratio with respect to leg and pod motion

$\vec{r}$ = radius vector originating at foot contact point

R = radius of cabin spheres for HOLAB plane change analysis (ballistic range in Appendix A)

S,C = sine and cosine, respectively

t = time

T = transporter kinetic energy

u_i = generalized velocity, $\dot{q}_i$, $i = 1,2,\ldots,n$

v = magnitude of velocity

V = transporter potential energy resulting from gravity and propulsion forces

V_c = volume of propulsion cylinder

V_p = propulsion unit potential energy

x,y,z = body-fixed coordinate system used in HOLAB plane change analysis (x is the independent variable of Appendix B)

X,Y,Z = coordinates of transporter center of mass measured from last footprint

y_i = dependent variable in Appendix B, $i = 1,2,\ldots,N$

z_P = leg displacement of HOLAB measured between foot and pod center of mass

α = launch angle for two-dimensional hops

β = landing angle for two-dimensional hops

γ = specific heat ratio of the working fluid

δ = plane change angle

Δ = determinant of the coefficient matrix $[a_{ij}]$

$\Delta_\varphi, \Delta_\theta, \Delta_\psi, \Delta_z$ = determinants which make up the numerators when applying Cramer's Rule corresponding to φ, θ, ψ, and z_P coordinates, respectively

ζ = distance between leg and vehicle centers of mass

η = distance between leg and pod centers of mass

μ = dummy variable used to reduce second order ordinary differential equations to first order

ξ = line of nodes defined by the intersect of the XY- and xy-planes in HOLAB plane change analysis

σ = surface slope angle

φ, θ, ψ = Euler angles used to specify HOLAB orientation during plane change maneuvers

ω = magnitude of angular velocity

Subscripts

$()_c$ = value taken about a center of mass

$()_{cm}$ = value taken about the vehicle center of mass

$()_d$ = value at disengagement

$()_e$ = value at engagement

$()_f$ = value at the end of hop

$()_L$ = thrust leg property

$()_o$ = value at beginning of the acceleration phase

$()_P$ = pod property

$()_x, ()_y,$
$()_z$ = value taken parallel to x, y, or z axes, respectively

Superscripts

$f(t_o^+)$ = limiting value of the dependent variable f at t_o when t_o is approached from a value greater than t_o

$f(t_o^-)$ = limiting value of the dependent variable f at t_o when t_o is approached from a value less than t_o

$\vec{()}$ = vector quantity

$\dot{()}$ = time derivative, d/dt of quantity below dot

I. INTRODUCTION

A. Motivation for a New Mobility System

The United States has made manned exploration of the Moon a national goal. On the first few Apollo missions astronauts will be limited to an operating radius on the lunar surface of a few hundred meters, because travel-by-foot will be the only mode of transportation. Many mobility systems for later flights have been proposed and are in initial development. However, these designs apparently will not satisfy the established mission requirements for lunar exploration. The most important recommendation of the 1967 Summer Study of Lunar Science and Exploration at Santa Cruz, California[1] was concerned with the expected low performance of these vehicles. The conference pointed out the imperative necessity for lunar transporters with much greater capabilities. Faced with an insufficient choice of devices, members of the Santa Cruz study were compelled to suggest a mobility system based on the concepts offered[2]. Their proposed solution was a redesign of the wheeled vehicle configuration which would then have the added capabilities of carrying two small flying units and dual mode operation, i.e., manned or automatic. This seemed to be the only way to satisfy observation and sampling requirements of both geochemists and geologists.

The prospects for currently planned mobility systems indicate that this is an appropriate time to consider a fresh approach to lunar surface transportation concepts. Steps taken with wheeled vehicles have been based on a philosophy offering little opportunity to apply modern aerospace technology and, even more seriously, taking little advantage of the unique environmental factors. Such concepts have led to discouraging

performance estimates, because design growth capabilities are practically non-existent. As a possible alternative and supplement to the wheeled devices, a group of flying unit designs have been introduced. These employ "brute-force" tactics with small chemical rockets, but offer a greatly improved range capability. Nevertheless, these two concepts, whether used separately or in combination, do not represent an optimum mobility system with respect to the fulfillment of mission objectives. One cannot expect to achieve efficient performance from a design based on principles which are not appropriate to the situation. Nominations for new mobility system concepts should be left open.

The Santa Cruz conference specifically pointed out the required areas of performance improvement: "To increase the scientific return from lunar surface missions after the first few Apollo landings, the most important need is for increased operating range on the Moon. On the early Apollo missions it is expected that an astronaut will have an operating radius on foot of approximately 500 meters. It is imperative that this radius be increased to more than 10 kilometers as soon as possible." As a further objective: "Exploration of lunar surface features such as large craters and their environs will require a range of approximately 25 kilometers or more." Proposed wheeled vehicles have inadequate range capabilities and lunar flying units have inadequate maneuverability for continuous ground coverage and low payload capacity.

In addition to the motivation of requirement, there is the satisfaction of technological achievement. The opportunity to develop a new mobility concept based on a unique application of modern technology is certainly a rewarding experience.

B. Survey of Past and Present Lunar Mobility Systems

In 1954, Herman Oberth published Man Into Space[3], which contained a brief description and sketches of a lunar transporter whose principal mode of locomotion was by a small tractor-like foot. A large cabin in which the crew could enjoy a shirt-sleeve environment was supported above this foot by a telescoping leg. This device was capable of executing jumps under certain conditions: to pass a rille, to negotiate a scarp, to turn around in a cul de sac, or to stop the vehicle in an emergency. Oberth's description represented the first serious effort in lunar mobility technology. Then, in 1959, he published a complete description with design drawings and operating details entitled, The Moon Car[4]. It is interesting to note that this concept was evolved through a consideration of the lunar environment and mission requirements, although the device, as described by Oberth, is largely impractical. It is very large and has many moving parts exposed to the lunar vacuum, thus possessing an inherently low reliability and safety factor. Furthermore, an extensive amount of construction is required upon arrival at the lunar surface in order to make the device operational.

In 1961, the Bendix Corporation initiated studies on a lunar roving vehicle concept which employs a unique metal-elastic wheel design[2]. Many versions of manned and unmanned models have been proposed which are intended to fulfill a wide range of lunar exploration requirements for the period from 1970 to 1980. Unmanned wheeled vehicles include the Surveyor Lunar Roving Vehicle and the "Pack Mule". The former device is an adjunct to the advanced Surveyor Program and its mission is to provide topographical information in the vicinity of the landed Surveyor spacecraft. Operation of this vehicle is controlled from earth. The Pack

Mule is a manually controlled vehicle used to carry exploration equipment during a manned, walking survey. One-man vehicle configurations offer either open or closed cabins and are known as the Local Scientific Survey Modules. This type of rover is designed to operate in conjunction with a fixed base or shelter. The open-cabin version has a range of 8 kilometers on a three to six hour trip. The closed-cabin version has a range of about 40 kilometers per twelve hour trip. Two-man vehicles have life support cabins, and are known as Lunar Mobile Laboratories. They are designed to be delivered to the lunar surface by a one-way Lunar Excursion Module and equipped to make 14-day scientific missions with a range of 80 kilometers. Maximum speed is 10 km/hr and slope limit is 35 degrees. A possible alternative to this vehicle type is a modified Lunar Excursion Module with wheels and extended life support capability. Finally, the Mobile Explorer is a three-man life-supporting vehicle capable of making a 42-day exploration mission and traveling a total of 1,600 kilometers. Its average speed is 5 km/hr.

Bell Aerosystems has performed a large amount of research and development work during the past few years on lunar flying devices[5]. These units can fly at a wide range of speed and altitude, indicating possible uses such as: in-flight sensor platform for photography, IR imagery and magnetometry, and carrier for dropping seismometers and communication relays from altitude. Such flying units have been considered for inclusion into the roving vehicle spectrum of mobility systems. When used as a supplement to wheeled vehicles, flying devices can be classified into three types: one-man surface-to-surface, multi-man surface-to-surface, and multi-man surface-to-orbit for emergency lunar orbit rendezvous. All surface-to-surface types have similar flight sequences:

boost, constant altitude cruise, descent, and land. Surface slope at the landing area must be less than 20 degrees. One-man flying units are minimum systems on which the pilot stands. These have been referred to as "pogo sticks", which is an unfortunate choice of terms since the devices considered in this work show much more similarity to the classic pogo stick design. Multi-man flying units have long rectangular bodies with support gear underneath. Astronauts sit on top of the body where they control the output of several lift and maneuver rockets. All versions of the flying vehicles are severely limited in performance capability because of inherent low payload capacity.

In 1967, Howard Seifert introduced the "Lunar Pogo Stick", a lunar transporter concept[6] which offers a vast improvement in expected performance over that of wheeled and flying vehicles. The proposed device employs neither roving nor flying techniques, but it is quite analogous to the classic pogo stick. Motion from one point to the next is achieved by hopping. A hop has three dynamic phases: acceleration of a primary mass upward along an inclined leg or pole, ballistic, and deceleration downward along an inclined leg or pole. The primary mass consists of at least structure, pilot, and payload. Between every two consecutive hops and during each ballistic phase, the leg or pole must be re-oriented. This can be done as an individual operation or as part of the dynamic sequence. Performance of such devices is limited only by the adverse effects of periodic accelerations on the pilots. Of course, a vehicle of this type can stop at the end of any given leap for rest and exploration purposes. The feasibility, based on calculated performance, of the Lunar Pogo Stick concept is the primary concern of this investigation. Therefore, further details of this device and its operation are presented in more appropriate sections of this manuscript.

C. Statement of the Problem and Approach

A lunar transporter represents a complete and somewhat complicated engineering system, consisting of several functional subsystems. It must provide several functions and has many operations to perform. To define, develop, and design a complete and detailed spacecraft system of this magnitude is a major program that requires a sophisticated multi-level engineering organization. Before such a program can be initiated, the merits of the basic concept must be demonstrated to the satisfaction of a sponsor. This has not been done in the past for the pogo stick principle. Therefore, the objective here is not to develop a detailed lunar mobility system but to investigate the feasibility of practically applying this concept and to demonstrate that a superior performance capability can be expected for missions of interest. This goal is achieved by studying the dynamic characteristics of somewhat idealistic pogo stick configurations which are based on realistic mission requirements. There are two dynamic models studied, which are different in operation and performance capabilities but are outgrowths of the same principle of locomotion. These, however, represent the two primary operating modes from which actual system designs may be developed.

With objectives defined, the following specific tasks must be addressed:

- Investigate influencing factors which directly or indirectly affect the design and operation of pogo vehicles. Define performance limiting phenomena.
- Develop general operating constraints and functions which are characteristic of such devices.

- Present two basic vehicle configurations, a small simple first-generation transporter and a large, advanced, and highly sophisticated vehicle.

- Develop the equations of motion for each of these two models. This will require specification of operating environment, kinematic relationships, control function, and propulsion law. Knowledge of operating environment leads to the determination of externally applied and dissipative forces. Kinematic relationships indicate the degree of freedom and type of dynamical problem at hand. The interaction of control forces and other inertia and applied forces significantly effects the dynamical behavior of a system. The locomotive force is determined directly from the propulsion law.

- Solve the equations of motion to simulate performance for each of the models. Some of these will be highly nonlinear differential equations which require numerical integration.

- Calculate hop performance data based on simulations of vehicle motions. Results should indicate dynamical performance quantities such as average speed, payload capacity, and range.

D. Summary of Work Presented

This investigation includes qualitative, as well as quantitative, components. In order to support introduction of the two designs studied, basic requirements and constraints are first presented. These include a

description of the lunar environment and its effect on vehicle design, definition of a basic dynamical operating sequence for hop simulation, formulation of a propulsion model, and a discussion of human limatitions and the nature of acceleration effects on astronauts.

Each of the two vehicles studied is presented separately for description, analysis, simulation, and performance calculations. Schematic designs are discussed in detail, including normal pilot and equipment operating functions and sequences. Equations of motion for two-dimensional hops are derived and a simulation technique developed. Computer programs for simulating vehicle motions were written and their logical structure described. Applications of interest of each design are briefly discussed to indicate the practical uses of hopping vehicles. Mass and configuration parameters were studied in order to obtain realistic estimates of vehicle hop performance. Resulting values are then compared with those of other proposed mobility systems.

In order to make full use of the inherent capabilities of vehicles based on this concept, the possibility of executing plane change maneuvers, while performing normal hop functions, was also investigated. Use of such a technique is shown to be feasible, with the more sophisticated transporter design, through computer simulations of a general rigid body problem related to vehicle motion during deceleration and acceleration events.

Finally, appendices are included to provide supporting material for the primary investigation. A generalization of the analysis and simulation of plane changing maneuvers has developed into an expeditious method for obtaining computer solutions to the motion of mechanical

systems. This technique is presented in detail as Appendix B. Actual computer simulation programs appear in Appendix C.

II. BASIC ASSUMPTIONS AND RELEVANT DATA

A. Lunar Environment

Lunar explorers and their equipment will be subjected to a unique environmental situation. Three aspects are of particular importance to pogo transporters: atmosphere, surface topography and properties, and gravitational strength. The nature and influence of each are briefly discussed below.

The existence and nature of lunar atmospheric gases have been investigated by two distinct approaches: proper interpretation of experimental measurements of the lunar disk properties at the Earth's distance and theoretical calculations concerning the capture and escape of gaseous molecules from the Moon. Data based on experimental observations is, at most, vague, because these measurements are only indirect sources of the desired information about atmospheric existence. Such methods can only give estimates on the upper limit of the surface pressure resulting from gaseous molecules. Three types of experimental measurements have given pressure bounds of 10^{-6}, 10^{-9}, and 10^{-13} atmosphere[7] at the lunar surface.

One of the basic theoretical approaches concerns the escape velocity and mean residence time of a molecule of gas in the weak gravitational field. Based on the estimated age of the Moon, this method indicates that all of the lighter gases would have quickly been lost, but there might still be a very rarefied combination of heavy gases, e.g., krypton and xenon. Singer[8] made an extensive theoretical study of a possible residual atmosphere. He concluded that no permanent atmosphere exists. However, there is an exosphere, i.e., atoms in the gaseous mantle at the

surface do not interact but describe free orbits under the influence of lunar gravity. Based on this information, the dynamic analysis of pogo transporters need not be concerned with atmospheric drag effects.

Although the rarified atmosphere does not affect performance, it may indirectly influence hardware design considerations. Contamination of existing gases deteriorates the potential scientific value of lunar exploration, because accurate knowledge of atmospheric density and composition should provide valuable information about the interior chemistry and radioactivity, possible volcanic processes, and composition of the solar wind. The lunar exosphere is so tenuous that it is particularly susceptible to contamination from exploration activities such as Apollo flight operations and manned and unmanned exploration equipment[1]. These newly introduced gases have relatively low molecule weights and, therefore, will escape the Moon. However, the elimination of these contaminants from descent rockets at the touchdown area may require a period of several days, about the same length of time as planned for Apollo explorations. This area may have a radius of several hundred meters, about the same as the operating range of astronauts on foot. This situation indicates a definite need for a small manned transporter in order to at least obtain accurate atmospheric data.

Contamination also results from transporter operation. Water vapor is expelled from astronaut pressure suits and cabin cooling system, while life support and propulsion units expel other contaminants. Minimization of the contamination problem may be an important factor in subsystem design considerations.

Lunar topographic features of prominence include maria, craters, mountain formations, and rille systems. Maria are smooth, dark areas

comprising about 40 percent of the visible disk and have diameters of up to 700 kilometers. There are three theories on the origin of these lunar seas presented by Gold, Urey, and Baldwin. However, Baldwin's logic seems to be the most convincing, because it is confirmed by lunar observations. Gold's theory postulates extremely thick dust layers in maria, but this is refuted on the basis of the existence of rille systems. Urey and Baldwin agree that maria resulted from large scale meteoritic collisions, followed with filling-in by molten rock of the blasted out craters. They disagree on the source of this molten material. Baldwin[9] suggests that it was internally originating lava. Flows from deep within the Moon covered the huge craters sometime after the actual impact. Therefore, it is widely agreed that the basic surface of lunar maria is composed of igneous rock with very gentle slopes.

Craters are much smaller in area than maria but are regarded as meteoritic impact locations which have not been filled in by lava flows. Many of the craters have thin sharp rims and steep slopes on either side of these edges. However, in general, the larger the crater, the gentler the slope of its inner wall. Crater floors are usually broad plains somewhat below the mean elevation of surrounding areas. On the visible disk there are five craters whose diameters exceed 200 kilometers, 32 others with diameters in excess of 100 kilometers, and thousands with smaller areas. Roving vehicles may have difficulties in exploring many of these craters, because their locomotive capabilities are limited to little more than gently sloping surfaces.

Mountain formations are thought to result from the huge planetesimal collisions which initiated the maria. These upland regions are observed to have relatively few crater marks, implying a young age for such

formations. The highest visible peaks occur at the lunar South Pole and reach to 6 kilometers in elevation. In contrast to the mountains are the shallow depressions known as rilles. These are typically located on the inside edges of maria and configured in huge sweeping arcs with radii of curvature of several hundred kilometers. Rilles are usually less than a kilometer deep and just a few kilometers wide. These are thought to be caused by thermal fracturing which occurred when the mare lavas cooled and shrank.

In addition to the four basic classes of topographic features: maria, craters, mountains, and rilles, there exist all sizes of debris resulting from all the meteoritic impacts. The lunar explorer has a large selection of surface features to investigate. However, some kind of transporter must be used. Debris will be one of the most serious mechanical obstacles to deal with. Also, the general composition of lunar soil will affect the design and performance of such vehicles.

Prior to "soft" landings of spacecraft, observations concerning the nature of lunar soils were made indirectly by infrared measurements, telescopic sightings, and radio and radar data.[7] These techniques lead only to gross conclusions about the surface composition, but they all agree that a layer of powered material covers most of the visible disk. Infrared measurements further reveal that this layer has a thickness on the order of centimeters and lies on a dense substratum. Of particular importance is knowledge of the dust layer in the prime landing zones for Apollo. However, the information can only be obtained by actually landing equipment in those areas.

Luna IX and Surveyor spacecraft have shed some light on this problem[10,11,12]. These unmanned lunar landers have confirmed the existence of a generous distribution of rock fragments, at least in the touchdown zones. Surface soil appears analogous to wet beach sand, in both behavior and appearance. Analysis of the Surveyor I dynamic touchdown experiment revealed the surface material has a static bearing strength on the order of 5 psi. (3.45×10^5 dyne/cm^2). Surveyor III data indicated a static bearing capacity of 2×10^5 to 6×10^5 dynes/cm^2 and this capacity increases with bearing size. Surveyor V data gave a capacity of about 2.7×10^5 dynes/cm^2 and a density of 1.1 g/cc. Penetration depth of footpads on Surveyors I and III was 2.5 to 5 cm. These results definitely indicate that the lunar surface can support landing vehicles and hopping transporters, at least in the mare regions where the Surveyor vehicles landed. However, proper design of a supporting foot for pogo vehicles is of major importance. For this work it is assumed that such a foot can be created and that its performance can be simulated by assuming a rigid and perfectly rough lunar surface. This idealization will give sufficiently accurate results for the performance estimates investigated here.

The surface temperature at the lunar equator varies between -250° and $+250^\circ$F during the period of one lunar day. This presents a serious heat transfer problem for transporters. However, no problem peculiar to pogo stick designs are anticipated and solutions to thermal problems common to all lunar mobility systems are either at hand or being developed.

Since pogo transporters will have trajectories with small dimensions compared to the lunar radius, a constant and uniform value of gravitational acceleration can be assumed. The mean surface value is 5.31 ft/sec^2 (162. cm/sec^2).

B. Basic Dynamical Sequence

The dynamical sequence discussed in this manuscript applies to a pogo transporter model of the following schematic description. A main body which consists of structure, control and operating equipment, and payload is supported by a "leg-with-foot" arrangement. The crew of one or more astronauts is located either on or in the main body. The leg and foot device initiates and brakes vehicle motion via the propulsion unit. Main body and leg mechanisms are assumed to act as rigid bodies even though the crew and some materials on board are, in fact, somewhat elastic. Most non-rigid body effects may be eliminated by a control and stabilization system. While the transporter is at rest the main body is stabilized by a set of supporting legs connected to this body. This description is general enough to apply to both configurations being studied. More specific descriptions will be given as each model is discussed in detail.

The sequence of motion for one hop can be thought of as a five step process. Assuming the vehicle initially at rest and deployed to move in the desired direction, the first step is an acceleration of the main body with respect to the leg and away from the lunar surface with the acceleration vector usually inclined to the local vertical so that horizontal motion is also achieved. The driving force is produced by a propulsive unit which acts between the leg and main body to produce relative motion. Since one end of the leg is fixed to the surface by foot traction, energy of propulsion is essentially transformed into kinetic and potential energy of the main body. The acceleration phase ends when the leg has either extended to a given length or the main body

has reached a specified velocity, depending on the control of performance parameters.

For the purposes of this study it is assumed that the relative translational motion between leg and main body ends instantaneously. In effect, this is an inelastic impact which occurs in infinitesimal time, resulting in partial loss of mechanical energy and in conservation of transporter linear and angular momenta. This transition is referred to as "engagement" (of the leg by the main body) throughout the manuscript.

The ballistic phase commences with engagement. This is a period in which the transporter is flying along a "free-fall" trajectory. A flat Moon approximation indicates that the vehicle center of mass follows the classic parabola. Leg orientation and attitude maneuvers are expected to be performed during this phase. This is necessary to prepare the vehicle for landing and possibly plane changing. The ballistic phase ends at the instant of foot contact with the lunar surface.

It is assumed that the foot makes an inelastic impact with the lunar surface in infinitesimal time, thereby losing all of its kinetic energy and momentum with respect to the Moon. The translational degree of freedom of the leg with respect to the main body is released simultaneously with the foot impact and the leg is again allowed to move against the propulsive force. Thus, this transition will be referred to as "disengagement". Consistent with the lunar surface model, it is assumed that the foot does not slide or sink after contacting the soil. Furthermore, the foot does not transmit torque to the leg and main body. Therefore, total angular momentum about the foot-leg joint is conserved during impact.

In conjunction with these events, the main body acceleration is immediately influenced by re-introduction of propulsive force.

The deceleration phase is similar to the acceleration phase in that the pilot experiences the same kind of forces in both instances. At the beginning of this last phase of a hop the vehicle has a certain amount of kinetic and potential energy. During deceleration the mechanical energy must be transformed back into propulsive energy, thus recovering much of the initial expenditure. This phase and the hop is terminated when the relative translational velocity between leg and main body reaches zero. The leg is then either locked to prevent further such motion or this relative velocity is allowed to change sign and the next hop begins. If the leg is locked a rest period will begin. During non-hopping periods the vehicle is assumed to be stabilized by its supporting structure. Operations which can be performed in these time intervals include vehicle re-orientation, acquisition of scientific data, sensor emplacement, human functions, and control system adjustment.

C. Propulsion Law

The propulsion law is a relationship between thrust force and other variables such as relative position and velocity of the leg with respect to the main body, and time. Each type of device has such characteristic relationships. For the application studied here, a propulsion unit which offers much versatility and adjustability is required. It must be capable of quickly changing its parameter values during ballistic phases and between hops. Of course, it should be compact and of minimum weight.

All these requirements can be satisfied by using a piston-in-cylinder device driven by an expanding gas. The working fluid may be nitrogen, products of decomposed hydrazine, or some other commonly used propellant.

Force exerted on the piston by gas pressure may be transmitted to the leg either directly or through a gear train[6] as illustrated in figure 1. The direct drive device (fig. 1a) incorporates a combination piston and leg, thus having a 1:1 gear ratio. This device is very simple and is especially useful for small transporters which require only short acceleration/deceleration displacements. The geared drive design (fig. 1b) permits a long acceleration/deceleration distance for a relatively small piston displacement. This is very useful for large vehicles. The gear ratio is defined by

$$r = \frac{z_P - z_{P_o}}{d - d_o}$$

From this, it is obvious that $r = 1$ for the direct drive version. For the geared model r is usually given and d is the desired quantity. Therefore,

$$d = \frac{z_P - z_{P_o}}{r} + d_o \quad . \tag{2-1}$$

The motive force, $\mathfrak{F}$ is related to the piston pressure force, F, by

$$\mathfrak{F} = \frac{F}{r} \quad .$$

Since this investigation is just a first order attempt to obtain performance figures, it is sufficient to assume an idealized situation. Calculations based on such assumptions give a reference from which designers may later work. The propulsion model used here injects and/or

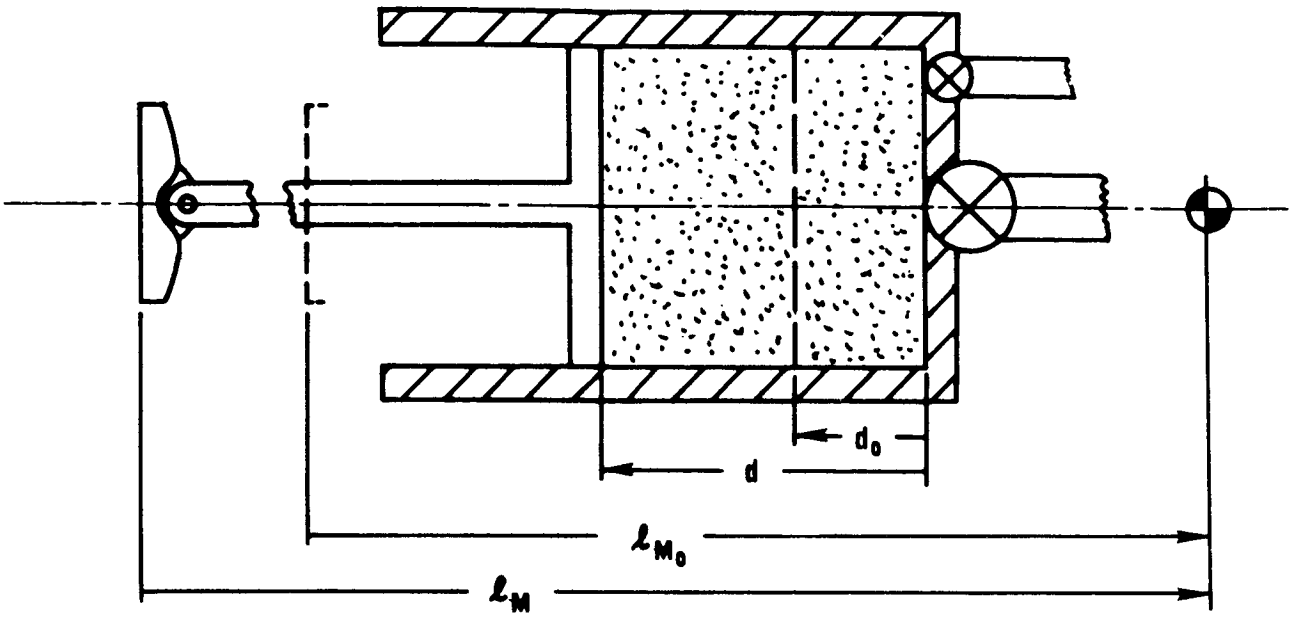

(a) Direct drive (acceleration phase)

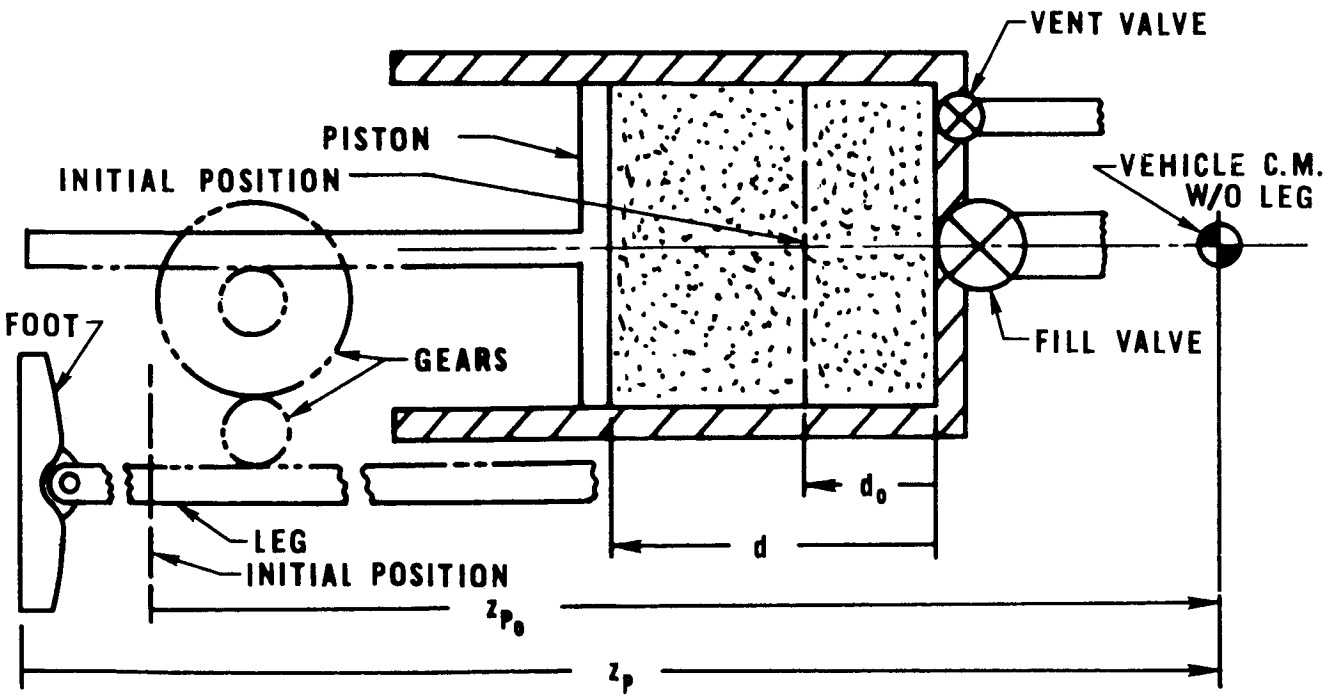

(b) Geared drive (acceleration phase)

Figure 1. Propulsion Models for Pogo Transporters

vents a given mass of working fluid into or out of the cylinder before the next acceleration or deceleration phase. This mass remains constant during expansion or compression. The corresponding thermodynamic processes are assumed to be adiabatic and reversible. Therefore, each expansion and compression is considered isentropic. At the temperatures and pressures of interest, most candidate fluids act quite like perfect gases. This leads to the perfect gas isentropic relation[13]

$$pV_c^{\gamma} = K \quad . \tag{2-2}$$

Typically, a unit mass of working gases may experience the following processes. At the beginning of a hop it is fed into a small displacement at relatively high pressure. During acceleration this gas experiences an isentropic expansion until engagement. Adjustments in pressure and volume may be required during the ballistic phase to prepare for landing. This can be done by changing both total mass of gases in the cylinder and piston position. Vent and fill values can be used to reduce and increase mass, respectively. During deceleration these gases experience an isentropic compression.

Since isentropic expansions and compressions have been assumed, the propulsive force is independent of time and depends only on piston displacement for the given initial conditions of any particular phase. The force on the piston is simply

$$F = pA \tag{2-3}$$

and the volume is

$$V_c = Ad \quad . \tag{2-4}$$

It is necessary to express F as a function of leg displacement, z_P, and given parameters. Therefore, combining expressions (2-1)-(2-4) to eliminate p, d, and V_c gives

$$\mathfrak{F} = \frac{F}{r} = \left(\frac{r}{A}\right)^{\gamma-1} \frac{K}{(z_P - z_{P_o} + d_o r)^{\gamma}} \quad . \tag{2-5}$$

D. Human Factors and Dynamic Limitations

The primary mission of lunar transporters is to move the human body around on the surface of the Moon. Therefore, the characteristics and limitations of astronauts are the most significantly influencing factors on design and performance of such vehicles. Designers of pogo transporters must take into account human factors problems common to other mobility systems and must deal with the peculiar problems brought about by the unique dynamic sequences of hopping vehicles. Considerations for detailed designs and missions must reflect the influences of physiological and psychological effects. However, at this stage of development, it is sufficient to assume that astronauts can be conditioned to cope with emotional problems such as fear, anxiety, and intolerance to discomfort. This will allow the investigation to disregard psychological factors.

It is the physiological factors which are of utmost importance to the operation and performance of pogo vehicles. In regard to human dynamic limitations, Stapp has said:[14] ". . . man is a thin flexible sack filled with thirteen gallons of fibrous and gelatinous material, inadequately supported by an articulated bony framework." The human body is normally subjected to 1g which is withstood without incident. As it is subjected to a slowly increasing acceleration upward in the

sitting position, the following sensations are experienced. At 2g an increase in weight and drooping of the soft tissues of face and body become evident. At 2-1/2 g it is nearly impossible to stand up, and by 4g arms and legs cannot be lifted. Exposure to 5g for several seconds may cause unconsciousness.

An extended stay on the Moon will result in a decrease of tolerance to accelerations because of reduced gravity. The body responds to a change in environmental stress. If the weight support requirements on a bone are reduced, a negative calcium balance eventually occurs and the bone strength becomes equal to the stress imposed. Of course, muscles become weaker when less work is required of them. However, these effects are thought to be avoidable through a proper exercise program[15]. Apollo crews will only be subjected to reduced gravity for a few days and astronauts stationed at lunar bases will probably have a physical maintenance program. Therefore, the acceleration tolerance levels of lunar astronauts should be comparable to those of earthbound men. Physical limitation data based on experiments conducted on earth will be used here.

The duration of acceleration, during acceleration and deceleration phases, on pogo vehicles is, at most, on the order of a second. This is fortunate, because human capabilities are very sensitive to exposure time, i.e., the shorter this time the greater the acceleration magnitude one can tolerate. Physical limits also depend on acceleration direction, rate of onset and decline, subject age, relative position of body limbs, and protective devices. Human accelerations of several g's are not uncommon. Table 1 gives some examples of aircraft pilot exposures[16].

Table 1. Approximate Magnitude and Duration of Accelerations Experienced by Aircraft Pilots

Situation	Magnitude (g)	Duration (sec)
Catapult take-off	2.5-6	1.5
Seat ejection	10-15	0.25
Parachute opening at 6,000 ft.	8.5	0.5

Figure 2 presents crew orientations and configurations of interest for pogo transporters. The direction of acceleration is given in each case by an arrow, i.e., crew members feel inertia forces in the opposite direction. Figure 3 presents estimated tolerance levels for each configuration in figure 2 as a function of duration. The magnitudes represent the highest levels of acceleration to which the subjects were willing to be exposed voluntarily.[14,16]

The curves of figure 3 clearly indicate there are preferred orientations with respect to acceleration direction and the tolerance level is higher for shorter durations. However, the optimum choice of position and acceleration profiles is also a function of other pilot operations such as navigation and reconnaissance observation. Furthermore, the actual acceleration must be well below the limits shown in figure 3 to insure satisfactory crew performance during hops. The long term effects of an extended period of hopping have not yet been investigated. However, the pilot can stop and rest at the end of any

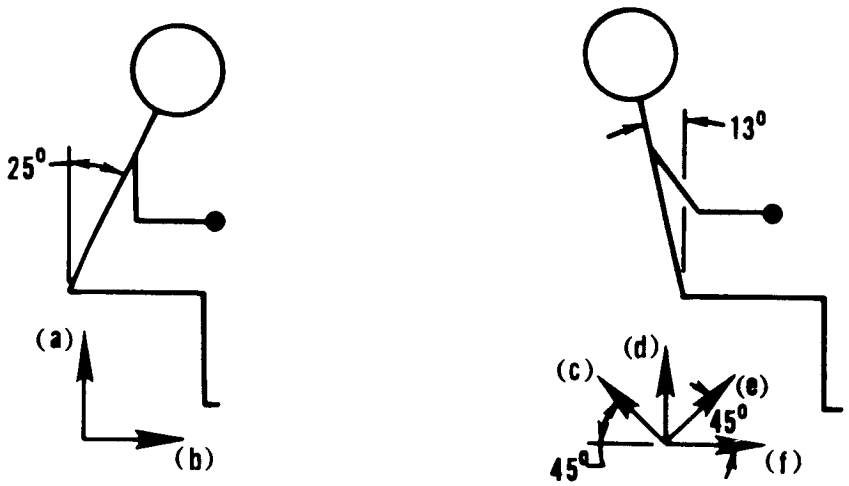

(LARGE ARROWS INDICATE ACCELERATION DIRECTIONS)

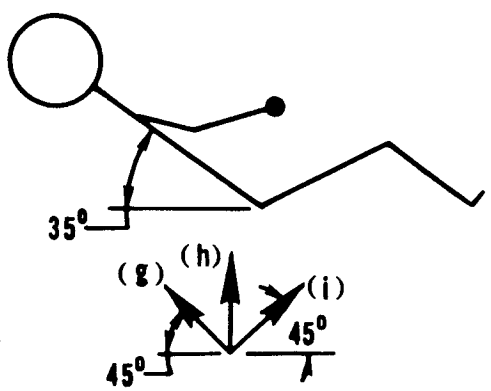

Figure 2. Possible Crew Orientations

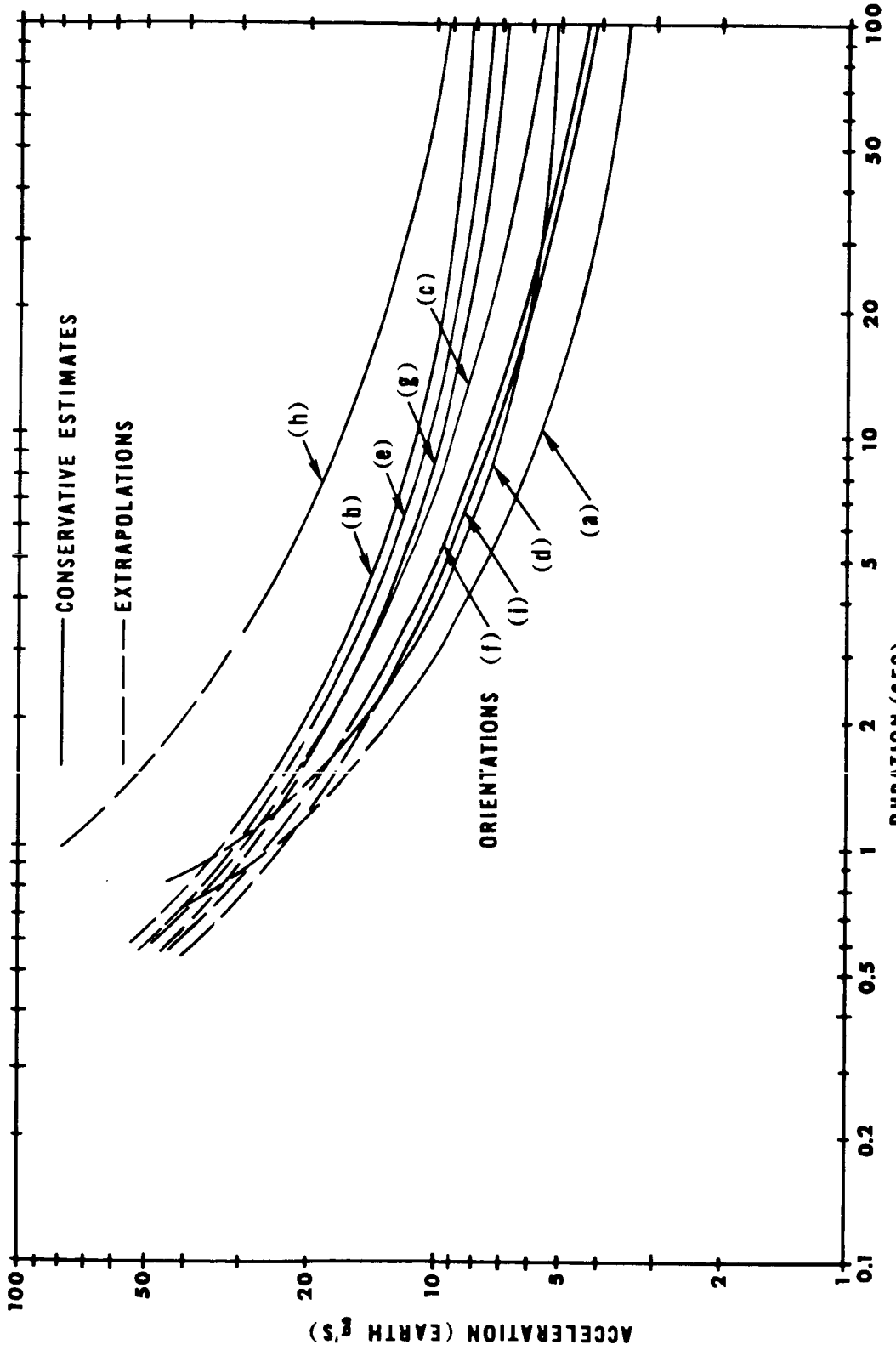

Figure 3. Human Tolerance to Acceleration

given hop. For the purposes of this study an upper acceleration level of 25% of the maximum values for given durations is assumed. This should insure comfortable and efficient operations.

III. SMALL HOPPING TRANSPORTER (SHOT)

A. Configuration Description and Operation

The Small Hopping Transporter (SHOT) is intended to be a minimum system with regard to weight, size, and complexity. Such vehicles could be incorporated into the last few flights of the Apollo series and into extended lunar base operations. Emphasis on early Apollo flights will be placed on successfully sending and returning the astronauts. Development and qualification test time required for a lunar transporter[17] is more than 4 years, thereby ruling out possible application of SHOT until at least 1972, beyond the time of initial Apollo missions. Final and optimum configurations will be somewhat different than those presented here, but in order to achieve desired objectives, one model configuration based on current technology and deductive reasoning is assumed.

Figure 4 presents a schematic profile of such a configuration[18]. The main body of SHOT consists of all equipment except the thrust leg, foot, and pilot with back pack. The main housing contains power supply; propulsion tanks, valves, and controls; attitude stabilization system; hop abort system; and possibly, a sample box and small scientific instruments. Surface stabilization and plane change mechanisms are used between hops to support and maneuver the main body for the next hop. If a plane change is necessary, the main body can be rotated about a vertical axis into the plane of the following hop. The surface stabilizing mechanism permits landing on slopes and rough terrain. In addition, it must provide transporter support while the leg and foot are re-positioned after each hop to the next take-off position and orientation.

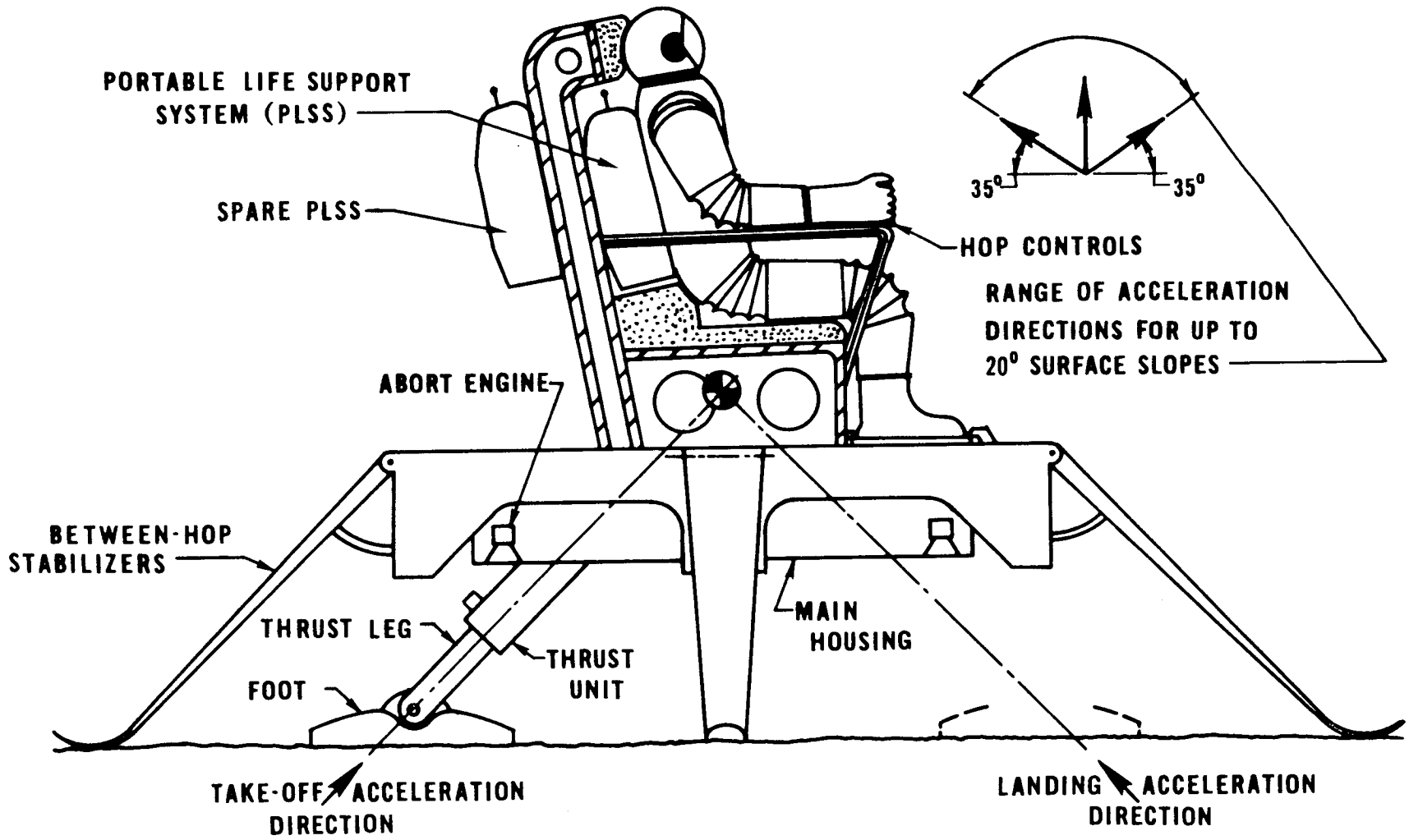

Figure 4. Schematic Profile of SHOT

Mounted on top of the main body are the pilot accommodations, instruments, flight controls, and emergency equipment. The seat design and relative orientation are critical from the standpoint of dynamic performance, navigation and reconnaissance observations, and pilot comfort. In order to keep SHOT simple the pilot is required to navigate by visual observation of landmarks. While resting between hops he must be comfortable and in a position to make observations and take pictures while seated. It should be easy for the pilot to get into and out of his harness. However, with all these requirements, he must also be in a position which allows a large enough acceleration to make the vehicle performance attractive. Careful consideration of the curves in figure 3 and the above factors leads to the seat configuration shown in figure 4. The range of acceleration directions to be experienced by the pilot for surface slopes between -20° and $+20^{\circ}$ are also shown in this figure. Using figure 3 and applying the 25% acceleration magnitude criterion, another set of curves can be constructed which give upper limits of acceleration on SHOT as a function of direction and duration. These are presented in figure 5. This represents the basic performance envelope for such a vehicle. All calculations of hop range and speed will be dependent upon accelerations falling below the corresponding curve in figure 5. These curves will be used extensively in later performance estimates.

During acceleration and deceleration phases the pilot will not have the time or capability to move his arms and hands in order to operate control switches. Therefore, these switches may be located in the arm rests near the hand positions. For safety purposes, pilot extremities

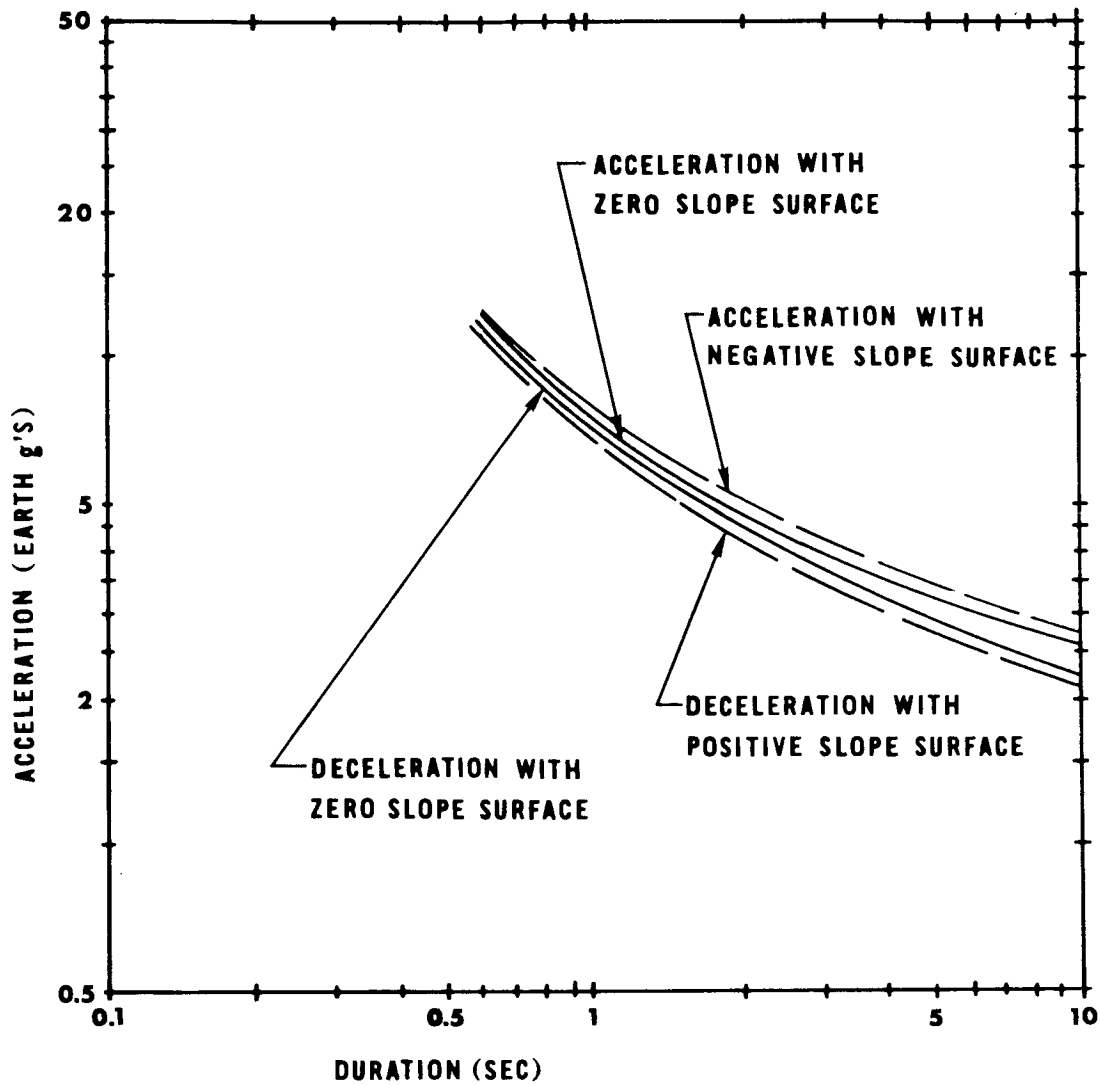

Figure 5. SHOT Acceleration Limits

should be secured in place during hopping periods to minimize perturbations to the stabilization system from pilot movements. His mass center should be near the vehicle center of mass.

The stabilization control system has a simple function on SHOT. It must maintain the main body as an inertial platform during each hop. However, the design of this system will require the application of modern control techniques. Disturbing torques will vary in type and size over the phases of each hop. During acceleration and deceleration phases moments about the foot will arise from the vehicle weight, thrust misalignment, pilot motion, and possible foot slippage. Ballistic phase torques result from leg and other mechanism reorientations, pilot motion, and propulsion exhaust and filling operations. Engagement and disengagement transitions are assumed to contribute, at most, minor perturbing moments. Candidate devices for solving these stabilization problems include reaction wheels[19] and twin-gyro controllers[20]. Since the main body will be essentially an inertial platform, the three disturbance axes are effectively decoupled. This indicates a linear control system is sufficient, and reaction wheels are well suited for this type of application because they require relatively simple control circuits and hardware. However, these devices may need large amounts of power, and main body rotations between hops to change planes would normally cause gyroscopic coupling among the reaction wheels. Unless such problems can be easily solved or avoided, a more sophisticated system may be required. Control systems employing twin-gyro sets need little power and can deal with dynamic coupling problems, but they require much more complicated circuitry and hardware. However, their overall weights may be comparable to those of simpler systems because of recent develops in design optimization[21].

Pilot and system functions involved in operating SHOT may be described as follows. Initially, the pilot mounts the main body and secures himself with harnesses and other safety locks. Before starting a hop he must decide upon the direction or plane of motion. If SHOT is not oriented in that plane, a rotation of the main body and thrust leg is required.* The landing area is visually observed and the hop profile selected. If visual sighting of the landing spot is blocked by an obstacle, a reconnaissance (vertical) hop may be in order. In most cases this situation will not occur. Once having selected the landing area, the pilot must estimate range, elevation, and local slope at this site. This information is entered into the propulsion and mechanism control devices which automatically adjust thrust leg orientation, initial piston displacement, and gas pressure in the cylinder. Once the ballistic phase is reached, these same devices will reorient the leg, adjust piston displacement and gas pressure, and reorient the between-hops stabilizing mechanism to match the slope at the landing site. It is assumed that vehicle motion is optimized in order to minimize working fluid expenditure for a given mission. A technique for doing this is discussed in Appendix A and is used in performance calculations.

As soon as the initial adjustments of propulsion parameters are completed, the pilot can press the piston-release button, thus beginning the acceleration phase. This lasts until the piston reaches a pre-set engagement displacement. During the hop, physical expenditures of energy by the astronaut are kept as low as possible. However, he must make

*The piston-in-cylinder thrust unit is hinged so that only rotation with respect to the main body about an axis normal to the pilot's plane of symmetry is allowed.

visual observations, while in ballistic flight, of future landing sites and topographic features of interest. Directional orientation of the thrust leg for disengagement is nominally coincident with the vehicle velocity vector at the end of the ballistic trajectory. This arrangement essentially eliminates angular impulses to the transporter when the leg and foot lose momentum and energy. Displacement and pressure adjustments made during the ballistic phase are based on constructing nearly symmetrical acceleration and deceleration phases so that the pilot will experience a peak accelerating force both at the beginning and end of each hop, and the magnitudes of these peaks will be approximately equal. Just before the piston is locked at the end of the deceleration phase, a set of springlike stabilizing legs engage the lunar surface around the main body. Pilot accuracy in choosing hop parameters: range, relative elevation, and local slope, will determine whether this last phase of motion is rough or smooth.

Before initiating the next hop, the pilot must, at least, reorient thrust leg, reset piston displacement and adjust cylinder gas pressure. However, if several hops on a large plane surface are in order, he need not enter new hop parameters into the control devices before each leap. In such situations a minimum of between hop time is required and a high average speed can be maintained. Performance estimates are based on computerized hop simulations. These are presented later in this chapter.

B. Analysis and Simulation of Vehicle Dynamics in Plane Motion

As a first step to obtaining quantitative performance data for pogo transporters, each distinct event occurring during the execution of a typical hop must be described by mathematical models. Then these

contributions to the dynamical character of the vehicle are fitted together to form a complete hop. Equations of motion are derived for acceleration, ballistic, and deceleration phases. Matching conditions are also developed for engagement and disengagement. A hop simulation sequence must be constructed which includes a terrain model, launch and landing orientations, and propulsion operating model. Discussion of techniques for obtaining performance data will then be in order.

The acceleration phase can be characterized by the model shown in figure 6. Since plane motion is assumed, only the two coordinates defined in this illustration are necessary to locate the transporter position at any time. Inertial stabilization of the main body by the control system permits only linear motion along the thrust leg direction during acceleration and deceleration phases. In effect, this stabilization eliminates all rotational degrees of freedom. Therefore, the acceleration phase model is a mass M with one degree of freedom moving under the influence of propulsion and gravity. The associated constraints are holonomic and scleronomous,* and the thrust force is a function of ℓ_M alone. These factors permit the application of the conservative form of Lagrange's equation[22],

$$\frac{d}{dt}\left(\frac{\partial L}{\partial \dot{\ell}_M}\right) - \frac{\partial L}{\partial \ell_M} = 0 \ . \qquad (3\text{-}1)$$

For this simple case

$$T = \frac{1}{2} M \dot{\ell}_M^2$$

$$V = Mg\ell_M \sin \alpha + V_p(\ell_M) \ .$$

*time-independent

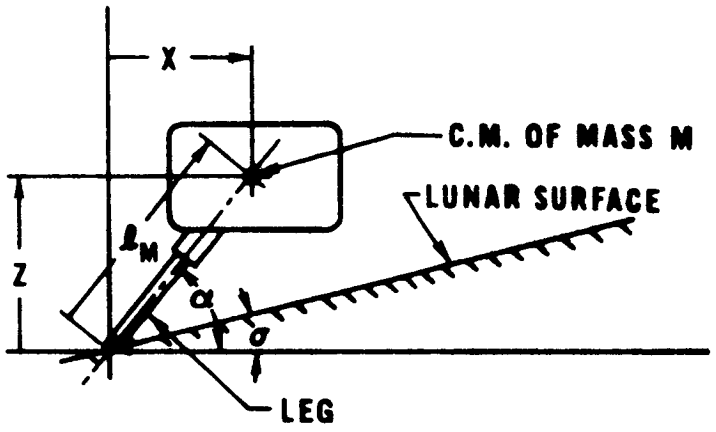

Figure 6. Acceleration Phase Model

Since $L = T - V$, equation (3-1) becomes

$$M\ddot{\ell}_M + Mg \sin \alpha + \frac{\partial V_p}{\partial \ell_M} = 0 .$$

Noting that the propulsion potential, V_p is defined by

$$\mathfrak{F} = - \frac{\partial V_p}{\partial \ell_M}$$

leads to

$$\ddot{\ell}_M = \frac{1}{M} \mathfrak{F} - g \sin \alpha .$$

Substituting expression (2-5) with $r = 1$ into this result leads to the desired form of differential equation for the acceleration phase. Hence,

$$\ddot{\ell}_M - \frac{1}{MA^{\gamma-1}} \frac{K_o}{(\ell_M - \ell_{M_o} + d_o)^{\gamma}} = - g \sin \alpha . \qquad (3\text{-}2)$$

where z_p has been replaced by ℓ_M,

$$K_o = p_o(Ad_o)^{\gamma} ,$$

and the time interval in which equation (3-2) applies is $t_o^+ \leq t \leq t_e^-$. Expression (3-2) is an ordinary nonlinear inhomogeneous second order differential equation which is generally solved numerically for arbitrary values of γ. In particular, since γ is the specific heat ratio of the working gas, its range of values indicates that numerical integration is most convenient for hop simulation objectives. This integration process is further discussed as part of the computer simulation program (part C of this chapter).

When the gas has expanded to a point at which ℓ_M has reached a preset engagement value, ℓ_{M_e}, the thrust leg is instantly locked and the transporter becomes a single rigid body. Since the time interval required for engagement is considered to be infinitesimal, impulses imparted by gravity and surface reaction forces are negligible and need not be included in this analysis. Therefore, linear and angular momenta are conserved during this transition of phases, and a simple set of relationships between velocity components, before and after engagement, result:

$$\left.\begin{aligned} \dot{X}(t_e^+) &= \left(\frac{M}{M+m}\right)\dot{X}(t_e^-) \\ \dot{Z}(t_e^+) &= \left(\frac{M}{M+m}\right)\dot{Z}(t_e^-) \ . \end{aligned}\right\} \tag{3-3}$$

Since these velocity components have finite values, no displacement of coordinates takes place during engagement. Thus,

$$\left.\begin{aligned} X(t_e^+) &= X(t_e^-) = \ell_{M_e} \cos\alpha \\ Z(t_e^+) &= Z(t_e^-) = \ell_{M_e} \sin\alpha \ . \end{aligned}\right\} \tag{3-4}$$

Relations (3-3) yield the initial conditions for ballistic flight. During this phase of the hop, the vehicle is essentially two rigid bodies connected by a hinge, so that thrust leg reorientations can be performed. In the real situation this operation will effect the location of the transporter center of mass and, thereby, range and speed performance calculations. However, the mass of these rotating parts is much less than that of the stabilized platform with crew. Furthermore, design details of propulsion components are still unknown. Therefore, it

seems reasonable to assume that the center of mass motion caused by reorientation operations can be ignored for this "first-order" analysis. In other words, the X,Z coordinates need not be adjusted for this effect but are simply coordinates of classical parabolic flight. The equations for this trajectory can be stated in integrated form immediately,

$$\left.\begin{aligned} \dot{X} &= \dot{X}(t_e^+) = \text{constant} \\ \dot{Z} &= \dot{Z}(t_e^+) - g(t - t_e) \end{aligned}\right\} \tag{3-5}$$

and

$$\left.\begin{aligned} X &= X(t_e) + \dot{X}(t_e^+)(t - t_e) \\ Z &= Z(t_e) + \dot{Z}(t_e^+)(t - t_e) - \tfrac{1}{2}g(t - t_e)^2 \end{aligned}\right\} \tag{3-6}$$

These relationships apply for the time interval $t_e^+ \leq t \leq t_d^-$. The ballistic phase ends at the instant of foot-surface contact t_d.

Disengagement is a combination of two simultaneous events. The foot contacts the lunar surface inelastically through infinitesimal distance and time. It loses all of its momentum and kinetic energy to this surface. The piston is also released at this time to move against decelerating gas pressure in the cylinder. To avoid angular impulses to the vehicle, the landing angle β is set to coincide with the velocity vector direction at the instant of contact. Therefore,

$$\beta = \tan^{-1}\left[\frac{\dot{Z}(t_d^-)}{\dot{X}(t_d^-)}\right] \tag{3-7}$$

where $0 < \beta < 90^\circ$. This condition results in total loss of linear and angular momenta and kinetic energy for the thrust leg at t_d. However,

these properties are conserved during disengagement for the main body and crew. Therefore, it is immediately evident that

$$\left.\begin{aligned} \dot{X}(t_d^+) &= \dot{X}(t_d^-) \\ \dot{Z}(t_d^+) &= \dot{Z}(t_d^-) \end{aligned}\right\} \tag{3-8}$$

and

$$\left.\begin{aligned} X(t_d^+) &= X(t_d^-) \\ Z(t_d^+) &= Z(t_d^-) \end{aligned}\right\} . \tag{3-9}$$

Equations (3-8) indicate that the speed of the main body with respect to the thrust leg at the beginning of deceleration is

$$\dot{\ell}_M(t_d^+) = \left[\dot{X}(t_d)^2 + \dot{Z}(t_d)^2\right]^{1/2} . \tag{3-10}$$

Relation (3-10) implies that acceleration and deceleration phases differ, at least, in the manner each is initiated, since each leap is started with zero velocity of the main body. However, these phases are similar in that both are constrained to one degree of freedom and motion is influenced by propulsion and gravity. The deceleration model is characterized in figure 7. Here again constraints are holonomic and scleronomous, and the thrust force is a function of ℓ_M alone. Hence, equation (3-1) is applicable here. Since

$$T = \frac{1}{2} M\dot{\ell}_M^2$$

$$V = Mg\ell_M \sin\beta + V_p(\ell_M)$$

for deceleration, then the differential equation of motion becomes

$$M\ddot{\ell}_M + Mg \sin\beta + \frac{\partial V_p}{\partial \ell_M} = 0 .$$

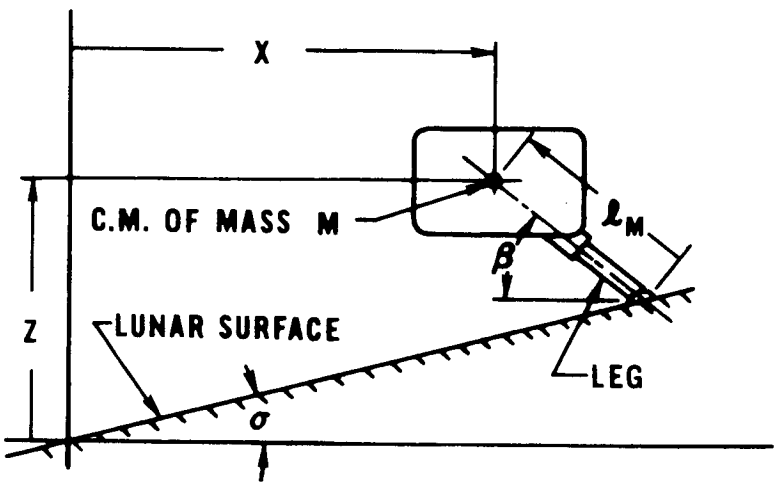

Figure 7. Deceleration Phase Model

During this phase the propulsion force is

$$\mathfrak{F} = -\frac{\partial V_p}{\partial \ell_M} = \left(\frac{1}{A}\right)^{\gamma-1} \frac{K_d}{(\ell_M - \ell_{M_d} + d_d)^{\gamma}}$$

where

$$K_d = p_d(AX_d)^{\gamma} .$$

These expressions lead to the desired form:

$$\ddot{\ell}_M - \frac{1}{MA^{\gamma-1}} \frac{K_d}{(\ell_M - \ell_{M_d} + d_d)^{\gamma}} = -g \sin\beta . \qquad (3\text{-}11)$$

The time interval in which this applies is $t_d^+ \leq t \leq t_f$. Expression (3-11) is a differential equation of the same class as equation (3-2) and may also be solved by numerical methods. This is accomplished in the computer simulation program discussed in part C of the chapter. These two differential equations indicate that propulsion unit operation can be simulated through gas pressure and displacement variations. Venting and filling effects on vehicle motion can be ignored, because these operations are executed between hops and during ballistic flight, and the control system will eliminate perturbing torques.

Deceleration and the hop are terminated at the instant the velocity $\dot{\ell}_M$ goes to zero. Simultaneously, with this event, the thrust leg is locked with respect to the main body, and between-hop stabilizing legs engage the local surface to secure the vehicle for reorientation maneuvers. Formally, the condition for hop termination is

$$\dot{\ell}_M(t_f) = 0$$

which defines t_f, time at which the hop ended. Final values of X and Z are obtained by extrapolating between the two appropriate numerical integration steps provided by the simulation program.

Before a computer simulation can be developed, all relevant parameters must be specified. These parameters are of three different types. A detailed design of the vehicle will determine accurate values of M, m, and A. Specific performance goals lead to desirable values of ℓ_{M_o}, ℓ_{M_e}, ℓ_{M_d}, d_o, p_o, and p_d. The lunar environment determines the value of g, and surface characteristics lead to values of launch angle α for minimum expenditure of working fluid. Estimates of design and basic performance parameter values for this investigation are obtained by studying other proposed mobility systems, where applicable, and by using "engineering judgement" in determining non-critical parameters. Actual values are developed and presented in part E of this chapter.

The launch angle α is an important parameter, because it can be used to help minimize gas expenditure. Typically, a certain percentage of this working fluid must be vented after each hop and/or during each ballistic phase. Therefore, it is desirable to have a minimum of gas in the cylinder at the beginning of the acceleration phase. The mass of this gas in the cylinder for a given thermodynamic state and given value of α is a minimum for minimum engagement velocity. Hence, it is desirable to have the launch angle set at a value which gives maximum range. Equation (3-2) indicates a certain dependence of engagement velocity $\dot{\ell}_M(t_e^-)$ on α. The average force of propulsion is, however, many (12 to 20) times larger than vehicle weight, and the effect of launch angle on this velocity is further reduced through the trigonometric operation $\sin\alpha$. It must be concluded that the initial ballistic

velocity is quite insensitive to variations in α about the optimum value for maximum range. Computed performance data confirms the relative independence of α and $\dot{\ell}_M(t_e^-)$. These observations indicate the optimization of α can be thought of as the problem of maximizing range for a given value of $\dot{\ell}_M(t_e^+)$. The hop profile associated with this problem is shown in figure 8. It is assumed ballistic flight occurs between points 0 and F which lie on a line parallel to a linear sloping terrain at an angle σ. There are two reasons for this assumption. The amount of algebra required to find the range is somewhat reduced, because only one slope angle need be considered. Second, and more important, when σ is positive, as is the case in figure 8, the deceleration distance is less than that for acceleration. This helps to make the peak accelerations felt by the pilot approximately equal, because vehicle kinetic energy is less at disengagement than at engagement for positive σ, implying a shorter stopping distance is required to obtain equal acceleration peaks at beginning and end of the hop. A similar equalization of these peak values occurs when σ is negative, because deceleration distance is greater than that for acceleration, and the kinetic energy to be taken out is greater for σ less than a small negative threshold value*. Typical acceleration profiles are presented with the performance figures in part F of this chapter. The condition which insures that points 0 and F lie on a line parallel to the surface is

*A slight loss of kinetic energy is experienced during engagement by inelastic locking of the thrust leg to the main body. Therefore, kinetic energies imparted by acceleration and dissipated by deceleration are equal when the conditions

$$\dot{X}(t_e^-) = \dot{X}(t_d^-) \quad \text{and} \quad \dot{Z}(t_e^-) = -\dot{Z}(t_d^-)$$ are satisfied.

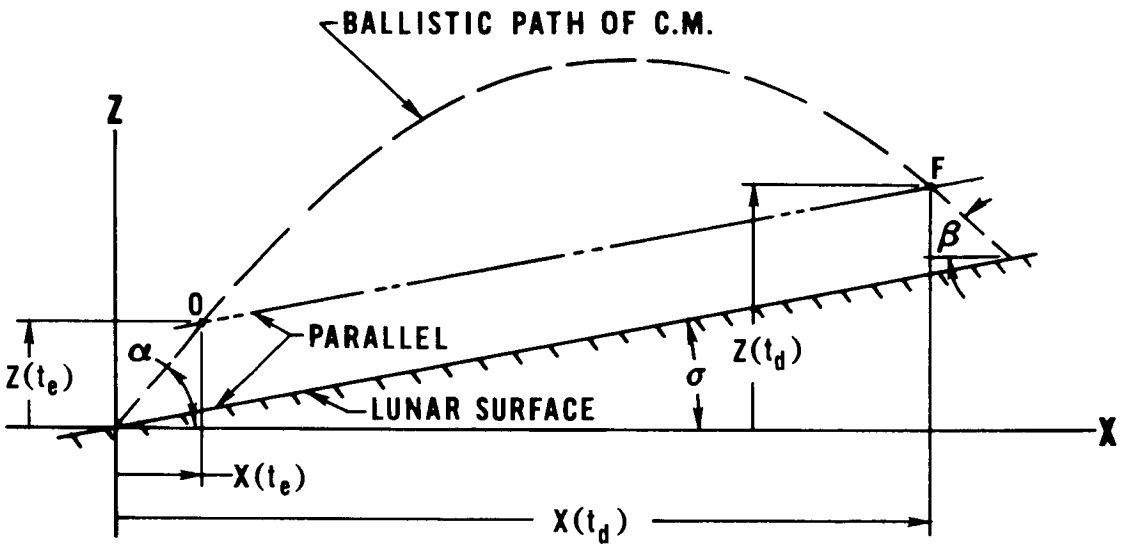

Figure 8. Hop Profile for SHOT Simulation

$$\ell_{M_e} \sin(\alpha - \sigma) = \ell_{M_d} \sin(\beta + \sigma) \ . \qquad (3\text{-}12)$$

Appendix A presents an analysis of launch angle optimization for maximum range, and it is found that

$$\alpha_{opt} = \frac{\pi}{4} + \frac{\sigma}{2} \qquad (3\text{-}13)$$

for $-90^{\circ} < \sigma < 90^{\circ}$.

C. Computer Simulation Program

Computer programs to simulate hopping motions of interest were designed in a manner which allows their continued expansion to provide increasingly detailed information as pogo transporter technology advances. A digital computer was used because of its versatility with respect to design projects. Actual computer listing of these programs are presented in Appendix C. Program logic, as discussed below, reflects the influence of the FORTRAN IV compiler language characteristics because these programs were finally written in this language.

The program constructed for SHOT performance simulation computes coordinates and velocities of the center of mass of vehicle minus thrust leg in plane motion over a linearly sloping surface with given initial conditions. Various elements of the dynamics analysis were presented in part B of this chapter. The technique of combining these factors to make a complete hop simulation is discussed here. Figure 9 presents the flow of logic in this simulation. Actual physical composition of such a program consists of a main program, a library subroutine for solving sets of first order ordinary differential equations, and other supporting subroutines. The program has five basic functions: accept configuration

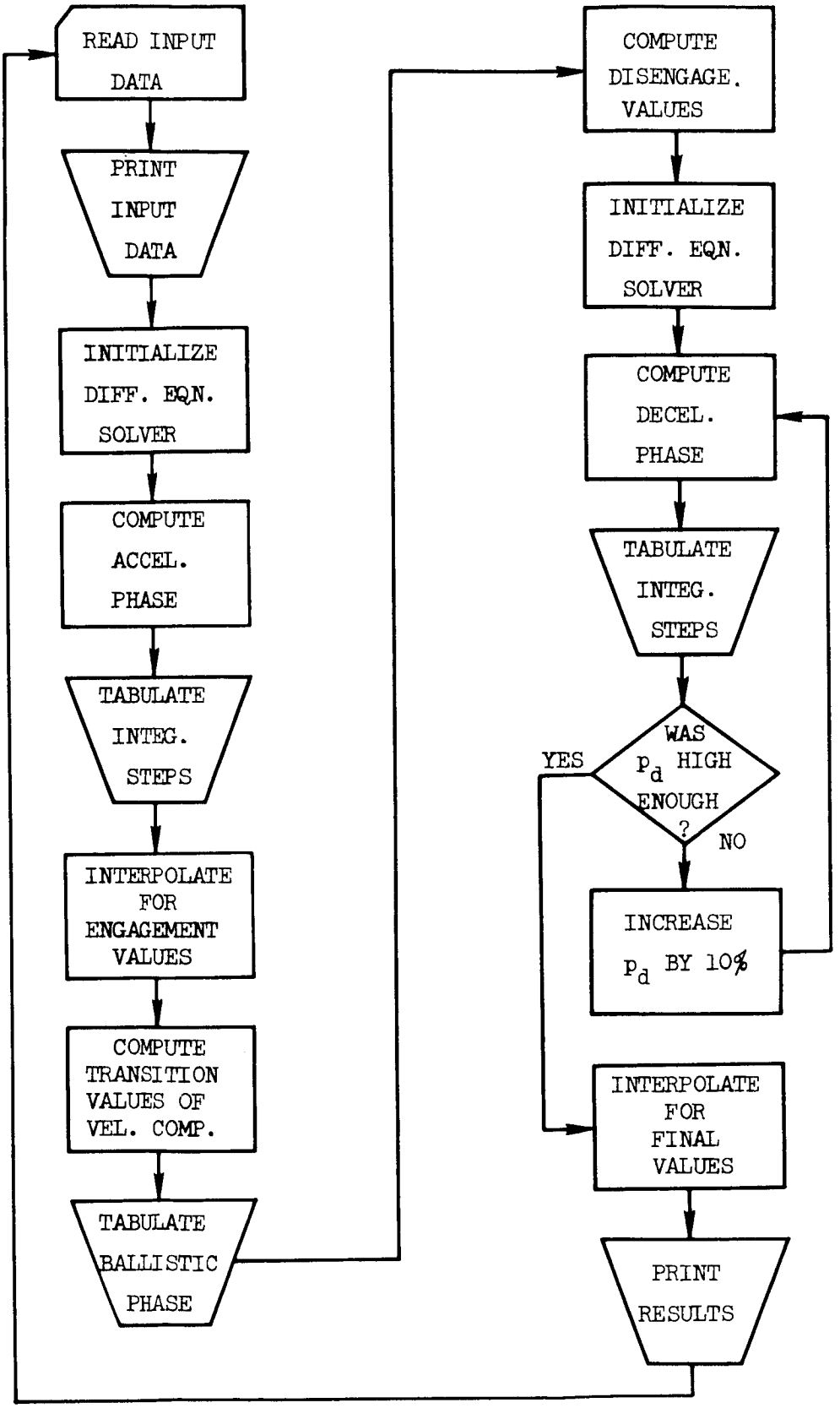

Figure 9. Schematic Flow Chart for SHOT Simulation

parameter and initial condition values, integrate the differential equations of motion, logically sequence hop events, compute hop performance figures, and print results. The flow chart of figure 9 is only schematic, and its purpose is to illustrate the sequence of computational events. A description of this sequence is now presented.

A digital computer program is a maze through which the computer takes input data values, these values being operated on with each sequential event. SHOT input data consists of values for γ, p_o, A, M, m, d_o, ℓ_{M_o}, ℓ_{M_e}, g, t_o, and σ. Within the framework of the dynamic model thrust magnitude and duration, working fluid, mass distribution, and environment can be selected. The program stores this input data and then prints these values as a heading on the output for run identification. Computation then begins on the acceleration phase differential equations,

$$\frac{\dot{\mu}}{M} = \frac{1}{MA^{\gamma-1}} \frac{K_o}{(\ell_M - \ell_{M_o} + d_o)^{\gamma}} - g \sin \alpha$$

$$\dot{\ell}_M = \frac{\mu}{M} \qquad (3\text{-}14a,b)$$

which are obtained from expression (3-2) by reducing it to first order with definition (3-14b). Several substitutions are first required before starting numerical integration of set (3-14). Solutions of the differential equations encountered in this investigation were obtained through the use of a library subroutine which employs a Hamming's modified predictor-corrector method for initial value problems. Desired accuracy and integration step size can be specified, and either part or all of these steps can be tabulated. Since the phase terminates on a test of the dependent variable ℓ_{M_e}, integration generally proceeds to within

one step beyond this desired value. Therefore, interpolation of independent and other dependent variables is required to obtain accurate data at the engagement point. Velocity components are then calculated from relations (3-3) to obtain initial ballistic values. The parabolic trajectory profile is then easily tabulated from equations (3-5) and (3-6) in ten equal time steps to the disengagement point. The ballistic range and time are calculated from

$$X(t_d) - X(t_e) = \frac{1}{g}[\dot{X}(t_e^+)^2 + \dot{Z}(t_e^+)^2](\sin 2\alpha - 2 \tan\sigma \cos^2 \alpha)$$

$$t_d - t_e = \frac{X(t_d) - X(t_e)}{\dot{X}(t_e^+)} \quad .$$

During the instant of disengagement, velocity components are unchanged for mass M and propulsion is again activated. Initialization for numerical integration is repeated. Before the deceleration differential equation, given by expression (3-11) and reduced to first order, can be solved, a cylinder pressure is calculated using a formula determined from experience,

$$p_d = (1 - \sin^2 \sigma)p_e \qquad (3\text{-}15)$$

so that $p_d \leq p_e$. This method of selecting p_d is necessary because some kinetic energy is lost in engagement and the value of ℓ_{M_d} is affected by σ through condition (3-12). Results indicate expression (3-15) is satisfactory for the purposes of this study. Numerical integration of the deceleration phase is carried out and terminated by testing for $\dot{\ell}_M \geq 0$. Here again tabulation is optional and interpolation is required. A further test is then made to determine the final value

of displacement d_f which corresponds with $\dot{\ell}_M = 0$. As a design criterion it has been decided that the value of d_f should not be less than d_o. If the case $d_f < d_o$ occurs, then deceleration is recomputed with a new value of p_d obtained from the formula,

$$(p_d)_{next} = 1.1\ (p_d)_{previous}\ .$$

This increase in disengagement pressure will result in a larger value of d_f. This process is repeated until the condition $d_d \geq d_o$ is satisfied. Then final hop performance data is printed. This includes t_e, t_d, t_f, ballistic flight time, $\dot{\ell}_M(t_e^-)$, $\dot{\ell}_M(t_e^+)$, range, maximum altitude, α, β, p_e, p_d, and d_f. The program reads in the next set of data and repeats the above cycle.

D. Applications of Interest

It is hoped that first operational SHOT models will be used in connection with the Apollo Applications Program which will commence shortly after initial Apollo successes. This program will consist of exploration missions to several areas of interest on the visible face of the Moon. Landing sites include the craters Copernicus and Alphonsus, and rille areas such as Schröter's Valley and Davy Rille. Hopefully, this transporter will be developed in such a manner that it can be taken with the astronauts in one launch vehicle, thus permitting a mobility equivalent to the combined performance of a lunar flying unit and roving vehicle, in addition to avoiding the extra expense and complexity of a second launch vehicle. Specific uses of SHOT on the lunar surface include reconnaissance observations, exploratory excursions, and possibly human factors experimentation. Reconnaissance information may

be obtained under two different circumstances. If the pilot sets the launch angle to 90°, then a vertical hop will be executed. This type of maneuver is designed for the sole purpose of making terrain observations, and it permits a maximum altitude and ballistic flight time to be attained for given propulsion parameter values. Reconnaissance data is obtained during normal travelling hops in which the launch angle was set to a value less than 90°. The pilot must make observations related to future landing sites and interesting topographical features during each ballistic phase. Exploration trips are required for carrying out the primary objective of lunar missions, i.e., to collect scientific data on the nature and origin of the Moon and its environment. On these excursions the pilot will be placing remote sensing devices for transmitting certain types of time-dependent data back to Earth over an extended period of time, making location-dependent measurements, collecting geological samples, and making surveys for the construction of accurate maps. Several interesting experiments can be done to obtain data related to the effects of low gravity on pilot performance. It is not yet known if the human senses will be greatly impaired and if an astronaut can quickly carry out navigation and control decision functions while being subjected to hopping motions.

After the Apollo Applications Program is completed, extended-stay lunar bases may be set up for further lunar and astronomical explorations. Members of these expeditions will need transportation devices for several purposes. A small vehicle, such as SHOT, can fill many of these requirements. Short range reconnaissance and exploration, as well as equipment maintenance trips are well within the capabilities of the

SHOT vehicle and are of primary importance to lunar base operations. Other possible uses of a small fast transporter include delivery of emergency life support equipment in rescue operations and transfer of astronauts between shelters during rotation-of-personnel maneuvers. With these application possibilities, SHOT may easily develop into a "Moon Jeep".

E. Parameter Values for Performance Calculations

Discussion of the SHOT simulation program in part C of this chapter indicates the requirement for determining certain parameter values before performance calculations can be executed. These parameters are separable into three classes: mass distribution, propulsion unit and working fluid, and environmental factors. Each of these classes and associated parameter values is separately discussed in the following paragraphs.

Only two mass distribution values M and m are required for this first-order performance analysis. However, vehicle mass is dependent upon the individual components which make up the system. Table 2 lists the various items required for an operating model of SHOT. This list also gives a conservative estimate for the mass of each item. These values were determined on the basis of other studies of lunar roving and flying vehicles[5,17]. An Apollo astronaut with portable life support system (PLSS) charged for a three hour excursion has a mass of 9.7 slugs. A spare PLSS has a mass of 2.1 slugs. These units also contain transceivers for astronaut communications. The primary propulsion unit can be a simple device. For example, if hydrazine is the propellant, the propulsion subsystem consists of valves, tubing, reaction chamber, propellant tank, pressurization tank, and a cylinder for the thrust leg.

A conservative mass estimate for this subsystem is 1.4 slugs. Assume hydrazine decomposition products of molecular weight 18 make up the propulsion working fluid, and the initial displacement volume is 0.3 cu. ft. Then, for a starting pressure of 150 psi and temperature of 600°F, the mass of gas in the cylinder at the beginning of a hop can be estimated through the equation of state of a perfect gas, and its value is 0.0022 slug. It is expected that a typical excursion of 3 hour duration and 6 mile range will require about 1200 hops. If the propulsion working fluid is utilized with an efficiency of 50%, then half of the initial fluid in the cylinder will be expelled during a nominal hop, and the total mass of hydrazine expelled is 1.32 slugs. Thus, 1.5 slugs is a conservative estimate for initial working fluid mass. Between-hop stabilizers and plane change mechanisms have an estimated mass of 3.4 slugs. The power source may be either batteries or fuel cells, with an estimated mass, including electronics for control and power distribution, of 2.1 slugs. A payload mass allowance of 0.7 slug will permit a significant number of experiments to be performed. The major perturbing torques to be eliminated by the stabilization control system will occur about the pitch axis. Of these, the largest will have an average magnitude of about 300 ft-lbs for as long as 0.7 sec. This will occur during acceleration and deceleration phases and result from the moment of vehicle weight about the foot position. An angular impulse of up to 210 ft-lb-sec must be eliminated by the control system if this torque has not been avoided through mechanism design techniques. Consider a cylindrical momentum wheel of 1.5 ft diameter. This could maintain stability through a braking process during the two critical phases if it is initially rotating at a rate of 6000 rpm and has a mass of 2.4 slugs.

Other disturbance torques are expected to be minor compared with those about the pitch axis. Therefore, a conservative estimate of the stabilization control system mass is 5.5 slugs. The main body structure is assumed to have a mass of 3.4 slugs, and the thrust leg-with-foot a mass of 0.5 slug. Each of the four nozzle units of the emergency abort system accounts for about 0.5 slug. It is estimated that a nominal abort maneuver requires a velocity change of 10 fps. If the propellant used has a specific impulse of 200 sec and the vehicle mass is 35 slugs, then about 0.19 slug of this expellant is used. Assuming 2% of the hops require abort maneuvers, then 4.5 slugs of propellant is needed. The total mass of the abort system is then estimated to be 6.6 slugs. Therefore, total vehicle mass is 36.9 slugs, of which $M = 36.4$ slugs and $m = 0.5$ slug. The magnitude of M is assumed to be constant throughout the excursion, even though working fluid and abort propellant are being expelled in addition to the possible unloading of remote sensing devices during an excursion. Some or all of this lost mass may be replaced by geological samples. The actual change in mass cannot be estimated at this time.

Propulsion unit configuration and working fluid selection are rather arbitrary at this point in SHOT development. For this study a satisfactory value for piston area seems to be 0.2 sq. ft. This permits peak pressure values to be of reasonable magnitude for hops of interest. A nominal value of specific heat ratio for hydrazine decomposition products is 1.2. The computer simulation program also requires values for d_o, ℓ_{M_o}, and ℓ_{M_e}. The dependence of vehicle performance on these parameters is determined by varying their values.

There are only two environmental factors required to simulate SHOT dynamics. The value of gravitational acceleration is constant and

uniform at 5.31 fpss. The linear slope angle will be varied to determine its effect on performance. Constant parameter values used as input are:

$M = 36.4$ slugs

$m = 0.5$ slug

$A = 0.2$ sq. ft.

$\gamma = 1.2$

$g = 5.31$ fpss.

Table 2. Estimated SHOT Mass Distribution

Item	Mass (slugs)
Pilot with PLSS	9.7
Spare PLSS	2.1
Primary propulsion	1.4
Propellant	1.5
Between-hop support equipment	3.4
Power supply and electronics	2.1
Payload	0.7
Control and stabilization	5.5
Main body structure	3.4
Thrust leg-with-foot	0.5
Emergency abort system	6.6
Total	36.9

F. Results of Performance Simulations

Two-dimensional hop simulations of SHOT were performed with the vehicle parameter values listed on page 54. In addition, the initial main body displacement value ℓ_{M_o} was assumed to be 4.0 ft in all cases studied. The following table indicates ranges of varied parameters for this study:

parameter	range
accel. distance, $\ell_{M_e} - \ell_{M_o}$	1 to 2.5 ft
initial cylinder displacement, d_o	0.5 to 2.0 ft
initial cylinder pressure, p_o	100 to 175 psi
linear surface shope, σ	-10^o to 10^o

Although p_o represents a critical quantity in a working transporter model, a more instructive parameter is the initial acceleration $\ddot{\ell}_{M_o}$ which is also the peak value of acceleration. Equation (3-2), evaluated at $t = t_o(\ell_M = \ell_{M_o})$, gives

$$\ddot{\ell}_{M_o} = \frac{p_o A}{M} - g \sin \alpha$$

Noting that $\alpha = \pi/4 + \sigma/2$, and inserting constant parameters values, gives

$$\ddot{\ell}_{M_o}(\text{fpss}) = 0.79\, p_o(\text{psi}) - 3.76(\sin \tfrac{\sigma}{2} + \cos \tfrac{\sigma}{2})$$

The maximum variation of $\ddot{\ell}_{M_o}$, resulting from surface slope values of use here, occurs when $\sigma = 10^o$. Therefore,

$$\ddot{\ell}_{M_o}(\text{fpss}) = 0.79\, p_o(\text{psi}) - 3.76 \qquad (3\text{-}16)$$

within 0.34 fpss. Now p_o can be replaced by $\ddot{\ell}_{M_o}$ through the application of formula (3-16).

Figure 10 illustrates the relationships between acceleration duration and peak acceleration for various values of acceleration distance and initial displacement. Comparing these curves with figure 5 indicates the acceleration levels used here are well within estimated limits of human endurance.

Figures 11 through 13 show hop range data for acceleration distances 1.0, 1.5, and 2.5 ft, respectively. As expected, for positively sloping surfaces, range is decreased if peak acceleration is maintained at a given level. Range is increased for negative slopes. Furthermore, range is increased for larger initial cylinder displacement, because pressure falls off at a slower rate with gas expansion. Finally, increased acceleration distance increases range, because propulsive pressure acts through a longer displacement, thus increasing the work of the gas on the vehicle. This then increases initial ballistic velocity and, therefore, range. Figure 14 illustrates this effect. Since gas pressure falls off as displacement increases, these curves approach asymptotes corresponding to infinite expansion of the working fluid.

Figure 15 illustrates the relationship of range to ballistic flight time and maximum altitude during flight. These curves appear to be independent of initial displacement values in the interval of interest and indicate that for given ballistic flight time, range is slightly increased for increased acceleration distance while the initial pressure required is reduced slightly. Alternately, for fixed range, ballistic

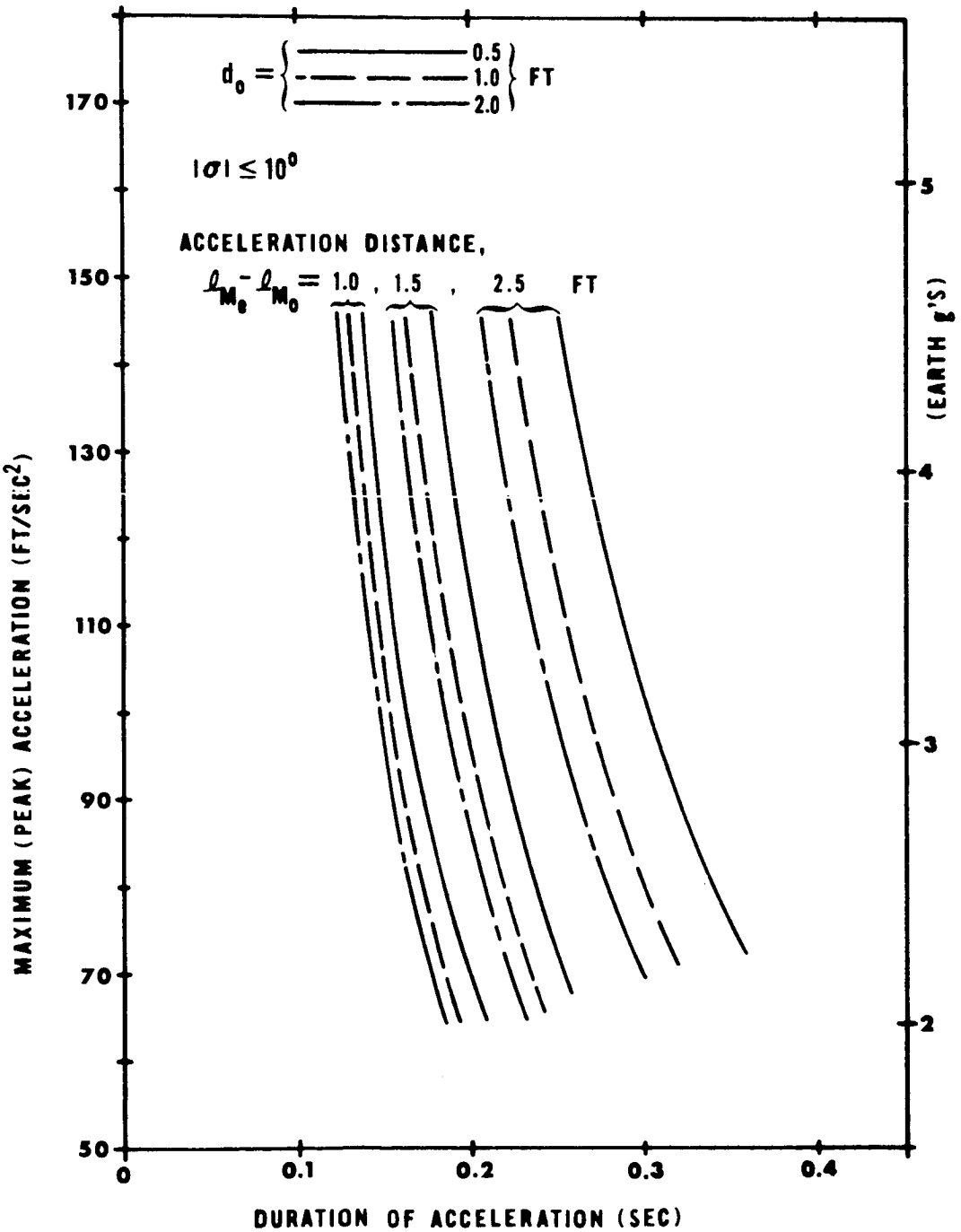

Figure 10. Vehicle Peak Acceleration vs. Duration

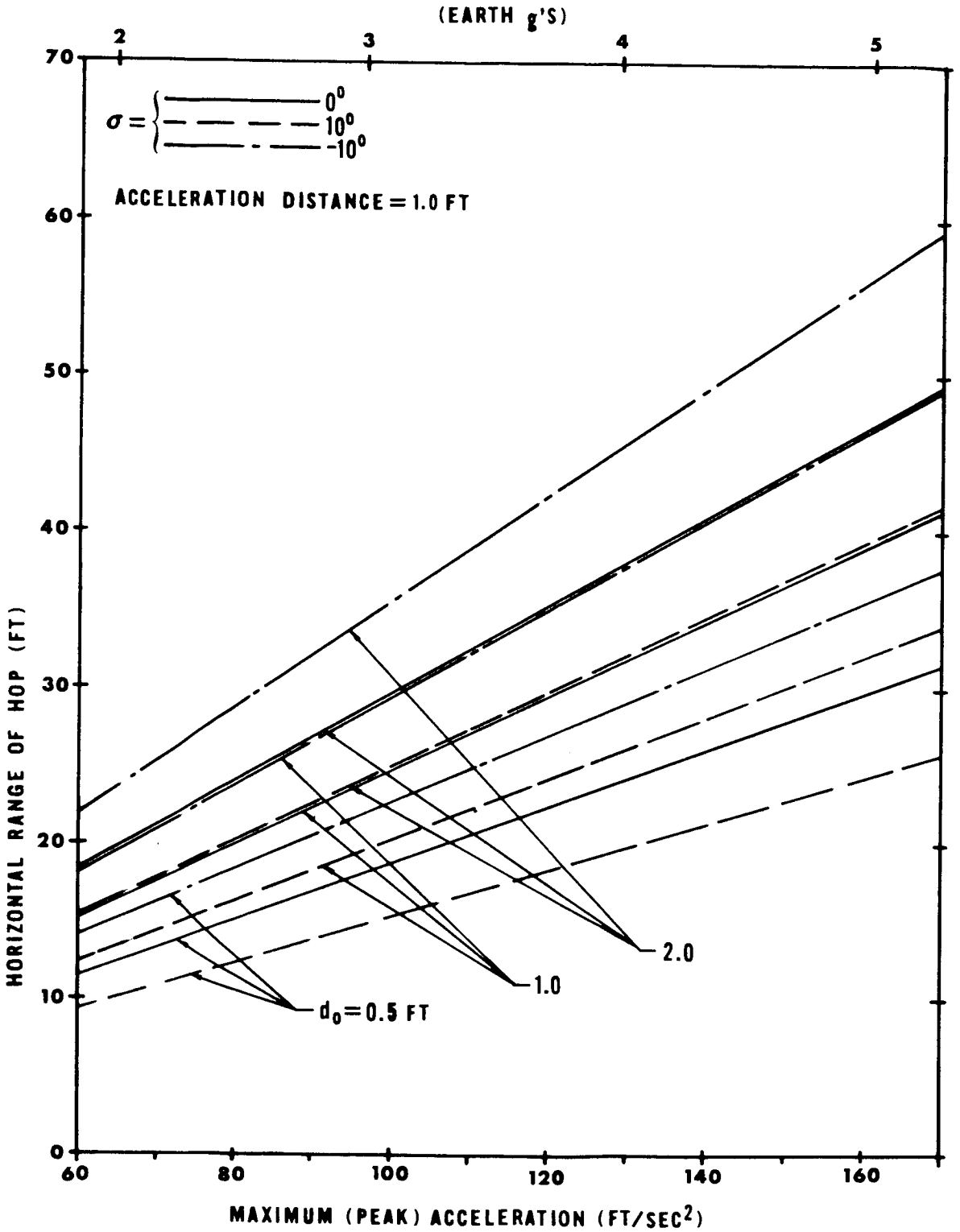

Figure 11. SHOT Hop Data for 1.0 ft. Acceleration Distance

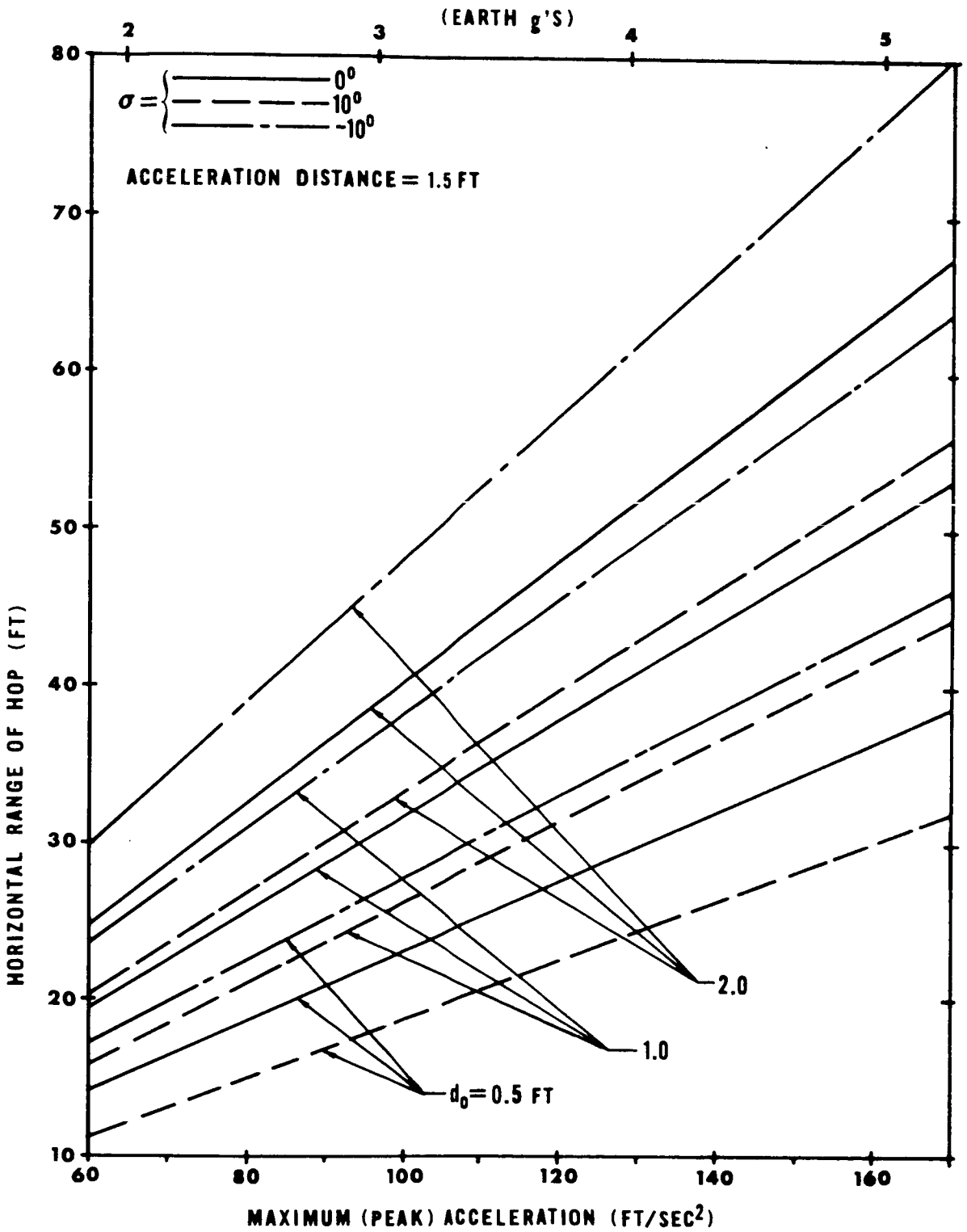

Figure 12. SHOT Hop Data for 1.5 ft. Acceleration Distance

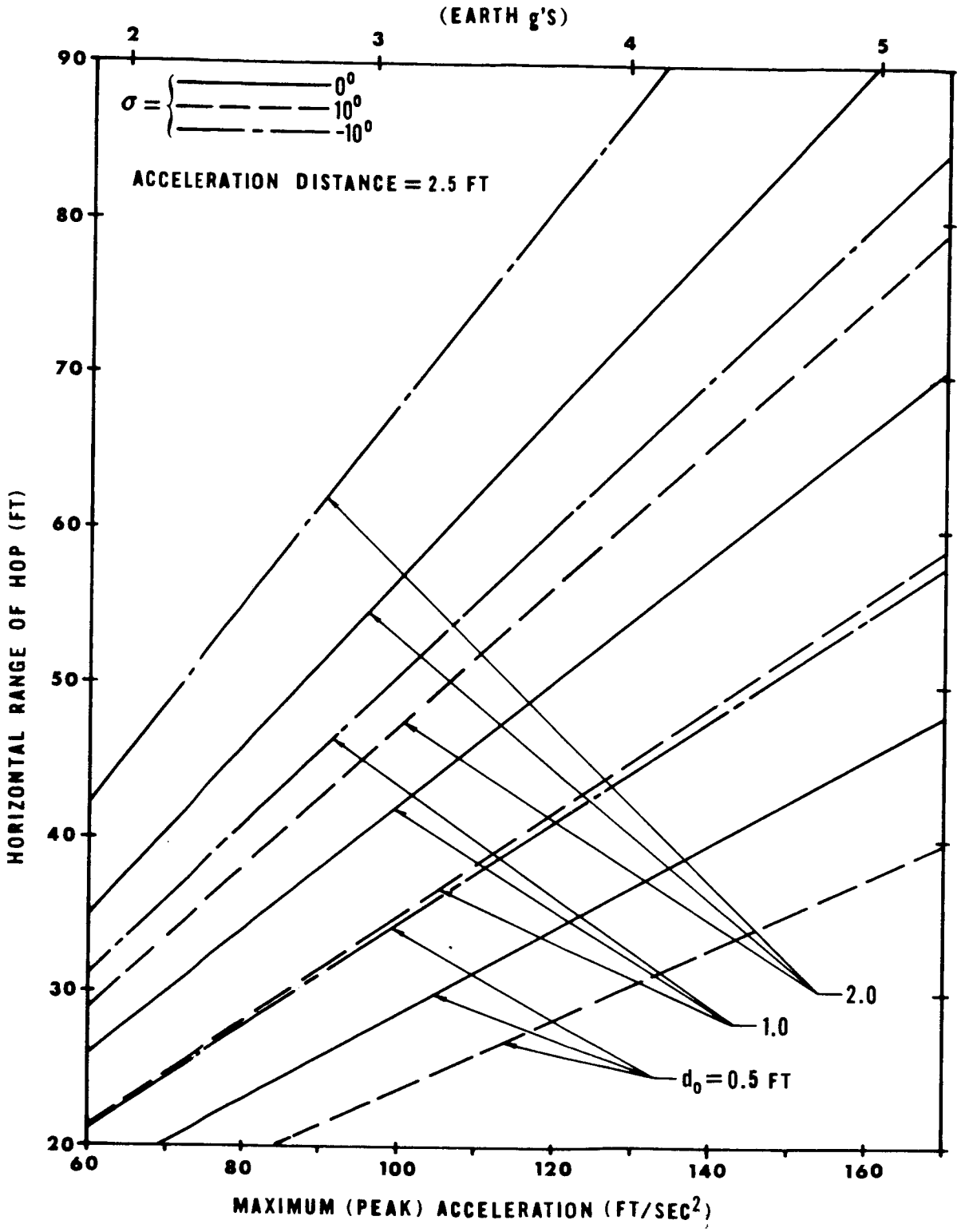

Figure 13. SHOT Hop Data for 2.5 ft. Acceleration Distance

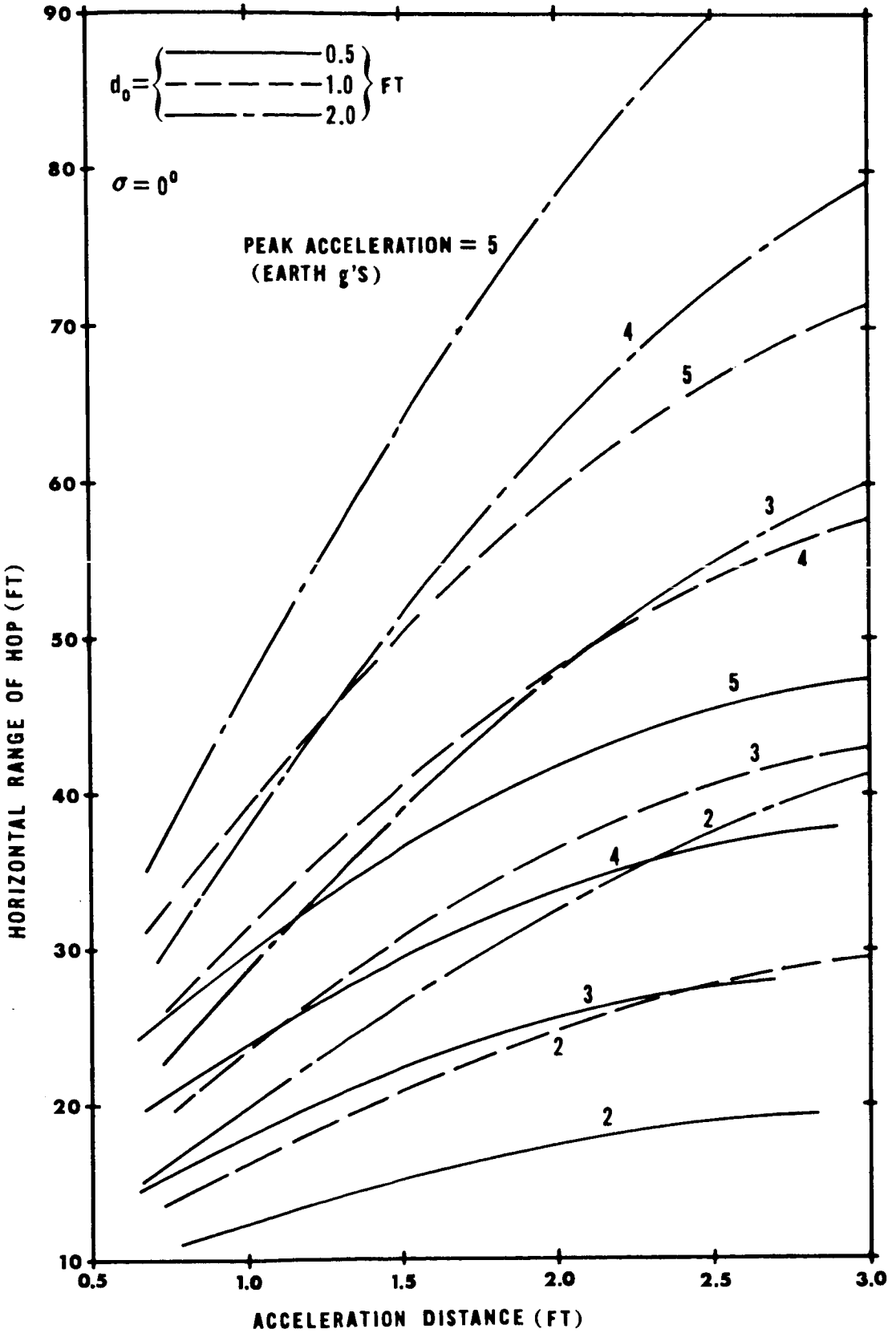

Figure 14. SHOT Hop Data with Peak Acceleration as the Parameter

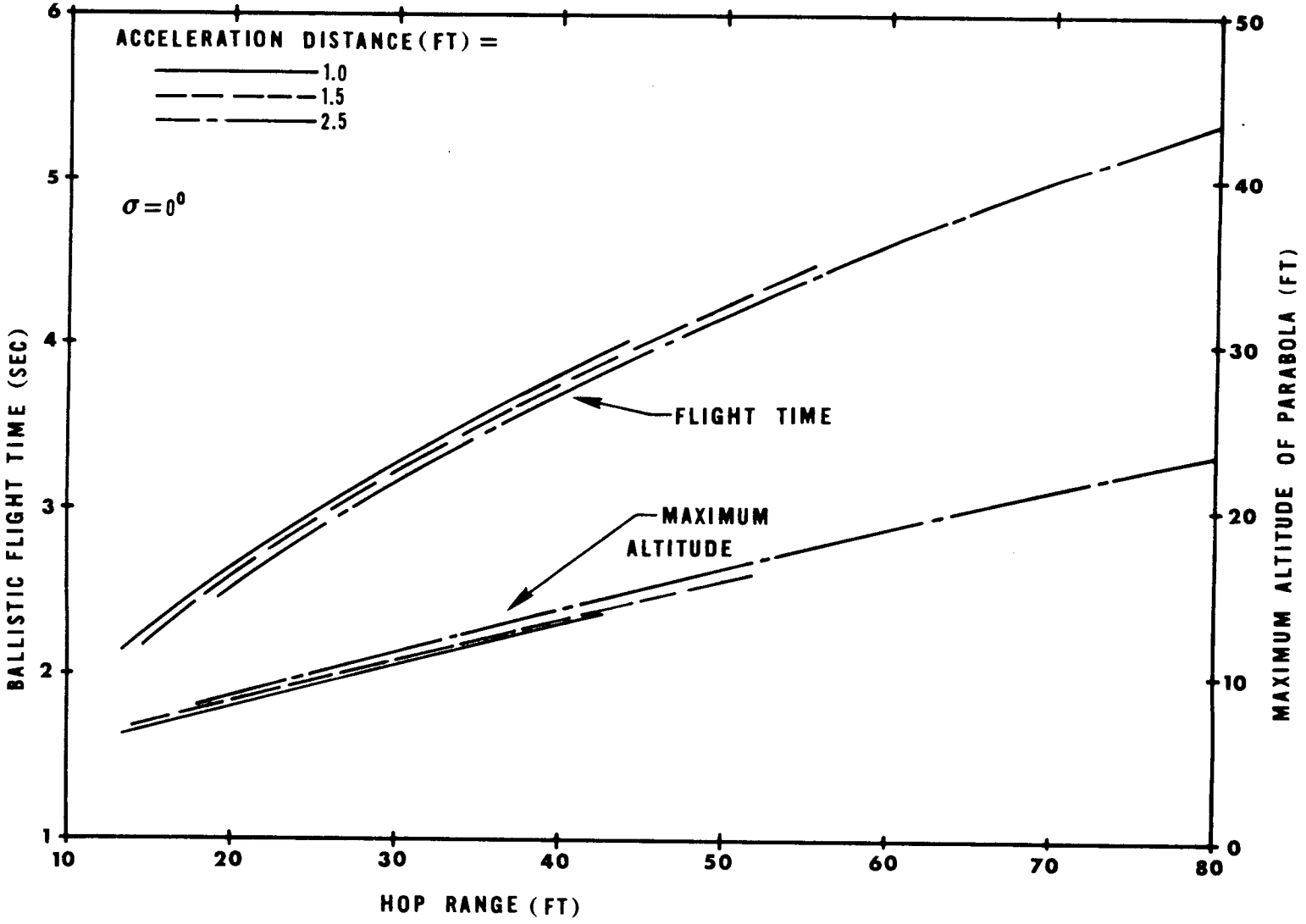

Figure 15. SHOT Hop Ballistic Data

flight time decreases slightly with increasing acceleration distance, because initial pressure must be decreased to maintain a given range and a longer leg decreases ballistic range required to achieve a given range. Furthermore, maximum altitude is indicated to increase slightly with increased acceleration distance for given range, because vehicle center of mass motions with respect to the main body center of mass are not accounted for in this simulation. Therefore, increased leg length adversely affects calculated altitudes for specified range. In fact, maximum altitude should decrease slightly for increased accleration distances.

To estimate an average speed for SHOT, between-hop maneuvering time must be taken into account. This interval is assumed to be 2 seconds. Figure 16 shows two typical acceleration profiles. For the p_o = 100 psi case, range is 43 ft and total hop time is 4.45 sec. Adding the 2 second between-hop interval, this vehicle has an average speed of only 6.7 fps. However, the p_o = 175 psi case corresponds to a range of 76.5 ft in 5.65 sec, giving an average speed of 10 fps (11 km/hr). This is more than twice the safe speed of currently proposed roving vehicles. Furthermore, during a 3 hr sortie, this transporter could travel over 20 miles in about 1,380 hops. A 420 lb (190 kg) one-man flying unit can carry the same payload as SHOT to a radius of only 4.4 miles without refueling.[23] Each such round trip requires an expenditure of 270 lbs of propellants. SHOT can carry this 23 lb payload to 10 miles and return with the expenditure of only 48 lbs of working fluid. A roving vehicle which can perform a 10 mile radius sortie requires several additional hours to make the trip and weighs 3,600 lbs.[17]

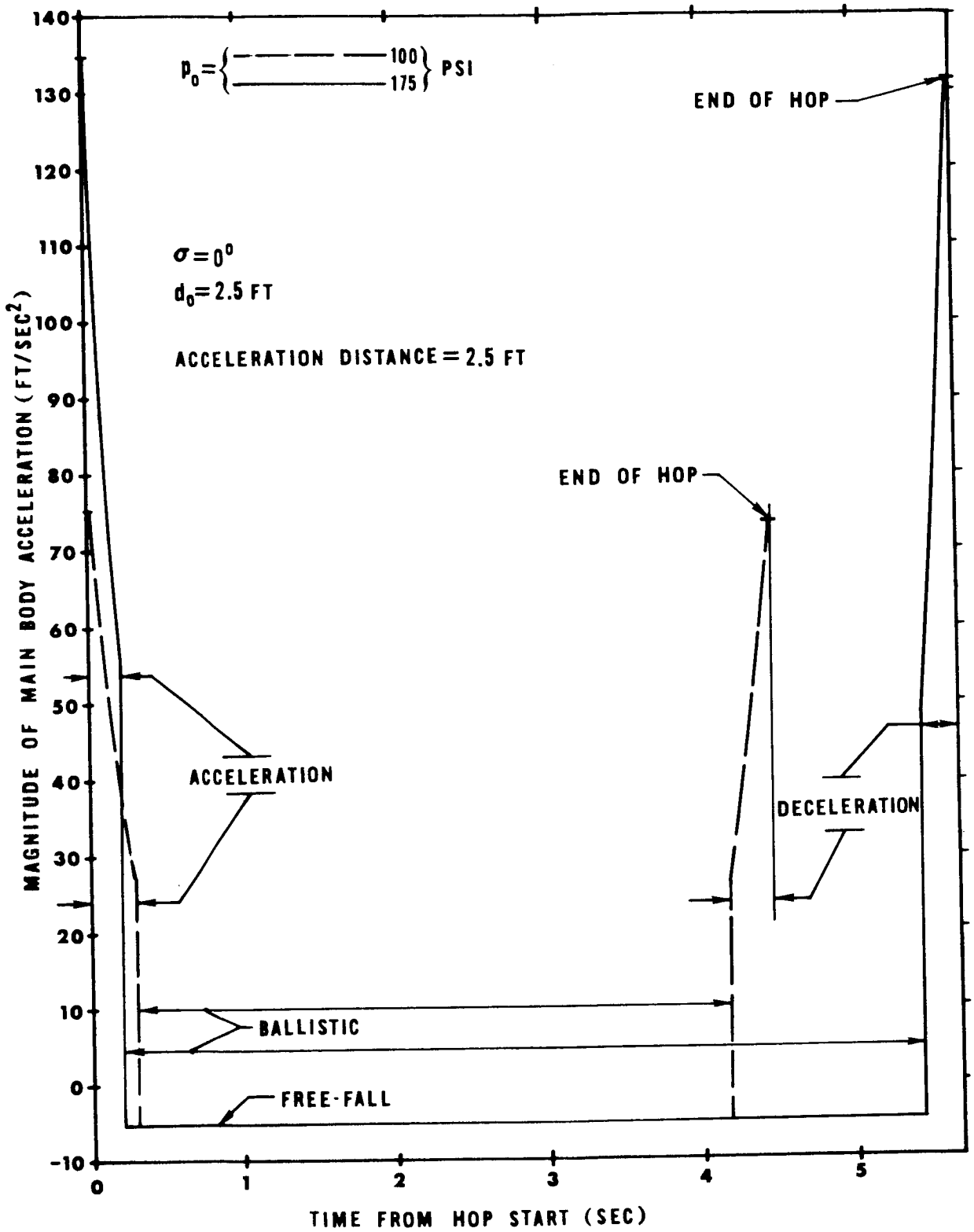

Figure 16. SHOT Hop Profile Examples

Based on the above performance figures and comparisons, it would seem that SHOT vehicles offer significant advantages to lunar explorers.

IV. LUNAR HOPPING LABORATORY (HOLAB)

A. Configuration Description and Operation

The Lunar Hopping Laboratory (HOLAB) is intended to be a sophisticated mobility system with extended range and duration capabilities. Such vehicles might be incorporated into the Apollo Applications Program and into extended lunar base operations. Use of this device would not be possible on early Apollo flights for two reasons. Initial emphasis will be on sending and returning astronauts with a single Saturn V launch vehicle. HOLAB would require a separate launch vehicle for its delivery to the lunar surface. Secondly, development and qualification test time, required for a lunar transporter of this complexity, is probably more than 5 years. Therefore, operational use of this device may not be realized before 1973, beyond the dates of initial Apollo missions. If this design can be shown to have superior performance and growth capabilities and at least equal reliability with respect to currently proposed roving vehicle designs, then HOLAB could replace its massive, slow competitor for lunar applications. Final and optimum configurations will differ from those presented here, but in order to achieve desired objectives, the only practical approach at this point in HOLAB development is to assume a specific model based on current technology and practical considerations.

Figure 17 presents a schematic profile of the entire transporter and a cutaway view of the crew cabin for the configuration studied here. The main body of HOLAB consists of a double pod and all other equipment except the thrust leg and foot. This pod is divided into two cabins which contain power supplies, primary propulsion unit, life support

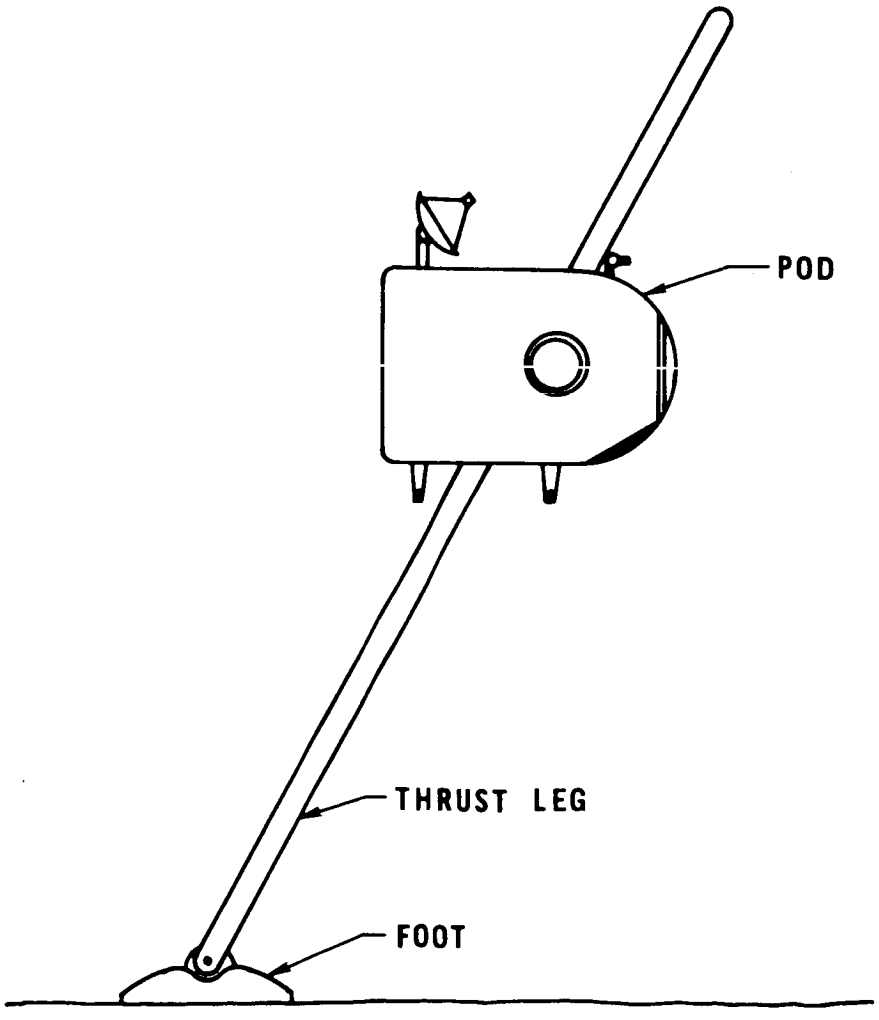

(a) Vehicle configuration

Figure 17. Schematic Profile of HOLAB

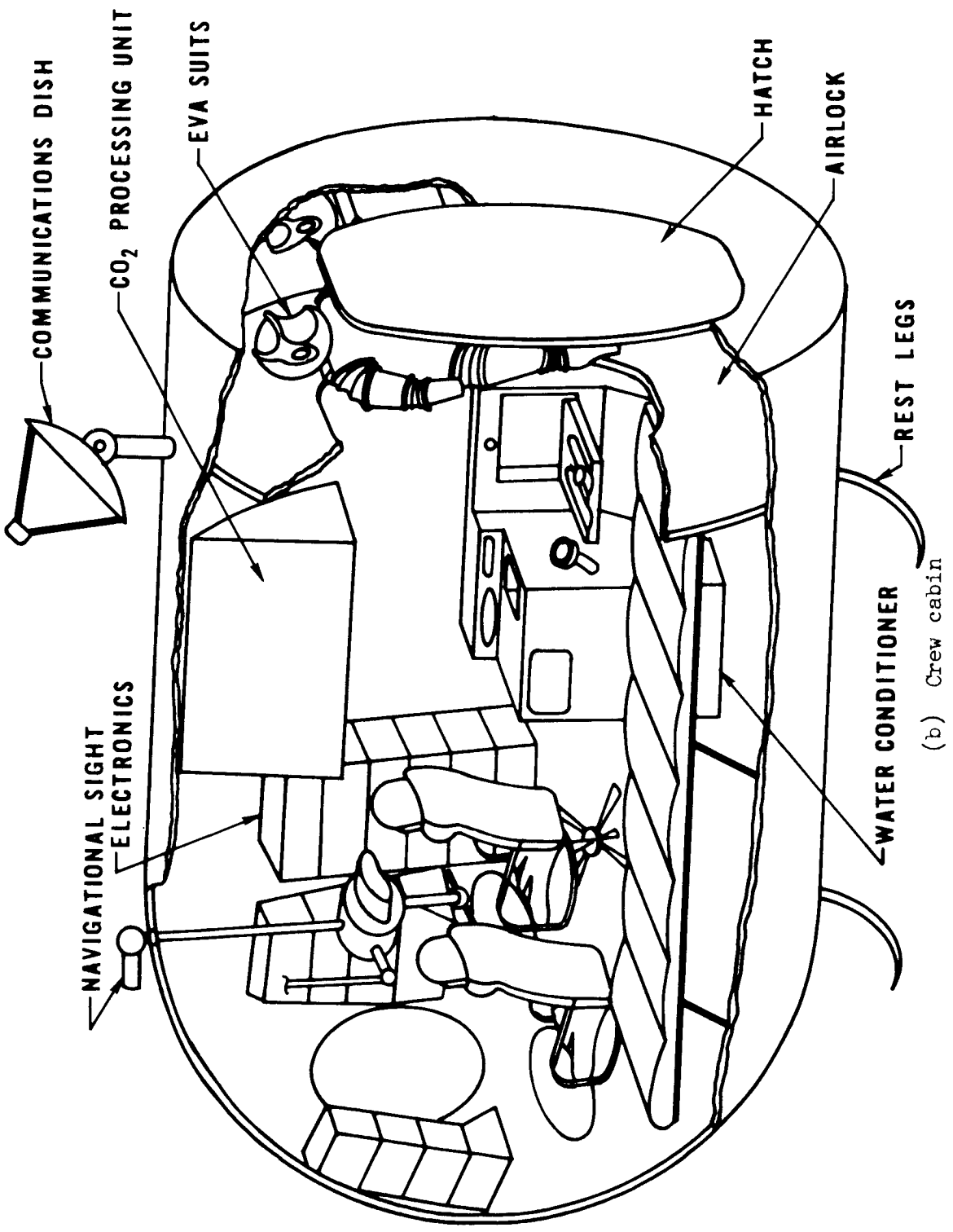

Figure 17. (Continued)

supplies, attitude control and navigational equipment, emergency abort propellant tanks, hop computer and electronics, scientific instruments, and sample box. The crew cabin is designed to accommodate two astronauts for about 10 earth days, thus providing life support, nutrition, and other necessary facilities for this period. Vehicle support during rest intervals is supplied by stabilizing legs. Unlike SHOT, this more sophisticated transporter can change planes and rotate the thrust leg without stopping. The former maneuver is accomplished by rotating the pod center of mass out of the plane of flight during the ballistic phase. Resulting moments during the deceleration and following acceleration phases cause a rotation of the thrust leg such that the plane of motion is changed. The thrust leg continuously rotates about the foot position during deceleration and acceleration into the next hop so that plane changing and leg reorientation occur simultaneously without stopping the vehicle between hops.

HOLAB can travel several hundred feet during each hop. Since the pilot cannot make unaided visual observations of future landing sites and manually determine proper control settings to arrive at these sites, navigational equipment and a hop profile computer are required. The sophistication of this vehicle permits crew orientations to be more favorable with respect to acceleration forces than were permitted on the SHOT configuration. However, acceleration and deceleration phases for this large transporter have durations of the order of 1 second. Figure 3 indicates a very high tolerance to acceleration for all body orientations given in figure 2. Because of this observation and the comfort of the crew, the seat configuration for HOLAB is essentially the

same as that for SHOT. Again imposing the 25% criterion on figure 3 for this design leads to a set of acceleration limit curves for this transporter. Since the pod is assumed to be pitch stabilized relative to an inertial frame, even though not so stabilized about other axes, this set of curves is essentially identical to those in figure 5 for SHOT. Therefore, these curves determine the basic performance envelope for both configurations.

During acceleration and deceleration phases the pilot is not required to perform any functions, because the plane change maneuver and propulsion unit adjustments are executed automatically during these phases. Therefore, normal control switches need not be located in the arm rests, although they must be easily reachable during the ballistic phase. Body movement while hopping should be minimized to keep perturbations at a low level. An emergency abort system is provided for those instances in which sighting errors and other unexpected events occur.

The attitude control system required for this vehicle is somewhat more sophisticated than that for SHOT. Primary function of this system is to insure that vehicle motion follows a sequence prescribed by the analysis of a mathematical model which assumes rigid bodies and idealized interactions without perturbations. This somewhat idealized model allows pod rotations about yaw and roll axes with respect to an inertial reference frame, indicating a high degree of dynamic coupling among degrees of freedom. Therefore, a highly nonlinear controls problem must be solved before developing satisfactory control circuits. This system must provide attitude stabilization during ballistic flight for vehicle and leg reorientation operations. Other disturbance torques will

vary in type and size over the phases of each hop, but are expected to have small magnitudes when compared with normal reorientation maneuvers. During acceleration and deceleration phases, unwanted moments about the foot joint may arise from misalignment, crew movement, and foot slippage. Engagement and disengagement transitions are assumed to contribute, at most, minor perturbing torques. Since the control devices must work with a high degree of coupling among coordinates, a promising candidate is a set of twin-gyro controllers[20], even though complex electronics are associated with these devices. The weight of such a system is, however, expected to be comparable with that of simpler systems[21].

Crew and system functions involved in operating HOLAB may be described as follows. Initially, the pilot and co-pilot enter the crew cabin through the airlock and secure the hatch. This cabin supports a shirt sleeve environment, thus allowing the crew to take off their EVA* suits. The two men then secure themselves in the contour seats and execute a pre-hop check list. Gyros are run up and propulsion cylinder is charged. If the first landing site has not yet been selected, the pilot sets controls for a reconnaissance hop to make appropriate observations. The piston-release button is then pressed and a vertical hop of more than 100 ft is initiated. The ballistic phase of this leap lasts for several seconds, allowing time for navigational readings to be taken. These readings are made by the co-pilot through the use of an optical instrument which is, in some respects, analogous to a submarine periscope. Range, elevation and azimuth are simultaneously adjusted by this astronaut. When he has fixed this instrument on a suitable site a button is pressed and the settings for this site, relative to HOLAB, are

*extravehicular activities

transmitted to a hop profile computer. This calculates required take-off orientation and gas charge in the cylinder to make a hop which takes the vehicle to within a few feet of the sighted landing point. Therefore, immediately after the reconnaissance hop is terminated, vehicle control equipment rotates pod and thrust leg to proper settings and adjusts propulsion parameters automatically. The piston-release button is again pressed and a series of continuous hops begins. During the first travelling ballistic phase other sightings of landing points are made with the navigational instrument, and the computer generates settings for succeeding travelling hops. These settings are transformed into disengagement attitude angle values and rates, and into propulsion adjustments. This maneuver allows the vehicle to move continuously from its present hop into the next hop, because values generated by the computer lead to proper compression of the working gases and rotation of transporter axes so that the next engagement occurs with the pre-calculated transporter orientation angles and velocity components which allow HOLAB to reach the second landing point. This process is repeated until the pilot elects to stop at the end of a given deceleration phase. An effort has been made here to optimize vehicle operation in order to minimize working fluid expenditure for the two-dimensional hop calculations, but continuous hopping with plane changing precludes this type of rigorous optimization. Any required maneuver may have a number of possible combinations of orientations, angular rates, and propulsion adjustments. In any given situation the combination which leads to the lesser fluid expenditure can be thought of as an optimization.

B. Analysis and Simulation of HOLAB Dynamics in Plane Motion

At this early stage of hopping vehicle development, most significant results are obtainable from basic first order approaches to the major problems concerned with the merits of such devices. It is desirable and practical to ignore minor influencing factors when estimating hop performance values whose foundations rest on approximations. This simplification also avoids confusing complications in the analysis. Therefore, immediately essential results, indicating the feasibility of this concept, must be concerned with performance estimates based on realistic assumptions. This type of investigation yields the dynamic sensitivities of these devices to variations of the major parameters.

Hopping motion is primarily 2-dimensional and can become 3-dimensional only during acceleration and deceleration phases. Motions in these phases contribute little to hop range, speed, and profile. Furthermore, differences between 2- and 3-dimensional motions occurring in these phases have very minor effects on single hop performance values. Plane change maneuvers are important to a larger part of the overall exploration mission, because most landing sites of scientific interest lie along non-coplanar paths. Therefore, vehicle performance, as estimated here, is based on a simple 2-dimensional hop model, assuming that no between-hop stopping is required. The ability to perform continuous hops is demonstrated through a simulation of the plane change maneuver in which disengagement orientation and angular rate values are used to determine rotations of the hopping plane. Successful implementation of this maneuver permits a maximum average speed to be achieved. The analysis related to this problem is presented in part C of this chapter.

The 2-dimensional hop simulation model for HOLAB is very similar to that used for SHOT. Figure 18 illustrates this configuration in the acceleration phase. Here the pod is represented by a double sphere of mass M and is assumed to be inertially stabilized and able to apply a controlling torque to a thrust leg of mass m such that only translational motion is allowed between leg and pod. This assures that HOLAB is a one degree of freedom system during acceleration and deceleration phases. Although rotations of the leg are in fact allowed in the general dynamical situation, this restriction of degrees of freedom results in only a very minor deviation between real and estimated hop performance figures, primarily because the thrust force is much greater than variations in gravitational and centrifugal forces resulting from a second degree of freedom.

The terrain model used for HOLAB is identical to that used for SHOT and the launch angle is again given by equation (3-13) and landing angle by expression (3-7). Propulsion is supplied to the thrust leg through a gear train as illustrated in figure 1b. Therefore, thrust is given by equation (2-5) with $r \neq 1$,

$$\mathfrak{F} = \left(\frac{r}{A}\right)^{\gamma-1} \frac{K_o}{(z_p - z_{p_o} + d_o r)^{\gamma}} \qquad (4\text{-}1)$$

with subscripts for the acceleration phase. For this hop model the associated constraints are again holonomic and scleronomous, and the thrust force is a function of z_p alone. Therefore, Lagrange's equation of form (3-1) is applicable to acceleration and deceleration phases:

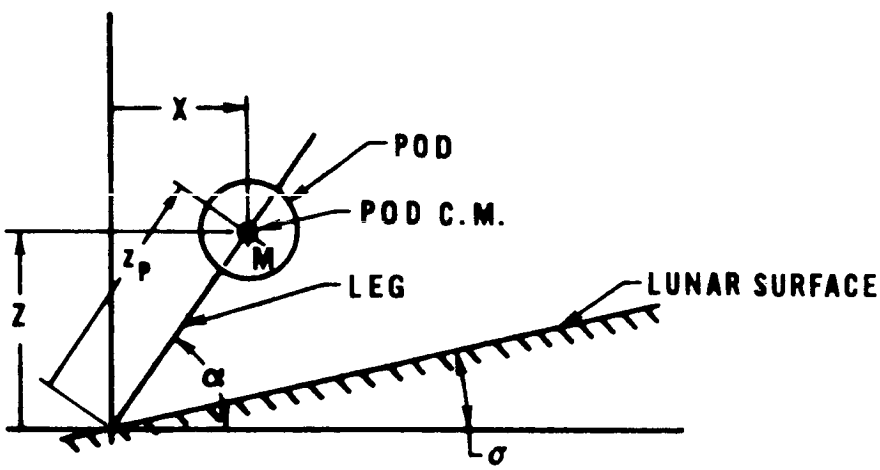

Figure 18. Acceleration Phase Model for HOLAB Hop

$$\frac{d}{dt}\left(\frac{\partial L}{\partial \dot{z}_p}\right) - \frac{\partial L}{\partial z_p} = 0 \ .$$

Kinetic and potential energy terms are analogous to those for SHOT. The resulting differential equations are

$$\ddot{z}_p - \left(\frac{r}{A}\right)^{\gamma-1} \frac{K_o}{M(z_p - z_{p_o} + d_o r)^{\gamma}} = - g \sin \alpha \qquad (4\text{-}2)$$

for acceleration, and

$$\ddot{z}_p - \left(\frac{r}{A}\right)^{\gamma-1} \frac{K_d}{M(z_p - z_{p_d} + d_d r)^{\gamma}} = - g \sin \beta \qquad (4\text{-}3)$$

for deceleration. Engagement and disengagement relations are simply those used for SHOT and are given by expressions (3-3), (3-4), (3-8), and (3-9). Ballistic trajectory equations have already been presented as sets (3-5) and (3-6). Furthermore, computer simulation logic for HOLAB hopping dynamics is given in figure 9. The only basic differences between the two simulation programs occur in differential equations (4-2) and (4-3) and in the input data requirements because $r \neq 1$ for HOLAB. (See Appendix C for the actual program statement listing.) In conclusion, parts B and C of Chapter III serve to explain the operation and structure of both hop simulation programs with the exception that ℓ_M becomes z_p for HOLAB.

C. Analysis and Simulation of Plane Changing Maneuvers

In order to visit interesting locations on the lunar surface, astronauts travelling in HOLAB must have the ability to change their hopping plane at will. Of course, this can be accomplished with

conventional rocket thrusters which operate during ballistic flight. However, this approach to the problem is extremely costly in terms of weight, thereby greatly reducing the inherent payload capability of this vehicle design. Another method of performing plane changes requires that the transporter stop between hops. During this rest period mechanical reorientation of leg and pod takes place. This is a time consuming operation and significantly reduces the average horizontal speed, probably to less than half the ballistic range rate. Since a maximum speed capability is important in all lunar missions, especially for rescue operations, it is quite desirable to perform plane change maneuvers while the vehicle is executing other required hop motions. Furthermore, this should not be done at the expense of payload capacity, i.e., with the use of rockets. Such a technique is possible and is presented in the following paragraphs.

A plane change is accomplished by allowing out-of-plane gravity torques to act on the vehicle during the interval in which the foot is on the surface, i.e., from the beginning of deceleration of one hop to the end of acceleration of the next hop. These torques are created primarily by rotating the pod about the leg axis such that the pod center of mass leaves the hop plane before disengagement occurs. Secondary moments are also produced when the leg is rotated out of this plane. The problem of determining the relationship between a given plane change requirement and the associated disengagement orientation and angular rates is a difficult one, but the dynamics of these maneuvers must be simulated in order to demonstrate the feasibility of this maneuvering technique. A complete study of this problem might include the following

items: sensitivity of plane change performance to variations in initial conditions and configuration parameters, resulting angles and angular rates which must be eliminated by the control system, acceleration profiles experienced by the crew, and maneuver profiles and duration. Demonstration of an actual plane change is presented in part G of the chapter.

Treatment of the plane change problem can be characterized as the description of the motion of a rigid slender rod, sliding pod configuration about a fixed point under the influence of propulsion and gravity. A complete study of this rigid body problem would have three steps: derivation of the appropriate differential equations, setting up of a computer program to solve these equations, and calculating enough data from the initial value solution to effectively determine the required boundary value relationships. These results would be used in an overall plane change computer program with disengagement, deceleration, acceleration, and engagement simulations. This rigid body problem represents only the deceleration/acceleration phases, but it is the "heart" of the plane change maneuver. The slender rod, sliding pod model used in this study is illustrated in figure 19. This configuration is a satisfactory representation of HOLAB for the purposes of dynamic simulations, because the primary concern at this point of pogo transporter development is the determination of gross configuration performance and related parameter sensitivities. The model of figure 19 incorporates these important configuration parameters. Each of the two cabins making up the pod of mass M is represented by a sphere. Both of these have equal mass, size, and uniform density. The connecting mechanism containing a gear box is assumed to be massless. Therefore, the pod accounts for

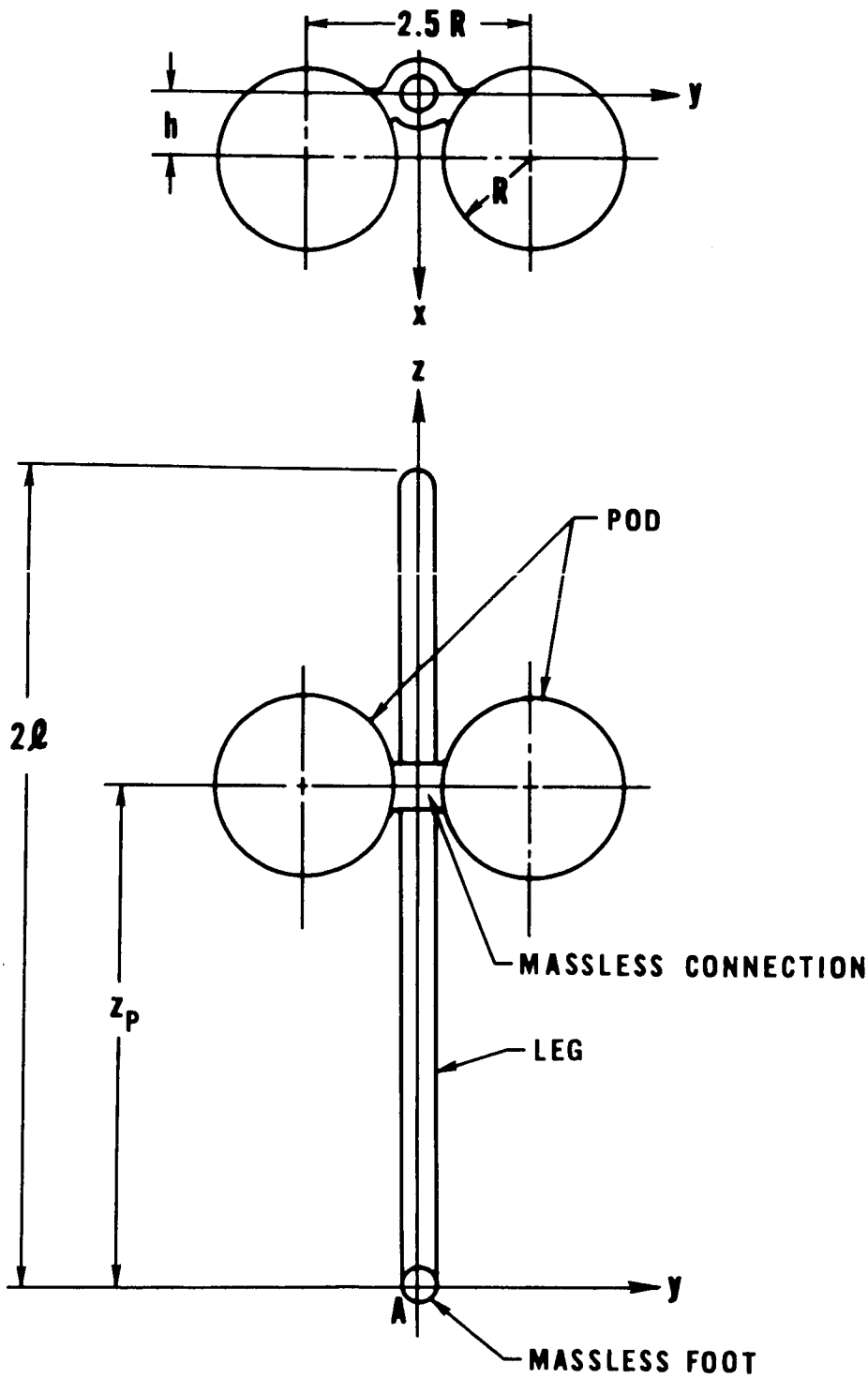

Figure 19. Configuration Model for Plane Change Maneuver Analysis

all vehicle mass except that of thrust leg and foot. This leg is a long thin, homogeneous rod of mass m and length 2ℓ. The foot is considered to be of small mass compared with other components and is ignored in this analysis. Radius of each cabin is R and distance between cabin centers is $2.5R$. Displacement of pod center of mass from the foot is z_p. Pod and leg centers of mass are separated by a distance h, the offset parameter which leads to an efficient plane change maneuver. The x,y,z set of axes are fixed to the vehicle at point A which coincides with the foot joint. Thrust leg symmetry axis coincides with the z-axis. The x-axis is normal to z and is in the plane of pod symmetry which also contains z. Finally, the y-axis is normal to both x and z. The only allowable pod rotations with respect to this body-fixed frame occur about an axis parallel to y and passing through the pod center of mass, i.e., about the line of cabin centers. Such rotations are executed by the control system so that the crew will not be subjected to pitching motions. This means that the cabins are inertially stabilized with respect to pitch, thus, allowing observational data to be taken during reorientation maneuvers and insuring proper acceleration positions for the crew.

Events related to plane changing operations experienced by the crew members may be described as follows. During any given ballistic phase navigational sightings are made. Data relevant to the landing site for the following hop is automatically transmitted to the computer. Then the required plane change to arrive at this site is computed with other parameters for the next hop. This result is again used by the computer, in conjunction with vehicle position and velocity values for the upcoming

disengagement time, to calculate angular orientation and rotation rates necessary at the instant of foot contact such that proper rotation into the following ballistic plane will be achieved. This computer will be constructed on the basis of plane change simulations similar to the one presented here. Values generated by these calculations will be automatically implemented by the control system. This device must also eliminate residual rotations after the following engagement event has occurred.

Although the crew will not be subjected to pitching motions, they will experience roll and yaw rotations because of the constraint relationships between leg and pod. During the actual plane change maneuver, they will feel both linear and angular accelerations. The former type always results in the familiar "eyeballs down" effect, but the latter type may change directions in the course of this maneuver. However, the magnitudes of forces resulting from angular accelerations will be much less than those caused by the propulsion unit. Therefore, human factor considerations related to total acceleration experienced by astronauts need only be concerned with forces produced by thrust. There may, however, be some problems related to astronaut senses and psychological makeup, which should be studied as part of a more comprehensive and sophisticated transporter development program.

The plane change simulation is analyzed in two separate steps and solved as one continuous process with respect to time. During a deceleration and subsequent acceleration phase, vehicle motion is essentially that of a sliding pod on a slender rigid rod, with one end pin-jointed, under the influence of propulsive and gravitational forces. In order to relate a solution of this rigid body problem to hop dynamics, it is

necessary to develop expressions which connect ballistic flight with plane change maneuvers. Once this is accomplished the desired relationships between disengagement conditions and resulting plane change magnitudes can be determined through a study of data obtained by solving the associated initial value problem on a digital computer. Analysis of the problem will follow a logical development. Differential equations of motion for the foot-on-surface time interval are first derived. Then engagement and disengagement conditions are developed. A method of solution and simulation is presented which lends itself to the determination of required plane change relations. Finally, the associated computer program logic is briefly discussed and its operation described.

To initiate the derivation of differential equations for deceleration/acceleration phases with plane changes, the basic configuration of figure 19 is used to obtain a more specialized mathematical model for this application. Figure 20 illustrates this model and defines relevant coordinates. X,Y,Z represent an inertial reference frame. Linear dimensions and body-fixed axes are identical to those defined in figure 19. A rigid body with one point fixed has three rotational degrees of freedom. Since the pod has only translational motion with respect to the leg, influenced by propulsion, this mechanical system has a total of four degrees of freedom.* The absence of pod pitch freedom can be easily treated by assuming the pod moment of inertia about its pitch axis to be

*This system has a fourth degree of freedom because the propulsive force is assumed to be a function of pod displacement z_p. If z_p is independent of coordinates, i.e., $z_p(t)$, then there would only be three degrees of freedom plus a time-dependent constraint.

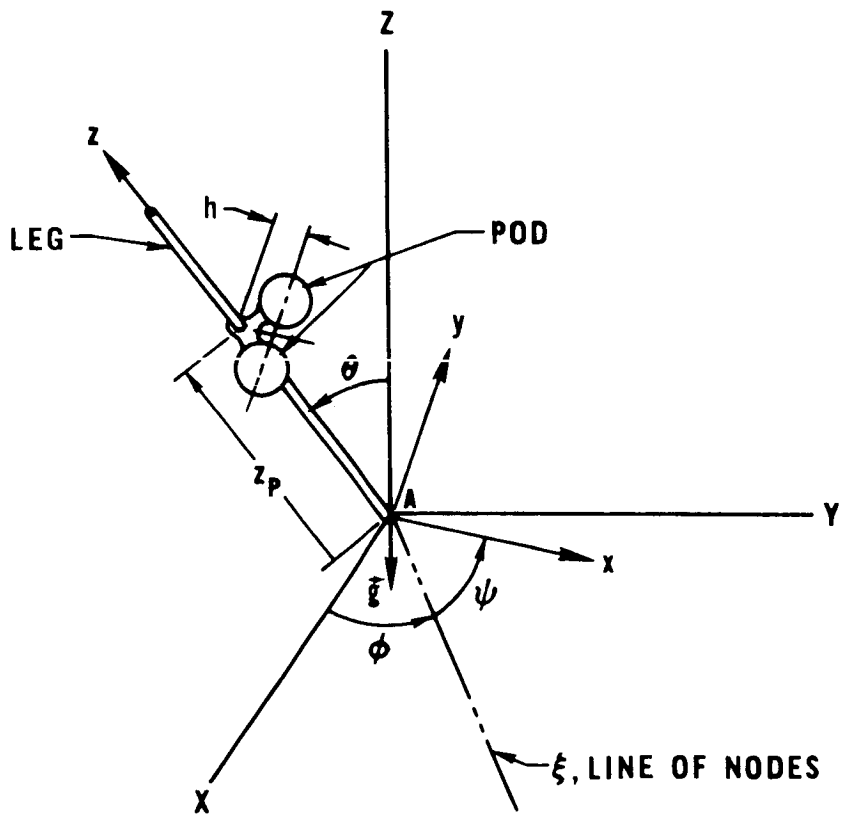

Figure 20. Mathematical Model of HOLAB for Plane Change Analysis

zero, because about this axis, no torque can exist between leg and pod and the pod can have no rotational kinetic energy. In effect, then, the pod moment of inertia about its pitch axis is zero. Generalized coordinates used here consist of the classic Euler angles[22], $\varphi,\theta,$ and $\psi,$ and the pod center of mass displacement z_p. The advantage of using these angles can be demonstrated by considering the rotation of a rigid body, with one point fixed, whose body-fixed axes originally coincided with X,Y, and Z. The reorientation of this body can always be described by applying the Euler angles in proper sequence. First, rotate the body about Z an amount φ. Then rotate it about the line ξ an amount $\theta,$ thus making ξ the line of intersection of XY and xy planes. Finally, rotate the body about its z-axis an amount $\psi,$ ariving at the desired orientation. These three angles completely and uniquely define the angular position of leg and pod. With the addition of z_p the translational position of the pod is defined. Therefore, these four coordinates, $\varphi,\theta,\psi,$ and $z_p,$ fully specify the state of this mechanical system at any instant during deceleration/acceleration phases. The initial dynamical conditions for this part of the plane change problem consist of the four coordinate values and their associated derivative values specified at time t_d^+. For this analysis it is assumed that all masses and moments of inertia are known and h is a constant parameter whose value is critical to efficient performance of this manuver.

Constraints associated with the model of figure 20 are holonomic and time independent, and do no work. Therefore, the Lagrangian formulation may be applied to the derivation of the differential equations of motion. Since gravitational and thrust forces are conservative, i.e., derivable

from a potential function of the coordinates alone, Lagrange's equations take the familiar form

$$\frac{d}{dt}\left(\frac{\partial L}{\partial \dot{q}_i}\right) - \frac{\partial L}{\partial q_i} = 0 \qquad (i = 1,2,3,4) \qquad (4\text{-}4)$$

where $L = T - V$,

T = total kinetic energy of the vehicle,

V = total potential energy of the vehicle including gravitational and propulsive,

and $q_1, q_2, q_3, q_4 = \varphi, \theta, \psi, z_p$, respectively. To construct the desired functional form of the Lagrangian L, it is first necessary to derive expressions for kinetic and potential energies in terms of the generalized coordinates and their derivatives. Applying the theory of rigid body dynamics leads to a general form of system kinetic energy,

$$T = \frac{1}{2} m v_{L_c}^2 + \frac{1}{2} M v_{P_c}^2 + \frac{1}{2} \vec{\omega} \cdot \overleftrightarrow{I}_L \cdot \vec{\omega} + \frac{1}{2} \vec{\omega} \cdot \overleftrightarrow{I}_P \cdot \vec{\omega} \qquad (4\text{-}5)$$

where v_{L_c} and v_{P_c} are the speeds of leg and pod centers of mass, respectively. $\overleftrightarrow{I}_L$ and $\overleftrightarrow{I}_P$ are inertia tensors of leg and pod about their centers of mass, respectively. $\vec{\omega}$ is the angular velocity vector which applies to both leg and pod (except pod pitch) because of their kinematic coupling. In order to avoid a great deal of algebraic manipulation, the body-fixed axes were selected to coincide with principal leg axes, and these are parallel to principal pod axes. Therefore, the leg kinetic energy becomes

$$T_L = \frac{1}{2} m v_{L_c}^2 + \frac{1}{2} \vec{\omega} \cdot \overleftrightarrow{I}_L \cdot \vec{\omega}$$

$$= \frac{1}{2}(I_{L_x} \omega_x^2 + I_{L_y} \omega_y^2 + I_{L_z} \omega_z^2) \qquad (4\text{-}6)$$

where I_{L_x}, I_{L_y}, and I_{L_z} are the leg moments of inertia about the x-, y-, and z-axes at point A, respectively. For the pod, principal axes of minimum moments of inertia pass through its center of mass and are parallel to the x,y,z set of coordinates. This situation permits the pod rotational kinetic energy about its center of mass to be written as

$$\frac{1}{2}\vec{\omega} \cdot \overleftrightarrow{I}_p \cdot \vec{\omega} = \frac{1}{2}(I_{P_{c_x}} \omega_x^2 + I_{P_{c_y}} \omega_y^2 + I_{P_{c_z}} \omega_z^2) \qquad (4\text{-}7)$$

where $I_{P_{c_x}}$, $I_{P_{c_y}}$, and $I_{P_{c_z}}$ are the pod moments of inertia about axes passing through its center of mass, which are parallel to the x,y, and z coordinates, respectively. Since the pod is pitch stabilized, $I_{P_{c_y}}$ is, in effect, zero and will be eliminated in the computer program. Before the total kinetic energy expression can be used in the Lagrangian, all contributing terms must be written as functions of $\varphi, \theta, \psi, z_p, \dot{\varphi}, \dot{\theta}, \dot{\psi}$, and $\dot{z}_P$. Therefore, the three components of angular velocity, ω_x, ω_y, and ω_z, must be expressed in terms of these variables.

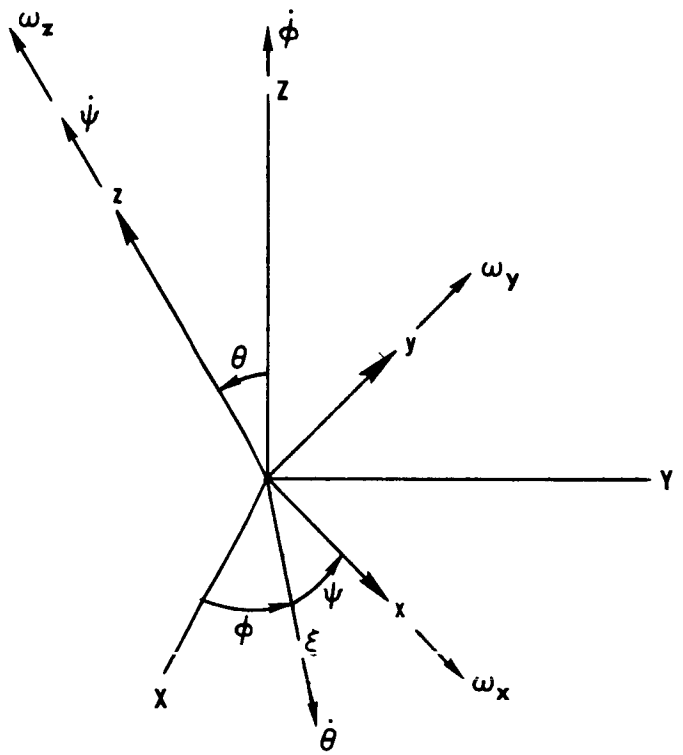

Thus,

$$\left.\begin{aligned} \omega_x &= \dot{\Phi} \sin\theta \sin\psi + \dot{\theta} \cos\psi \\ \omega_y &= \dot{\Phi} \sin\theta \cos\psi - \dot{\theta} \sin\psi \\ \omega_z &= \dot{\Phi} \cos\theta + \dot{\psi} \end{aligned}\right\} \qquad (4\text{-}8a,b,c)$$

In addition, $v_{P_c}^2$ must be written in these variables. Note that $\vec{v}_{P_c}$ is considered to be a vector in the inertial frame, because kinetic energy is measured in this frame. However, the body-fixed and inertial systems are related by an orthogonality transformation because of their common origin. The radius vector $\vec{r}_{P_c}$ is invariant under such a transformation and its magnitude is identical in both frames. Thus, the algebra of deriving a suitable expression for $v_{P_c}^2$ is greatly simplified:

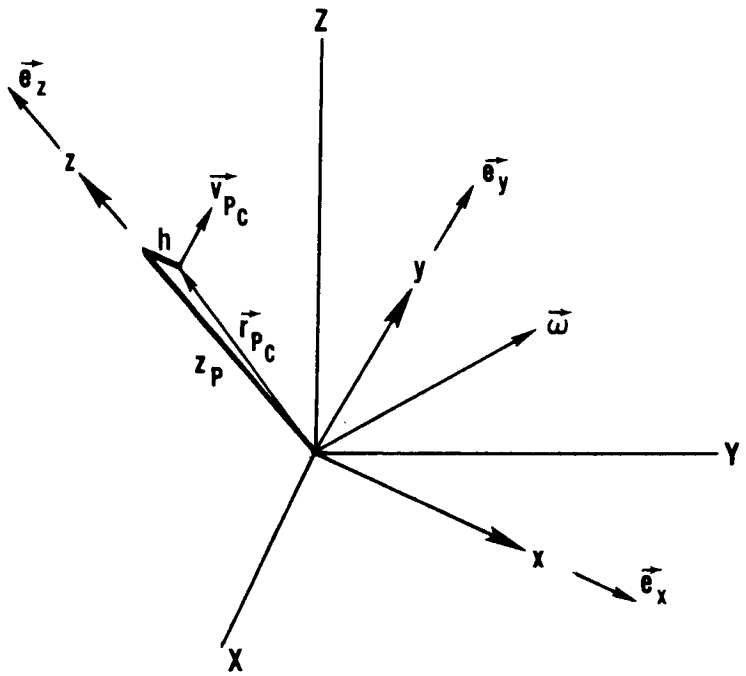

$$\vec{r}_{P_c} = h\vec{e}_x + z_P\vec{e}_z$$

which gives

$$\vec{v}_{P_c} = \dot{\vec{r}}_{P_c} = h\dot{\vec{e}}_x + z_P\dot{\vec{e}}_z + \dot{z}_P\vec{e}_z \ .$$

From the theory of infinitesimal rotations,

$$\dot{\vec{e}}_x = \vec{\omega} \times \vec{e}_x = \omega_z\vec{e}_y - \omega_y\vec{e}_z$$

$$\dot{\vec{e}}_z = \vec{\omega} \times \vec{e}_z = \omega_y\vec{e}_x - \omega_x\vec{e}_y$$

so that

$$\vec{v}_{P_c} = z_P\omega_y\vec{e}_x + (h\omega_z - z_P\omega_x)\vec{e}_y + (\dot{z}_P - h\omega_y)\vec{e}_z \ .$$

Finally,

$$v_{P_c}^2 = \vec{v}_{P_c} \cdot \vec{v}_{P_c} = \dot{z}_P^2 + h^2(\omega_y^2 + \omega_z^2) + z_P^2(\omega_x^2 + \omega_y^2)$$

$$- 2hz_P\omega_x\omega_z - 2h\dot{z}_P\omega_y \ . \qquad (4\text{-}9)$$

Combining expressions (4-5) through (4-9) gives the desired form of kinetic energy. Before writing this equation, it is convenient to introduce some simplifying definitions. To shorten the trigonometric notation in future equations, the following conventions were borrowed from celestial mechanics,

$$\sin\theta = S_\theta, \ \sin\varphi = S_\varphi, \ \sin\psi = S_\psi$$

$$\cos\theta = C_\theta, \ \cos\varphi = C_\varphi, \ \cos\psi = C_\psi .$$

It is possible to combine some constants by letting

$$\left.\begin{aligned} I_{L_x} + I_{P_{c_x}} &= I_x \\ I_{L_y} + I_{P_{c_y}} &= I_y \\ I_{L_z} + I_{P_{c_z}} &= I_z \ . \end{aligned}\right\} \qquad (4\text{-}10a,b,c)$$

Now T becomes

$$T = \tfrac{1}{2} I_x(\dot{\varphi}S_\theta S_\psi + \dot{\theta}C_\psi)^2 + \tfrac{1}{2} I_y(\dot{\varphi}S_\theta C_\psi - \dot{\theta}S_\psi)^2$$

$$+ \tfrac{1}{2} I_z(\dot{\varphi}C_\theta + \dot{\psi})^2 + \tfrac{1}{2} M\{\dot{z}_P^2 + z_P^2(\dot{\varphi}^2 S_\theta^2 + \dot{\theta}^2)$$

$$+ h^2[\dot{\psi}^2 + \dot{\theta}^2 S_\psi^2 + \dot{\varphi}^2(C_\psi^2 + C_\theta^2 S_\psi^2) + 2\dot{\varphi}\dot{\psi}C_\theta - 2\dot{\varphi}\dot{\theta}S_\theta S_\psi C_\psi] \quad \text{(continued)}$$

$$- 2hz_P[\dot{\phi}^2 S_\theta C_\theta S_\psi + \dot{\theta}\dot{\psi}C_\psi + \dot{\phi}\dot{\psi}S_\theta S_\psi + \dot{\phi}\dot{\theta}C_\theta C_\psi]$$

$$+ 2h\dot{z}_P[\dot{\theta}S_\psi - \dot{\phi}S_\theta C_\psi]\} \ . \qquad (4\text{-}11)$$

The total potential energy is immediately obtainable from figure 20,

$$V = mg\ell C_\theta + Mg(z_P C_\theta + hS_\theta S_\psi) + V_p(z_P) \qquad (4\text{-}12)$$

where $V_p(z_P)$ is again the potential energy of propulsion, a function of z_P alone. The thrust force need not be expressed as a potential, since it appears in the differential equations as $\partial V_p/\partial z_P$, the negative of the thrust force between leg and pod given by equation (4-1). That is,

$$\mathfrak{F} = - \frac{\partial V_p}{\partial z_P} \ .$$

For this problem it is assumed that the mass of working fluid in the cylinder is constant throughout the entire plane change maneuver.* Therefore K has a constant value for deceleration and subsequent acceleration. Thus,

$$\mathfrak{F} = \left(\frac{r}{A}\right)^{\gamma-1} \frac{K_d}{(z_P - z_{P_o} + d_d r)^\gamma} \qquad (4\text{-}13)$$

is the thrust expression which applies during the entire simulation of each maneuver computed.

Observations of equations (4-11) and (4-12) indicate that set (4-4) can be written in a somewhat more specific form:

*In the actual case, working fluid properties must be changed during plane change maneuvers to effect changes in hop range. This will probably involve an increase or a decrease of fluid mass in the cylinder.

$$\left.\begin{aligned}
&\frac{d}{dt}\left(\frac{\partial T}{\partial \dot{\phi}}\right) - \frac{\partial T}{\partial \phi} + \frac{\partial V}{\partial \phi} = 0 \\
&\frac{d}{dt}\left(\frac{\partial T}{\partial \dot{\theta}}\right) - \frac{\partial T}{\partial \theta} + \frac{\partial V}{\partial \theta} = 0 \\
&\frac{d}{dt}\left(\frac{\partial T}{\partial \dot{\psi}}\right) - \frac{\partial T}{\partial \psi} + \frac{\partial V}{\partial \psi} = 0 \\
&\frac{d}{dt}\left(\frac{\partial T}{\partial \dot{z}_P}\right) - \frac{\partial T}{\partial z_P} + \frac{\partial V}{\partial z_P} = 0
\end{aligned}\right\} \qquad (4\text{-}14a,b,c,d)$$

Performing the indicated differentiations on expressions (4-11) and (4-12) will transform set (4-14) to the desired relationships between coordinates and their derivatives. Since Ψ is cyclic (does not appear explicitly) in L, partial derivatives with respect to this variable are zero, thus making equation (4-14a) simply

$$\frac{\partial T}{\partial \dot{\phi}} = \text{constant},$$

or

$$\begin{aligned}
&I_x(\dot{\phi}S_\theta^2 S_\psi^2 + \dot{\theta}S_\theta S_\psi C_\psi) + I_y(\dot{\phi}S_\theta^2 C_\psi^2 - \dot{\theta}S_\theta S_\psi C_\psi) \\
&+ I_z(\dot{\phi}C_\theta^2 + \dot{\psi}C_\theta) + M[z_P^2\dot{\phi}S_\theta^2 - h\dot{z}_P S_\theta C_\psi \\
&+ h^2(\dot{\phi}C_\psi^2 + \dot{\phi}C_\theta^2 S_\psi^2 + \dot{\psi}C_\theta - \dot{\theta}S_\theta S_\psi C_\psi) \\
&- hz_P(2\dot{\phi}S_\theta C_\theta S_\psi + \dot{\psi}S_\theta S_\psi + \dot{\theta}C_\theta C_\psi)] \\
&= \text{constant.} \qquad (4\text{-}15a)
\end{aligned}$$

Unfortunately, this type of simplification is not possible for equations (4-14b,c,d) which now become

$$I_x[\ddot{\varphi}S_\theta S_\psi C_\psi + \dot{\varphi}\dot{\psi}S_\theta(C_\psi^2 - S_\psi^2) + \ddot{\theta}C_\psi^2 - 2\dot{\theta}\dot{\psi}S_\psi C_\psi - \dot{\varphi}^2 S_\theta C_\theta S_\psi^2]$$

$$- I_y[\ddot{\varphi}S_\theta S_\psi C_\psi + \dot{\varphi}\dot{\psi}S_\theta(C_\psi^2 - S_\psi^2) - \ddot{\theta}S_\psi^2 - 2\dot{\theta}\dot{\psi}S_\psi C_\psi + \dot{\varphi}^2 S_\theta C_\theta C_\psi^2]$$

$$+ I_z(\dot{\varphi}^2 S_\theta C_\theta + \dot{\theta}\dot{\psi}S_\theta) + M\{2z_P\dot{z}_P\dot{\theta} + z_P^2\ddot{\theta} - z_P^2\dot{\varphi}^2 S_\theta C_\theta$$

$$+ h^2[\ddot{\theta}S_\psi^2 + 2\dot{\theta}\dot{\psi}S_\psi C_\psi - \ddot{\varphi}S_\theta S_\psi C_\psi + 2\dot{\varphi}\dot{\psi}S_\theta S_\psi^2 + \dot{\varphi}^2 S_\theta C_\theta S_\psi^2]$$

$$- hz_P[\ddot{\psi}C_\psi - \dot{\psi}^2 S_\psi + \ddot{\varphi}C_\theta C_\psi - 2\dot{\varphi}\dot{\psi}C_\theta S_\psi + \dot{\varphi}^2 S_\psi(S_\theta^2 - C_\theta^2)]$$

$$+ h\ddot{z}_P S_\psi\} - mg\ell S_\theta + Mg(-z_P S_\theta + hC_\theta S_\psi) = 0 \qquad (4\text{-}15b)$$

$$I_z(\ddot{\varphi}C_\theta - \dot{\varphi}\dot{\theta}S_\theta + \ddot{\psi}) - (I_x - I_y)(\dot{\varphi}^2 S_\theta^2 S_\psi C_\psi - \dot{\varphi}\dot{\theta}S_\theta S_\psi^2 + \dot{\varphi}\dot{\theta}S_\theta C_\psi^2 - \dot{\theta}^2 S_\psi C_\psi)$$

$$+ M\{h^2[\ddot{\psi} + \ddot{\varphi}C_\theta - 2\dot{\varphi}\dot{\theta}S_\theta S_\psi^2 - \dot{\theta}^2 S_\psi C_\psi + \dot{\varphi}^2 S_\theta^2 S_\psi C_\psi]$$

$$- 2h\dot{z}_P(\dot{\theta}C_\psi + \dot{\varphi}S_\theta S_\psi) - hz_P(\ddot{\theta}C_\psi + \ddot{\varphi}S_\theta S_\psi + 2\dot{\varphi}\dot{\theta}C_\theta S_\psi$$

$$- \dot{\varphi}^2 S_\theta C_\theta C_\psi)\} + MghS_\theta C_\psi = 0 \qquad (4\text{-}15c)$$

$$M[\ddot{z}_P - z_P(\dot{\varphi}^2 S_\theta^2 + \dot{\theta}^2) + h(\ddot{\theta}S_\psi - \ddot{\varphi}S_\theta C_\psi + \dot{\varphi}^2 S_\theta C_\theta S_\psi$$

$$+ 2\dot{\theta}\dot{\psi}C_\psi + 2\dot{\varphi}\dot{\psi}S_\theta S_\psi)] + MgC_\theta - \left(\frac{r}{A}\right)^{\gamma-1} \frac{K_d}{(z_P - z_{P_o} + d_d r)^\gamma}$$

$$= 0 \qquad (4\text{-}15d)$$

These four expressions represent the set of second order ordinary differential equations of the plane change maneuver. There is a high

degree of coupling among coordinates. This and the nature of the propulsion law make these equations extremely non-linear in a rather complicated manner. In general, the motion is neither periodic nor of small amplitude, indicating that the only practical method of solution is by application of computer techniques.

Before solving set (4-15) it is necessary to complete the problem description by developing disengagement and engagement relations. When this is accomplished, these differential equations can be solved by simulating motion initiated at time t_d^- and computing coordinates until engagement occurs at time t_e^+. At the instant of disengagement the foot makes contact with the lunar surface, and the pod is simultaneously unlocked and becomes free to move along the leg under the influence of propulsive, gravitational, and acceleration forces. Loss of all momentum and kinetic energy is experienced by the foot. No torque is transmitted between foot and leg during this event. Therefore, angular momentum about point A is conserved, while linear momentum and kinetic energy of leg and foot are partially lost to the lunar surface. Coordinates used for deriving disengagement relations are the instantaneous body-fixed axes x,y,z, which may be thought of as inertially fixed during this event, because no actual displacements occur in this infinitesimal interval. Since the pod is released to move down the leg at time t_d^-, it does not experience any impact effects along the z-direction during this event. No displacement between pod and leg takes place in this instant so that propulsive forces do no work on the pod. Therefore, the velocity along the leg of a point on the pod-leg connection mechanism which also lies on the z-axis will not be affected by disengagement. These conditions can now be expressed in quantitative form. Figure 21 illustrates the appropriate geometric

relationships. Thus, conservation of angular momentum about point A takes the form

$$[(I_{L_{c_x}} + I_{P_{c_x}})\omega_x - m\ell v_{L_{c_y}} - Mz_P v_{P_{c_y}}]\Big|_{t_d^-}^{t_d^+} = 0 \qquad (4\text{-}16a)$$

$$[(I_{L_{c_y}} + I_{P_{c_y}})\omega_y + m\ell v_{L_{c_x}} + M(z_P v_{P_{c_x}} - h v_{P_{c_z}})]\Big|_{t_d^-}^{t_d^+} = 0 \qquad (4\text{-}16b)$$

$$[(I_{L_{c_z}} + I_{P_{c_z}})\omega_z + Mh v_{P_{c_y}}]\Big|_{t_d^-}^{t_d^+} = 0 \qquad (4\text{-}16c)$$

where only the values of the angular and linear velocity components are affected by disengagement. The pod-leg connecting point condition is expressed as

$$v_{P_{c_z}}(t_d^+) = v_{L_{c_z}}(t_d^-) - h\omega_y(t_d^+) \; . \qquad (4\text{-}17)$$

To completely determine disengagement effects on the state of this vehicle, kinematic relations between leg and pod are needed. At t_d^-

$$\left.\begin{aligned} v_{L_{c_x}} &= v_{P_{c_x}} - (z_P - \ell)\omega_y \\ v_{L_{c_y}} &= v_{P_{c_y}} - h\omega_z + (z_P - \ell)\omega_x \\ v_{L_{c_z}} &= v_{P_{c_z}} + h\omega_y \end{aligned}\right\} \qquad (4\text{-}18a,b,c)$$

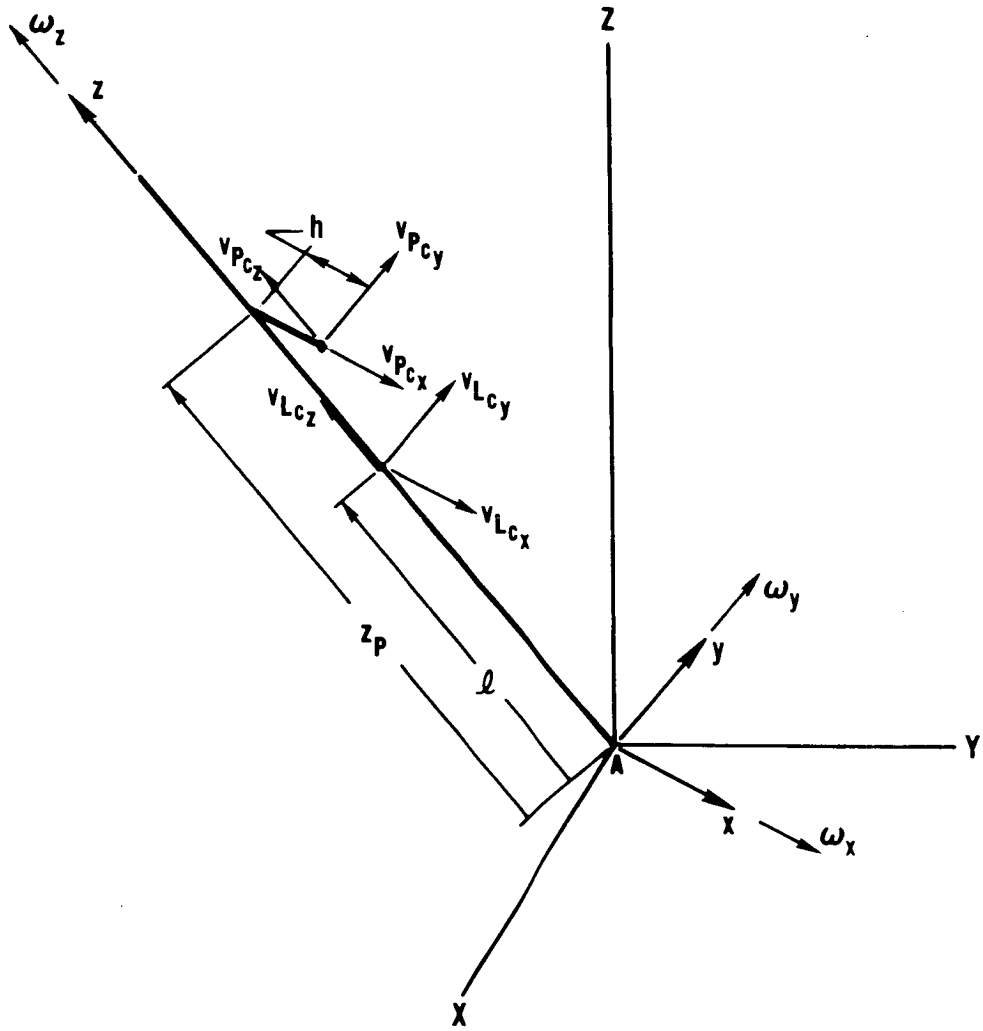

Figure 21. Nomenclature for Transition Analysis

and at t_d^+

$$\left.\begin{aligned} v_{L_{c_x}} &= \ell\omega_y \\ v_{L_{c_y}} &= -\ell\omega_x \\ v_{P_{c_x}} &= z_P\omega_y \\ v_{P_{c_y}} &= h\omega_z - z_P\omega_x \end{aligned}\right\} \qquad (4\text{-}19a,b,c,d)$$

Given angular and linear velocity components of the leg or pod at time t_d^-, then conditions (4-16) through (4-19) uniquely determine all required values of the state of the vehicle at time t_d^+.

At the end of the plane change maneuver, engagement occurs. Since pod and leg engage in a perfectly inelastic manner over an infinitesimal time interval, no displacements or outside impulses take place with this event. Therefore, vehicle angular and linear momentum are conserved through engagement. By applying this principle to the components of angular and linear momentum, in addition to appropriate kinematic relations, initial ballistic coordinate and velocity values at t_e^+ can be uniquely determined from conditions at t_e^-, the end of the plane change maneuver. Here again body-fixed coordinates are used. Equating angular momentum components about point A at times t_e^- and t_e^+ gives

$$\left[(I_{L_{c_x}} + I_{P_{c_x}})\omega_x - m\ell v_{L_{c_y}} - Mz_P v_{P_{c_y}}\right]\Big|_{t_e^-}^{t_e^+} = 0 \qquad (4\text{-}20a)$$

$$\left[\left(I_{L_{c_y}} + I_{P_{c_y}}\right)\omega_y + m\ell v_{L_{c_x}} + M\left(z_P v_{P_{c_x}} - h v_{P_{c_z}}\right)\right]\Big|_{t_e^-}^{t_e^+} = 0 \qquad (4\text{-}20b)$$

$$\left[\left(I_{L_{c_z}} + I_{P_{c_z}}\right)\omega_z + M h v_{P_{c_y}}\right]\Big|_{t_e^-}^{t_e^+} = 0 \qquad (4\text{-}20c)$$

which are similar to set (4-16), but apply at engagement rather than disengagement. Equating linear momentum components at times t_e^- and t_e^+ gives

$$\left.\begin{aligned} \left[m v_{L_{c_x}} + M v_{P_{c_x}}\right]\Big|_{t_e^-}^{t_e^+} &= 0 \\ \left[m v_{L_{c_y}} + M v_{P_{c_y}}\right]\Big|_{t_e^-}^{t_e^+} &= 0 \\ M v_{P_{c_z}}\Big|_{t_e^-} &= \left[m v_{L_{c_z}} + M v_{P_{c_z}}\right]\Big|_{t_e^+} . \end{aligned}\right\} \qquad (4\text{-}21a,b,c)$$

In addition to their use at disengagement, kinematic relations, (4-19) apply at t_e^- and (4-18) apply at t_e^+. Therefore, expressions (4-18) through (4-21) uniquely determine engagement events.

The primary objective of this analysis is to relate an initial ballistic flight plane to a new flight plane. These planes are defined by the vehicle center of mass velocity components which lie in the XY-plane. In order to simulate the entire maneuver in a realistic manner, the inertial velocity components $\dot{X}_{cm}(t_d^-)$ and $\dot{Z}_{cm}(t_d^-)$ are assumed to be

given in addition to $z_p(t_d^-)$ and the Euler angles and their rates at time t_d^-. These vehicle center of mass velocities must be converted to body-fixed coordinates before disengagement conditions can be calculated. This is done by performing an orthogonality transformation on these components,

$$\begin{pmatrix} v_{cm_x} \\ v_{cm_y} \\ v_{cm_z} \end{pmatrix} = \mathbf{A} \begin{pmatrix} \dot{X}_{cm} \\ \dot{Y}_{cm} \\ \dot{Z}_{cm} \end{pmatrix} \tag{4-22}$$

where $\mathbf{A}$ is the orthogonal matrix,

$$\mathbf{A} = \begin{pmatrix} C_\psi C_\varphi - C_\theta S_\varphi S_\psi & C_\psi S_\varphi + C_\theta C_\varphi S_\psi & S_\psi S_\theta \\ -S_\psi C_\varphi - C_\theta S_\varphi C_\psi & -S_\psi S_\varphi + C_\theta C_\varphi C_\psi & C_\psi S_\theta \\ S_\theta S_\varphi & -S_\theta C_\varphi & C_\theta \end{pmatrix} . \tag{4-23}$$

In expanded form relation (4-22) gives

$$\begin{Bmatrix} v_{cm_x} \\ v_{cm_y} \\ v_{cm_z} \end{Bmatrix} = \begin{Bmatrix} C_\psi C_\varphi - C_\theta S_\varphi S_\psi \\ -S_\psi C_\varphi - C_\theta S_\varphi C_\psi \\ S_\theta S_\varphi \end{Bmatrix} \dot{X}_{cm} + \begin{Bmatrix} C_\psi S_\varphi + C_\theta C_\varphi S_\psi \\ -S_\psi S_\varphi + C_\theta C_\varphi C_\psi \\ -S_\theta C_\varphi \end{Bmatrix} \dot{Y}_{cm}$$

$$+ \begin{Bmatrix} S_\psi S_\theta \\ C_\psi S_\theta \\ C_\theta \end{Bmatrix} \dot{Z}_{cm} . \tag{4-24a,b,c}$$

These velocity components are related to the leg center of mass components through plane geometric considerations:

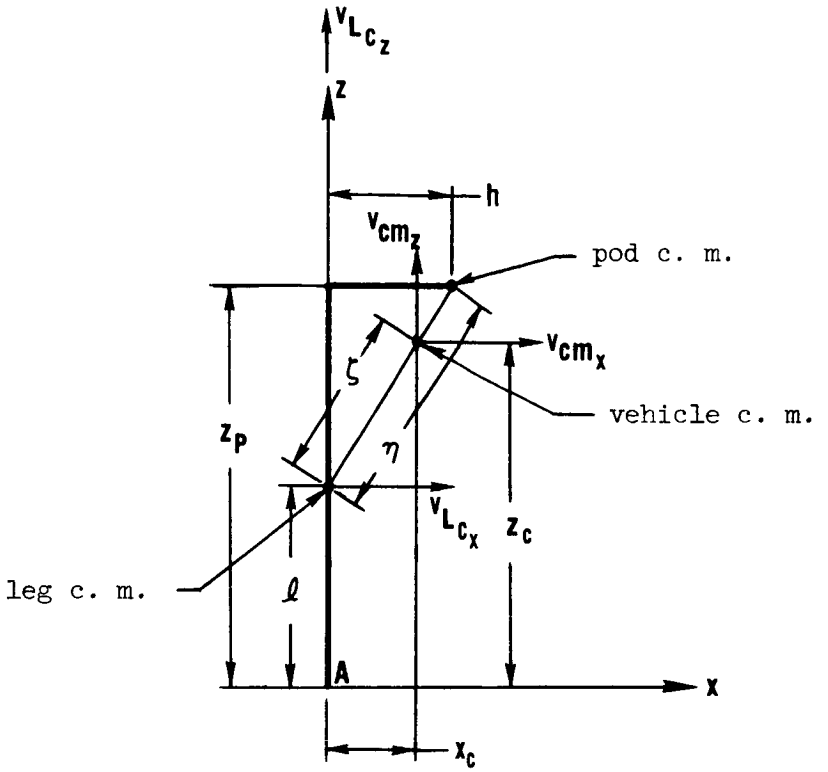

$$\left.\begin{aligned} v_{L_{c_y}} &= v_{cm_x} - (z_c - \ell)\omega_y \\ v_{L_{c_y}} &= v_{cm_y} - x_c\omega_z + (z_c - \ell)\omega_x \\ v_{L_{c_y}} &= v_{cm_z} + x_c\omega_y \end{aligned}\right\} \qquad (4\text{-}25a,b,c)$$

where

$$\left.\begin{aligned} x_c &= \frac{\zeta}{\eta}\, h \\ z_c &= \frac{\zeta}{\eta}\,(z_P - \ell) + \ell \\ \zeta &= \frac{M\eta}{M+m} \\ \eta &= \sqrt{(z_P - \ell)^2 + h^2} \end{aligned}\right\} \qquad (4\text{-}26a,b,c)$$

Values given by set (4-25) are used with disengagement conditions to convert vehicle center of mass components into leg and pod components.

At the subsequent engagement event values of vehicle center of mass velocity components must be obtained in terms of the inertial frame. First, these components are calculated in body-fixed coordinates from components of the leg center of mass velocity at time t_e^+ by rearranging set (4-25):

$$\left.\begin{aligned} v_{cm_x} &= v_{L_{c_x}} + (z_c - \ell)\omega_x \\ v_{cm_y} &= v_{L_{c_y}} + x_c\omega_z - (z_c - \ell)\omega_x \\ v_{cm_z} &= v_{L_{c_z}} - x_c\omega_y \ . \end{aligned}\right\} \qquad (4\text{-}27a,b,c)$$

Then an orthogonal transformation to inertial coordinates is performed,

$$\begin{pmatrix} \dot{X}_{cm} \\ \dot{Y}_{cm} \\ \dot{Z}_{cm} \end{pmatrix} = \mathbf{A}^{-1} \begin{pmatrix} v_{cm_x} \\ v_{cm_y} \\ v_{cm_z} \end{pmatrix} \ . \qquad (4\text{-}28)$$

Expressions (4-28) can be expanded to get a form similar to set (4-24). Noting a characteristic property of othrogonal matrices,

$$\mathbf{A}^{-1} = \mathbf{A}^T \ ,$$

leads to

$$\begin{Bmatrix} \dot{X}_{cm} \\ \dot{Y}_{cm} \\ \dot{Z}_{cm} \end{Bmatrix} = \begin{Bmatrix} C_\psi C_\varphi - C_\theta S_\varphi S_\psi \\ C_\psi S_\varphi + C_\theta C_\varphi S_\psi \\ S_\theta S_\psi \end{Bmatrix} v_{cm_x} + \begin{Bmatrix} -S_\psi C_\varphi - C_\theta S_\varphi C_\psi \\ -S_\psi S_\varphi + C_\theta C_\varphi C_\psi \\ S_\theta C_\psi \end{Bmatrix} v_{cm_y}$$

$$+ \begin{Bmatrix} S_\theta S_\varphi \\ -S_\theta C_\varphi \\ C_\theta \end{Bmatrix} v_{cm_z} . \qquad (4\text{-}29a,b,c)$$

The expressions presented to this point completely describe the dynamical state of this vehicle model in the interval $t_d^- \leq t \leq t_e^+$. Given the vehicle center of mass velocity components and angular state with z_p at time t_d^-, then these relationships can be solved to generate the entire state of vehicle dynamics at time t_e^+.

Solution and simulation of plane change conditions and equations are performed by a digital computer program. Resulting data is used to develop relations between final and initial ballistic flight planes. Various elements of the dynamical analysis have been presented above, and the method of combining these into a complete simulation can now be discussed. The actual program is listed in Appendix C. Here, programming methods, logic, and objectives are briefly presented. A schematic flow chart of computational events is illustrated in figure 22. A program run is initiated with the input of data containing configuration and mass distribution information, ballistic approach, linear and angular velocity components related to vehicle center of mass, propulsion and working fluid specifications, and the gravity constant. These values are immediately printed out. Then this data is operated on as indicated

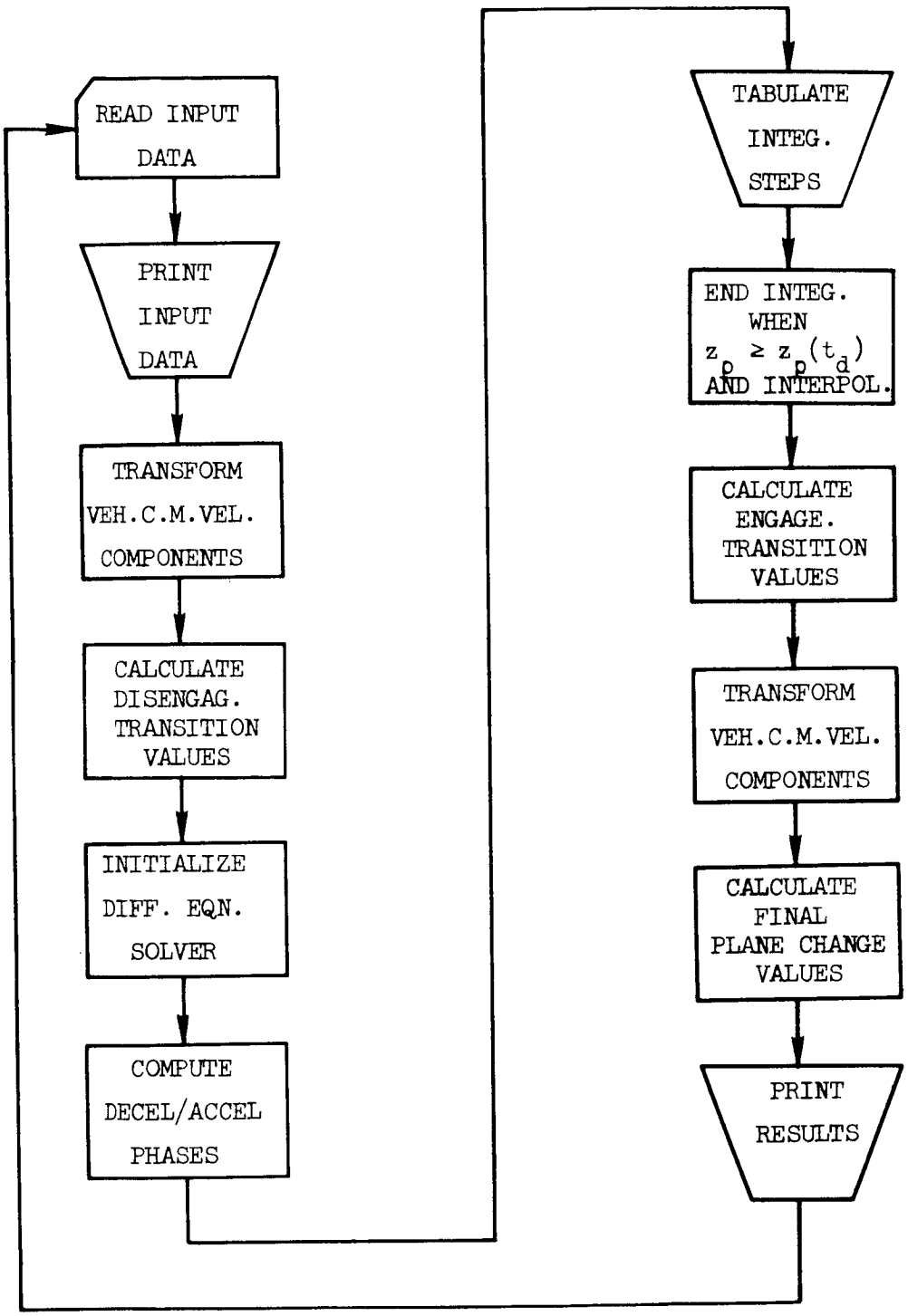

Figure 22. Schematic Flow Chart for HOLAB Plane Change Simulation

by relations (4-24) and (4-25) to obtain velocity components of the leg center of mass in body-fixed coordinates. These are used with expressions (4-16) through (4-19) to calculate disengagement conditions at t_d^+. Numerical integration of differential equations (4-15) can then commence. However, these expressions are much more complicated than those encountered in the two-dimensional hop programs. Setting these equations into a library subroutine for integrating differential equations requires an extensive amount of algebraic manipulation. The amount of work required to construct a program which handles these equations in their present form is even greater. Therefore, the method developed in Appendix B for quickly formulating these expressions for computer solution is employed in this section of the simulation program.

The rigid body problem considered here falls within the class of conservative systems discussed in this appendix. Differential equations (4-15) can be expressed in form (B-10b) with $n = 4$. Coefficients a_{ij} and factors C_i are defined by equations (B-12) and (B-11b), respectively. Applying these to the case at hand, with indices 1,2,3, and 4 referring to φ,θ,ψ, and z_P, respectively, gives the following results:

$$a_{11} = (I_x S_\psi^2 + I_y C_\psi^2) S_\theta^2 + I_z C_\theta^2 + M[h^2 C_\psi^2 + (z_P S_\theta - h C_\theta S_\psi)^2] \qquad (4\text{-}30a)$$

$$a_{12} = a_{21} = (I_x - I_y) S_\theta S_\psi C_\psi - MhC_\psi (hS_\theta S_\psi + z_P C_\theta) \qquad (4\text{-}30b)$$

$$a_{13} = a_{31} = I_z C_\theta + Mh(hC_\theta - z_P S_\theta S_\psi) \qquad (4\text{-}30c)$$

$$a_{14} = a_{41} = - MhS_\theta C_\psi \qquad (4\text{-}30d)$$

$$a_{22} = I_x C_\psi^2 + I_y S_\psi^2 + M(z_P^2 + h^2 S_\psi^2) \qquad (4\text{-}30e)$$

$$a_{23} = a_{32} = - Mhz_P C_\psi \qquad (4\text{-}30f)$$

$$a_{24} = a_{42} = MhS_\psi \qquad (4\text{-}30g)$$

$$a_{33} = I_z + Mh^2 \qquad (4\text{-}30h)$$

$$a_{34} = a_{43} = 0 \qquad (4\text{-}30i)$$

$$a_{44} = M \, . \qquad (4\text{-}30j)$$

To eliminate second order terms let

$$\begin{Bmatrix} \dot{\varphi} \\ \dot{\theta} \\ \dot{\psi} \\ \dot{z}_P \end{Bmatrix} = \begin{Bmatrix} \omega_\varphi \\ \omega_\theta \\ \omega_\psi \\ v_z \end{Bmatrix} \qquad (4\text{-}31a,b,c,d)$$

then the C_i factors become

$$C_1 = (I_x - I_y)[\omega_\theta \omega_\psi S_\theta (S_\psi^2 - C_\psi^2) - S_\psi C_\psi (2\omega_\varphi \omega_\psi S_\theta^2 + \omega_\theta^2 C_\theta)]$$

$$-2(I_x S_\psi^2 + I_y C_\psi^2)\omega_\varphi \omega_\theta S_\theta C_\theta + I_z \omega_\theta S_\theta (2\omega_\varphi C_\theta + \omega_\psi)$$

$$-M\{2z_P \omega_\varphi S_\theta (v_z S_\theta + z_P \omega_\theta C_\theta) - 2hv_z C_\theta (\omega_\varphi S_\theta S_\psi + \omega_\theta C_\psi)$$

$$- h^2[2\omega_\varphi (\omega_\psi S_\theta C_\psi + \omega_\theta C_\theta S_\psi) S_\theta S_\psi + 2\omega_\theta \omega_\psi S_\theta C_\psi^2 - \omega_\theta^2 C_\theta S_\psi C_\psi]$$

$$- hz_P[2\omega_\varphi \omega_\theta S_\psi (C_\theta^2 - S_\theta^2) + S_\theta C_\psi (2\omega_\varphi \omega_\psi C_\theta + \omega_\psi^2 - \omega_\theta^2)\} \qquad (4\text{-}32a)$$

$$C_2 = (I_x - I_y)\omega_\psi[2\omega_\theta S_\psi C_\psi - \omega_\varphi S_\theta(C_\psi^2 - S_\psi^2)]$$

$$+ (I_x S_\psi^2 + I_y C_\psi^2)\omega_\varphi^2 S_\theta C_\theta - I_z \omega_\varphi S_\theta(\omega_\varphi C_\theta + \omega_\psi)$$

$$- M\{z_P(2v_z\omega_\theta - z_P\omega_\varphi^2 S_\theta C_\theta)$$

$$+ h^2 S_\psi[2\omega_\psi(\omega_\theta C_\psi + \omega_\varphi S_\theta S_\psi) + \omega_\varphi^2 S_\theta C_\theta S_\psi]$$

$$+ hz_P S_\psi[(\omega_\psi + \omega_\varphi C_\theta)^2 - \omega_\varphi^2 S_\theta^2]\}$$

$$+ mg\ell S_\theta + Mg(z_P S_\theta - hC_\theta S_\psi) \qquad (4\text{-}32b)$$

$$C_3 = (I_x - I_y)[S_\psi C_\psi(\omega_\varphi^2 S_\theta^2 - \omega_\theta^2) + \omega_\varphi\omega_\theta S_\theta(C_\psi^2 - S_\psi^2)]$$

$$+ I_z\omega_\varphi\omega_\theta S_\theta - M\{h^2 S_\psi[C_\psi(\omega_\varphi S_\theta^2 - \omega_\theta^2) - 2\omega_\varphi\omega_\theta S_\theta S_\psi]$$

$$- 2hv_z(\omega_\theta C_\psi + \omega_\varphi S_\theta S_\psi) - hz_P\omega_\varphi C_\theta(2\omega_\theta S_\psi - \omega_\varphi S_\theta C_\psi)\}$$

$$- MghS_\theta C_\psi \qquad (4\text{-}32c)$$

$$C_4 = M\{z_P(\omega_\varphi^2 S_\theta^2 + \omega_\theta^2) - h[\omega_\varphi S_\theta S_\psi(\omega_\varphi C_\theta + 2\omega_\psi) + 2\omega_\theta\omega_\psi C_\psi]\}$$

$$- MgC_\theta + \left(\frac{r}{A}\right)^{\gamma-1} \frac{Kd}{(z_P - z_{P_o} + d_d r)^\gamma} \qquad (4\text{-}32d)$$

Equations (B-10b) represent a set of simultaneous linear equations in the $\dot{u}_j$'s($\dot{\omega}_\varphi, \dot{\omega}_\theta, \dot{\omega}_\psi$, and $\dot{v}_z$ here), which must be solved for these quantities before integration can be performed by a library subroutine. This algebraic operation can be accomplished as part of the computer program at each step of integration or manually before setting up the program. Here,

this was done by the latter method using Cramer's Rule. This procedure gives

$$\begin{Bmatrix} \dot{\omega}_\varphi \\ \dot{\omega}_\theta \\ \dot{\omega}_\psi \\ \dot{v}_z \end{Bmatrix} = \frac{\begin{Bmatrix} \Delta_\varphi \\ \Delta_\theta \\ \Delta_\psi \\ \Delta_z \end{Bmatrix}}{\Delta} \qquad (4\text{-}33a,b,c,d)$$

where Δ is the determinant of the coefficient matrix $[a_{ij}]$ and Δ_φ, Δ_θ, Δ_ψ, and Δ_z are determinants obtained by replacing the column of the coefficients of $\dot{\omega}_\varphi, \dot{\omega}_\theta, \dot{\omega}_\psi$, and $\dot{v}_z$ of set (B-10b), respectively, in $[a_{ij}]$ by the column $\{C_1 \quad C_2 \quad C_3 \quad C_4\}$. When expanded, these determinants take the forms

$$\begin{aligned} \Delta = {} & a_{14}[2a_{24}(a_{12}a_{33} - a_{13}a_{23}) + a_{14}(a_{23}^2 - a_{22}a_{33})] \\ & + a_{24}^2(a_{13}^2 - a_{11}a_{33}) + a_{44}[a_{22}(a_{11}a_{33} - a_{13}^2) \\ & + a_{23}(2a_{12}a_{13} - a_{11}a_{23}) - a_{12}^2 a_{33}] \end{aligned} \qquad (4\text{-}34a)$$

$$\begin{aligned} \Delta_\varphi = {} & a_{14}[C_4(a_{23}^2 - a_{22}a_{33}) + a_{24}(C_2 a_{33} - a_{23}C_3)] \\ & + a_{24}[C_4(a_{12}a_{33} - a_{13}a_{23}) + a_{24}(a_{13}C_3 - C_1 a_{33})] \\ & + a_{44}[C_1(a_{22}a_{33} - a_{23}^2) + C_2(a_{13}a_{23} - a_{12}a_{33}) \\ & + C_3(a_{12}a_{23} - a_{13}a_{22})] \end{aligned} \qquad (4\text{-}34b)$$

$$\Delta_\theta = a_{14}[a_{14}(a_{23}C_3 - C_2a_{33}) + C_4(a_{12}a_{33} - a_{13}a_{23})]$$
$$+ a_{24}[C_4(a_{13}^2 - a_{11}a_{33}) + a_{14}(C_1a_{33} - a_{13}C_3)]$$
$$+ a_{44}[a_{11}(C_2a_{33} - a_{23}C_3) + a_{12}(a_{13}C_3 - C_1a_{33})$$
$$+ a_{13}(C_1a_{23} - a_{13}C_2)] \qquad (4\text{-}34c)$$

$$\Delta_\psi = a_{14}[C_2(a_{14}a_{23} - a_{13}a_{24}) + C_3(a_{12}a_{24} - a_{14}a_{22})$$
$$+ C_4(a_{13}a_{22} - a_{12}a_{23})] + a_{24}[C_1(a_{13}a_{24} - a_{14}a_{23})$$
$$+ C_3(a_{12}a_{14} - a_{11}a_{24}) + C_4(a_{11}a_{23} - a_{12}a_{13})]$$
$$+ a_{44}[C_1(a_{12}a_{23} - a_{13}a_{22}) + C_3(a_{11}a_{22} - a_{12}^2)$$
$$+ C_2(a_{12}a_{13} - a_{11}a_{23})] \qquad (4\text{-}34d)$$

$$\Delta_z = a_{14}[C_1(a_{23}^2 - a_{22}a_{33}) + C_3(a_{13}a_{22} - a_{12}a_{23})$$
$$+ C_2(a_{12}a_{33} - a_{13}a_{23})] + a_{24}[C_1(a_{12}a_{33} - a_{13}a_{23})$$
$$+ C_3(a_{11}a_{23} - a_{12}a_{13}) + C_2(a_{13}^2 - a_{11}a_{33})]$$
$$+ C_4[a_{22}(a_{11}a_{33} - a_{13}^2) + a_{23}(2a_{12}a_{13} - a_{11}a_{23})$$
$$- a_{12}^2a_{33}] \qquad (4\text{-}34e)$$

Sets (4-31) and (4-33) represent the eight differential equations in proper form to be integrated by a library subroutine. Although the above expressions are complicated, they represent a minimum of effort with

respect to setting this problem into a computer program. Expressions (4-34) are coded directly into the function subroutine which supports this differential equation routine, so that values of $\dot{\omega}_\varphi$ $\dot{\omega}_\theta$ $\dot{\omega}_\psi$, and $\dot{v}_z$ are computed from relations (4-33) at each step of the integration.

The plane change maneuver simulation continues until engagement displacement is reached. This is assumed to be equal to the initial displacement, i.e.,

$$z_P(t_e) = z_P(t_d) \ .$$

Then conditions (4-20) and (4-21) are applied to determine linear and angular velocity components of leg and pod in body-fixed coordinates at time t_e^+. Expressions (4-27) are then used to convert these into velocity components of the vehicle center of mass. Finally, set (4-29) gives these last velocities in terms of inertial directions X,Y, and Z. Since these are the initial ballistic flight velocity components of the new hop, the resulting plane of interest is defined by the angle δ, calculated from

$$\delta(t_e^+) = \tan^{-1}\left(\frac{\dot{Y}_{cm}(t_e^+)}{\dot{X}_{cm}(t_e^+)}\right) \ . \qquad (4\text{-}35)$$

The desired value of plane change is just the difference of this and the initial plane angle $\delta(t_e^-)$. A plane change is demonstrated and related results presented and discussed in part G of this chapter.

D. Applications of Interest

It is not intended to restrict applications of the pogo transporter to lunar operations, because the concept offers inherent advantages in any low gravity, low atmosphere environment where there is a sufficiently substantial surface to support vehicle interactions. However, immediate and near-future manned-space objectives are focused on exploration of the Moon. Consequently, HOLAB applications related to lunar missions are of primary concern. First operational models could be used in connection with the more sophisticated missions of the Apollo Applications Program in the late 1970's. Extended surface explorations to areas of scientific interest require mobility systems which provide sufficient life support facilities, payload capacity, and versatility to perform satisfactorily in the harsh lunar environment. At the same time, this vehicle must be light enough to be carried by existing launch vehicles. The inherent ability of HOLAB to fulfill these requirements within technological constraints of weight and size will be at least partially confirmed by the results obtained from dynamical models studied here and presented in parts F and G of this chapter.

Specific uses of this transporter include extended reconnaissance and cartographic vehicle, scientific data collection equipment carrier, and human factors research laboratory. As with SHOT, reconnaissance information may be obtained by two techniques. A vertical hop can be executed for the sole purpose of making terrain observations, while attaining a maximum altitude and ballistic flight time for given propulsion parameter values. This type of data is also collected during normal travelling hops. Scientific data collection is the primary

objective of these trips. With HOLAB any particular site of interest may be visited for an extended period of probing and placing of sensing devices. In addition to these applications, several interesting and essential experiments can be performed to learn more about low gravity and isolation effects over extended periods on human beings. Of particular importance is the extent to which crew abilities are impaired with respect to control and navigational functions.

Beyond the Apollo Applications Program are the extended-stay lunar bases. HOLAB may fulfill several requirements here, including those uses mentioned above in addition to "crew bus" and "lunar ambulance" applications. Since HOLAB is fast and has a large payload capacity, it is ideal for transferring several crew members between shelters and for emergency rescue and equipment delivery operations.

E. Parameter Values for Hop and Plane Change Calculations

Both HOLAB simulation programs require several parameter and initial condition values as input data. Most important parameters are related to vehicle mass distribution, primary propulsion unit and working fluid, and lunar environment. For the plane change program, initial dynamical conditions consist of vehicle orientation angles and velocity components at time t_d^-, which are varied with each of the computer runs in order to determine relations between successive ballistic flight planes. The two-dimensional hop program requires only cylinder pressure and surface slope as the primary variables. Nevertheless, many other parameters related to vehicle configuration may be changed, at will, in either program. Those parameters which are considered constants for this study are evaluated in the following paragraphs.

The hop simulation program requires only two mass distribution values, m and M. Several quantities in addition to these two are needed for the other program because of the associated rigid body problem. Pod mass, M is dependent upon the individual components making up the cabins. Table 3 displays the various items contained in an operating pod. This list gives a conservative estimate of each component mass, obtained from a survey of studies on lunar transporter vehicles[17] and preliminary design and performance calculations. The crew consists of two astronauts, each weighing about 175 earth pounds without their vacuum suits. Life support equipment and supplies for a 10 earth day duration have a total mass of about 18 slugs. The extravehicular activity (EVA) suits each include a PLSS of mass 2.1 slugs. Total mass of both suits is estimated at 5 slugs. The primary propulsion unit is basically a simple device. It is bigger than that used on SHOT and has a gear train, increasing its mass to an estimated 6 slugs. A 500 km (1.65×10^6 ft.) excursion with hops of 500 ft. in range would require a total of 3300 hops. If hydrazine is the working fluid, its decomposition products have a molecular weight of 18. Assuming a displacement volume of 4.5 cu. ft. at the beginning of the acceleration phase, then for a maximum pressure of 450 psi and temperature of 600°F, the mass of gas in the cylinder during each hop is estimated at .0099 slugs. If the working fluid has a utilization efficiency of 85%, then 15% of this fluid will be lost in the course of the excursion. Therefore, about 49 slugs of hydrazine will be required. A promising candidate for power source is the fuel cell. Its estimated mass, including electronics, of 15 slugs seems large, but this device must supply all electrical power to control, navigation, communications, and propulsion systems for a period

Table 3. Estimated HOLAB Pod Mass Contributers

Item	Mass (slugs)
Crew (2)	11
Life support	18
EVA suits	5
Propulsion and gear train	6
Working fluid (3300 hops)	49
Power and electronics	15
Navigation and computer	5
Communications	3
Structure	60
Control system	17
Payload	10
Between-hop support	4
Abort system	26
Total	229

of 10 days. Navigational sighting and computing equipment can be made using miniature circuit techniques and its estimated mass is 5 slugs. Communications will be required between HOLAB and its logistics vehicle. Associated equipment is estimated to have a mass of 3 slugs. Pod structure must withstand accelerations of several earth g's, and its mass is about 60 slugs. The control system for HOLAB is much more complicated than that of SHOT because of the highly non-linear nature of coordinate coupling associated with plane change maneuvers. However, maximum disturbance torques will occur during ballistic flight in reorientation operations. Three sets of turn gyro stabilizers of mass 5 slugs each should be sufficient for this requirement. Total control system mass, including electronics, is estimated at 17 slugs. A payload of 10 slugs, including scientific instruments and sensing devices, is permitted here. Between-hop supports for rest periods are very simple because plane changing is done without the use of surface stabilizing mechanisms. Therefore, these have an estimated mass of 4 slugs. It is assumed that a nominal HOLAB abort maneuver requires a velocity change of 10 fps. If the propellant has a specific impulse of 200 sec and the vehicle mass is 250 slugs, then each abort requires 0.4 slug of propellant. Assuming 2% of the hops require abort maneuvers, the total abort system mass is about 26 slugs. Finally, the total pod mass is 229 slugs (3340 kg).

Leg mass can be estimated on the basis of buckling instability. Assuming a thin aluminum tube of circular cross-section exposed to a maximum critical load (including 1.5 safety factor) of 55,000 earth pounds at a maximum length of 20 ft, then Euler's load formula for pinned ends gives a minimum leg radius of 5" for a wall thickness of 0.1". Therefore,

a 36 ft. long leg has a mass of less than 5 slugs. With other structural supports and gear teeth added, the leg mass is estimated at 8 slugs.

There are six principal moments of inertia required by the plane change program. From figure 19 it is apparent that five have the forms

$$I_{L_{c_x}} = I_{L_{c_y}} = \frac{1}{3} m \ell^2$$

$$I_{L_{c_y}} = 0$$

$$I_{P_{c_x}} = I_{P_{c_z}} = 1.96\ MR^2.$$

Inertial pitch stabilization of the pod leads to

$$I_{P_{c_y}} = 0 \quad .$$

Configuration parameters ℓ and R have the values 18 ft and 5 ft, respectively. The offset parameter, h will be varied with successive computer runs. Therefore,

$$I_{L_{c_x}} = I_{L_{c_y}} = 864 \text{ slug-ft}^2$$

$$I_{P_{c_x}} = I_{P_{c_z}} = 11{,}200 \text{ slug-ft}^2$$

At this point in HOLAB development, propulsion and working fluid parameters can only be selected on an arbitrary basis. For this study assume

$A = 3$ sq. ft

$r = 5$

$\gamma = 1.2$

Other related parameters will vary with program runs.

There are only two environmental factors required in the hop simulation and one for the other program. The value of gravitational acceleration is needed by both, and is 5.31 fpss. To simulate hops, the linear slope angle is required, but this will be varied to determine its effect on performance. Parameters not mentioned in this part are discussed in parts F and G of this chapter.

It should be noted that an actual detailed design effort for such a complex vehicle will introduce many more variables related to transporter performance. These must be considered and their affects on design and operation determined. For example, a parametric analysis of the control system should be performed early in the development program. Mass of the flight version of this device will be affected by vehicle dynamics, navigational equipment accuracy and crew functions. Vehicle mass and performance will, in turn, be affected by the control system mass and operation.

F. Results of Hop Simulations

Two-dimensional hop simulations of HOLAB were carried out using the following parameter values as constants:

$M = 229$ slugs

$m = 8$ slugs

$z_{P_o} = 6$ ft.

$d_o = 1.5$ ft

$r = 5.0$

$A = 3.0$ ft.^{2}

$\gamma = 1.20$

$g = 5.31$ ft/sec^2

The combination of values for A, r, and d_o were selected on the basis of maintaining reasonable propulsion unit dimensions and operating pressures. The following table indicates ranges of varied parameters for this study:

parameter	range
pod accel. distance, $z_{P_e} - z_{P_o}$	10 to 25 ft
initial cyl. pressure, p_o	170 to 425 psi
linear surface slope, σ	-10^o to 10^o

Here again, p_o is a critical quantity, but is more useful when transformed to initial acceleration magnitude. Equation (4-2), evaluated at $t = t_o$ $(z_P = z_{P_o})$ gives

$$\ddot{z}_{P_o} = \frac{p_o A}{Mr} - g \sin \alpha \ .$$

As in Chapter III, noting that $\alpha = \pi/4 + \sigma/2$, and inserting constant parameter values where possible, initial acceleration becomes

$$\ddot{z}_{P_o}(\text{fpss}) = 0.377\ p_o(\text{psi}) - 3.76 \qquad (4\text{-}36)$$

within 0.34 fpss. Therefore, peak acceleration can again be considered a function of p_o only, for values of σ used here. Performance data presented here are expressed as functions of maximum acceleration, $\ddot{z}_{P_o}$ given by formula (4-36).

Figure 23 illustrates the relationship of acceleration duration to peak acceleration for various values of pod acceleration distance which correspond to configurations studied here. Comparison with figure 5 indicates the acceleration levels used for HOLAB simulation are well below tolerable limits of human discomfort. Figure 24 presents hop range data for four pod acceleration distances and three linear slope angles. Curves tend to support expected sensitivities. For given peak acceleration, range is decreased by increasing slope angles and vice versa. In addition, range is increased for longer acceleration distances, because the pressure force acts through a larger displacement. This increases initial ballistic velocity and, therefore, range. Figure 25 illustrates this effect more descriptively. Here again, these curves approach asymptotes because gas pressure does not fall to zero until the limit of infinite expansion is reached.

Figure 26 illustrates the relationship of range to ballistic flight time and maximum altitude of flight for various pod acceleration distances. These curves will be useful in determining opportunities for making navigational and reconnaissance observations. These curves have

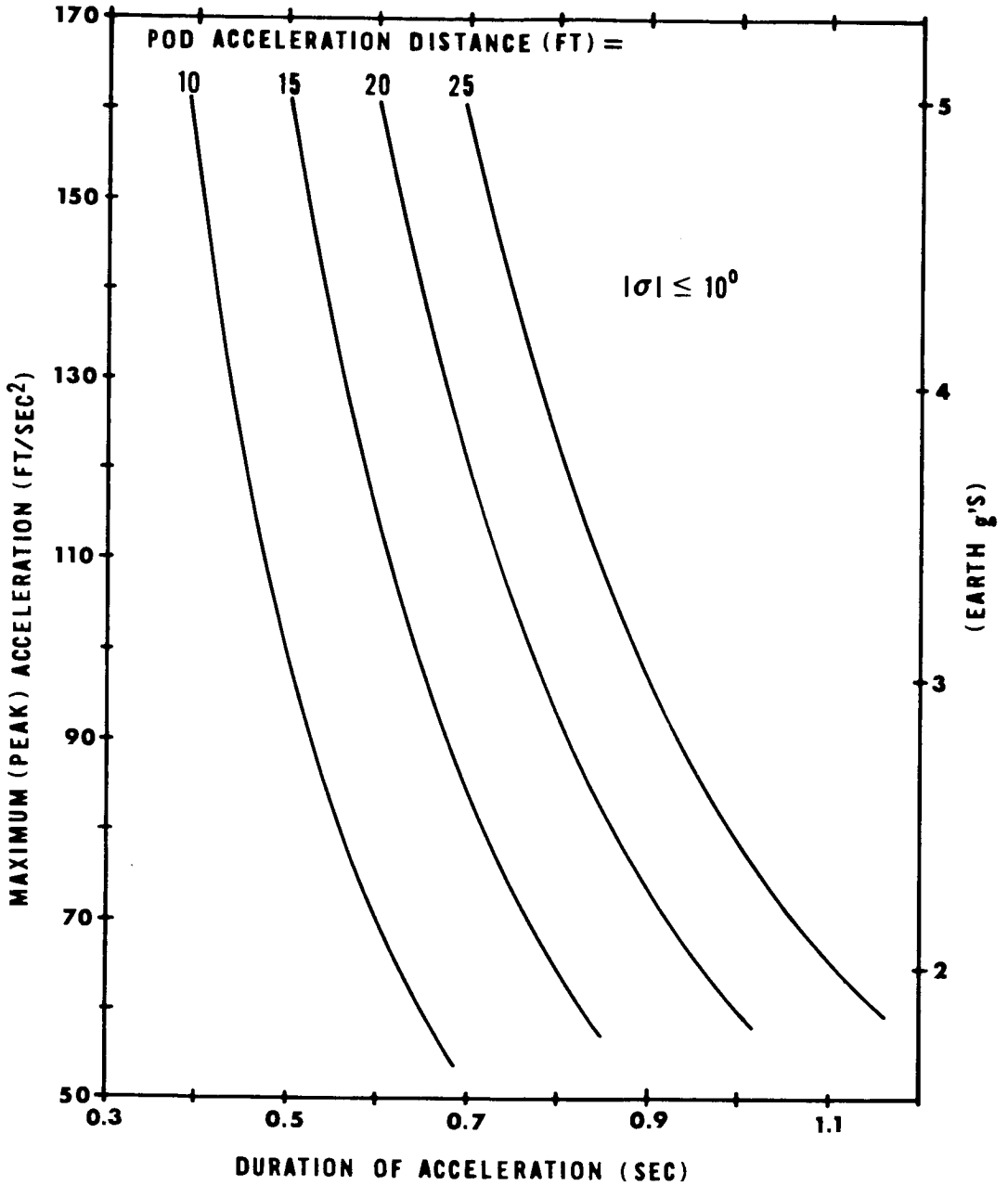

Figure 23. HOLAB Acceleration vs. Duration

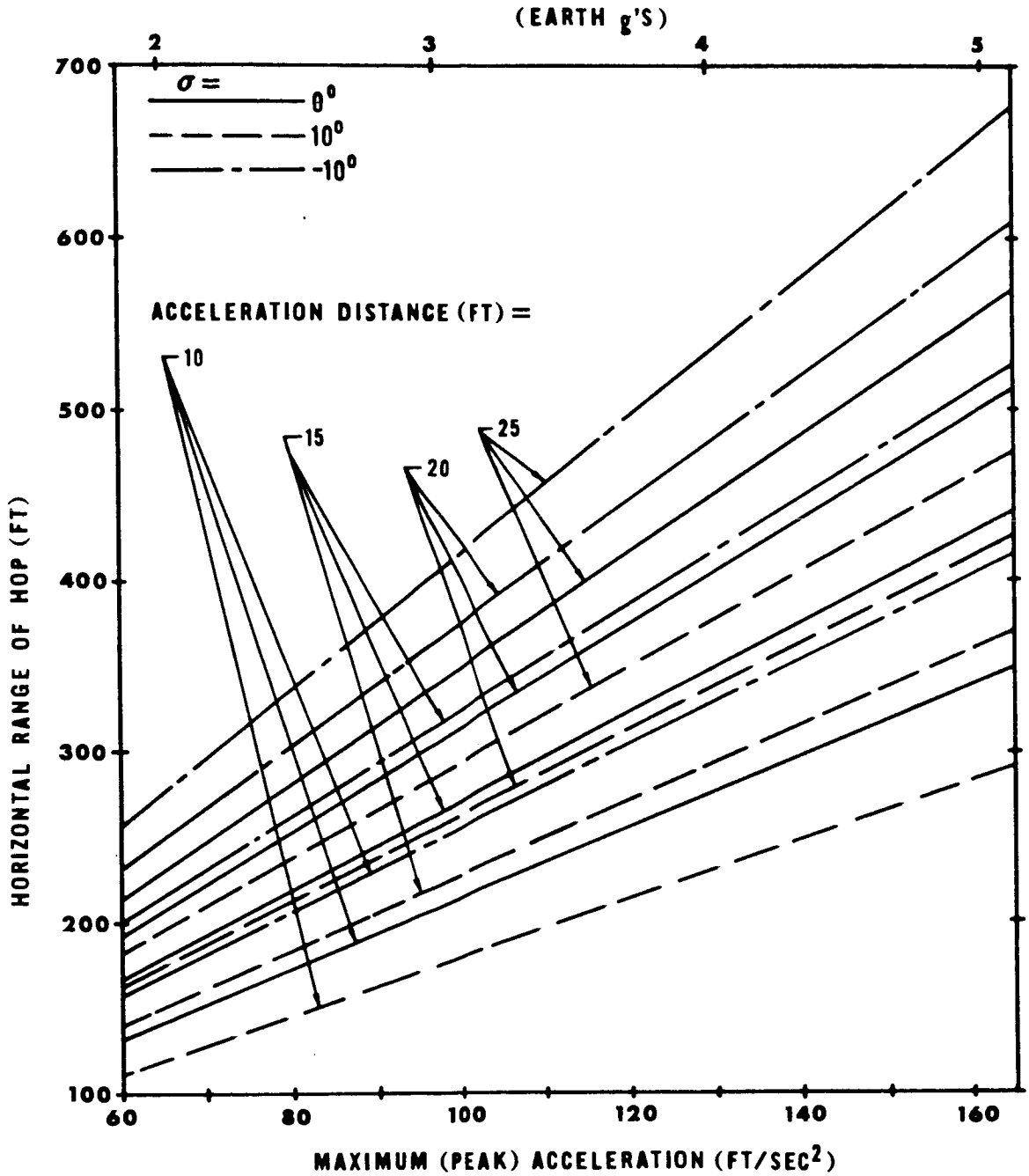

Figure 24. HOLAB Hop Data with Acceleration Distance and Surface Slope as Parameters

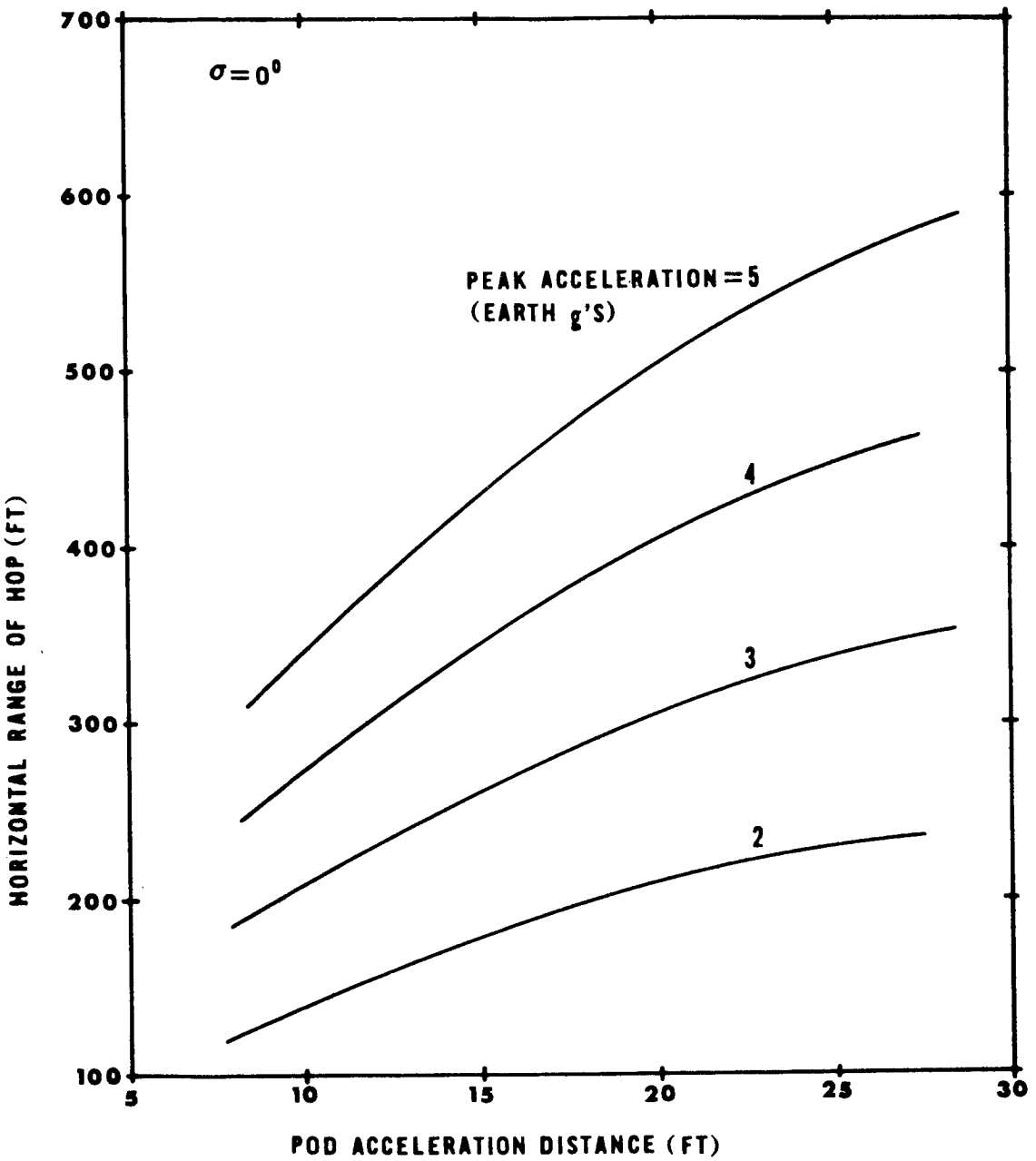

Figure 25. HOLAB Hop Data with Peak Acceleration as the Parameter

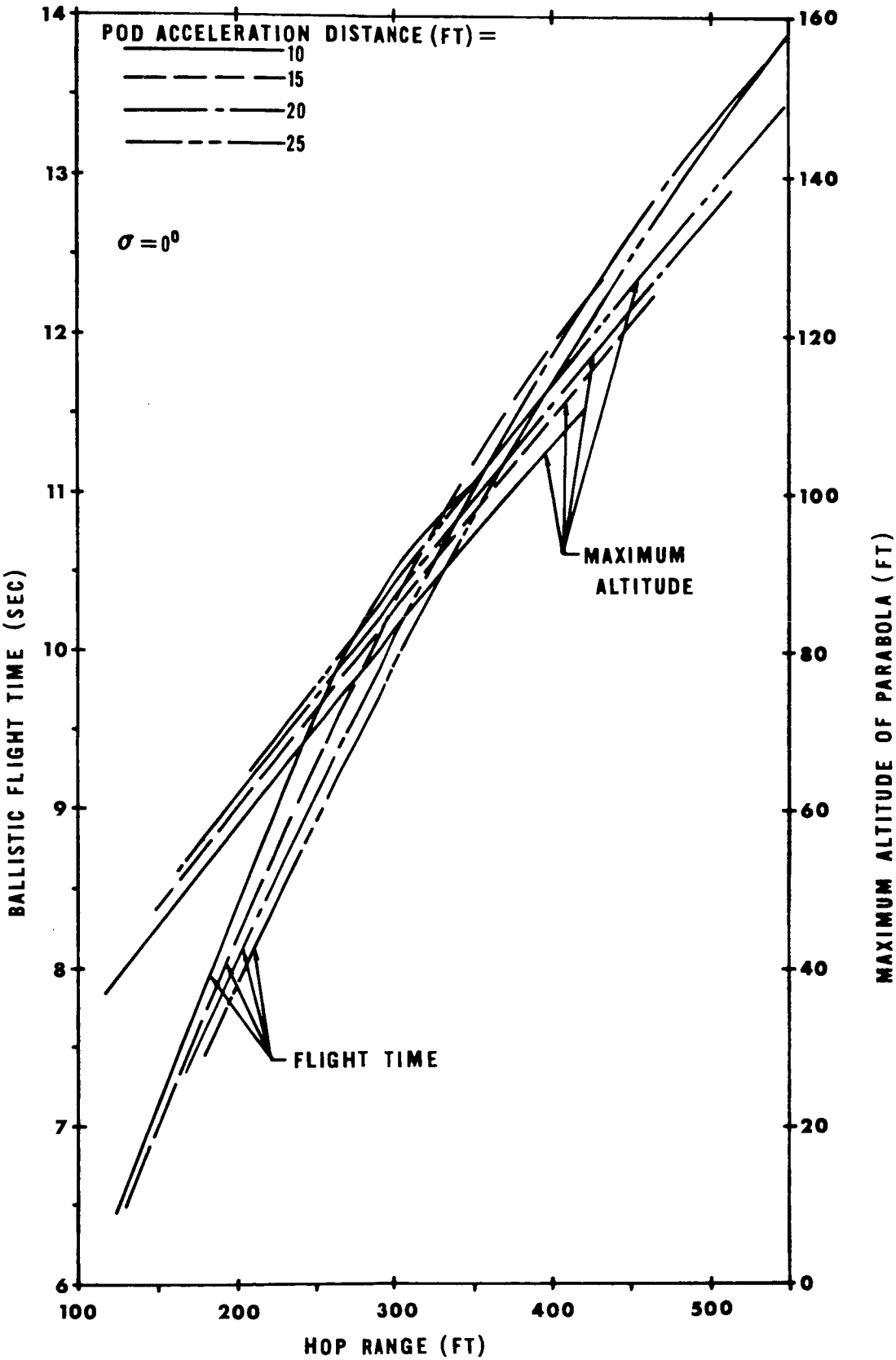

Figure 26. HOLAB Ballistic Data

characteristics similar to those of SHOT. For given ballistic flight time, range is slightly increased for increased acceleration distance while initial pressure is reduced slightly. Furthermore, for fixed range, ballistic flight time decreases slightly with increased acceleration distance, because pressure is reduced to maintain range and additional leg length subtracts from ballistic range. Finally, maximum altitude is indicated to increase slightly with increasing acceleration distance for given range, because vehicle center of mass motions with respect to the pod center of mass are not accounted for in this simulation. Therefore, increased leg length adversely affects calculated altitudes for specified range. In fact, maximum altitude should decrease slightly for increasing acceleration distances.

Since HOLAB need not stop between hops to reposition the leg or change planes, high average speeds may be easily obtained. Figure 27 illustrates two typical acceleration profiles. For the p_o = 171 psi case, the hop range is 210 ft. and total hop time is 10.6 sec., giving a speed of 16.1 fps. However, the p_o = 426 psi case corresponds to a range of 545 ft. in 15.3 sec., giving a speed of 35.6 fps. (39 km/hr). This is more than seven times the safe speed of proposed roving vehicles. During a 10 day sortie HOLAB can easily travel a total distance of 500 km and provide a generous stopover time at each site of interest. A comparable roving vehicle[17] has a mass of 277 slugs and requires at least 14 days to traverse 250 km. No reasonable flying unit configuration can make a mission of this range without stopping to pick up propellants.[23]

Based on the above performance figures and comparisons, HOLAB seems to offer a completely new range of capabilities for extended lunar operations.

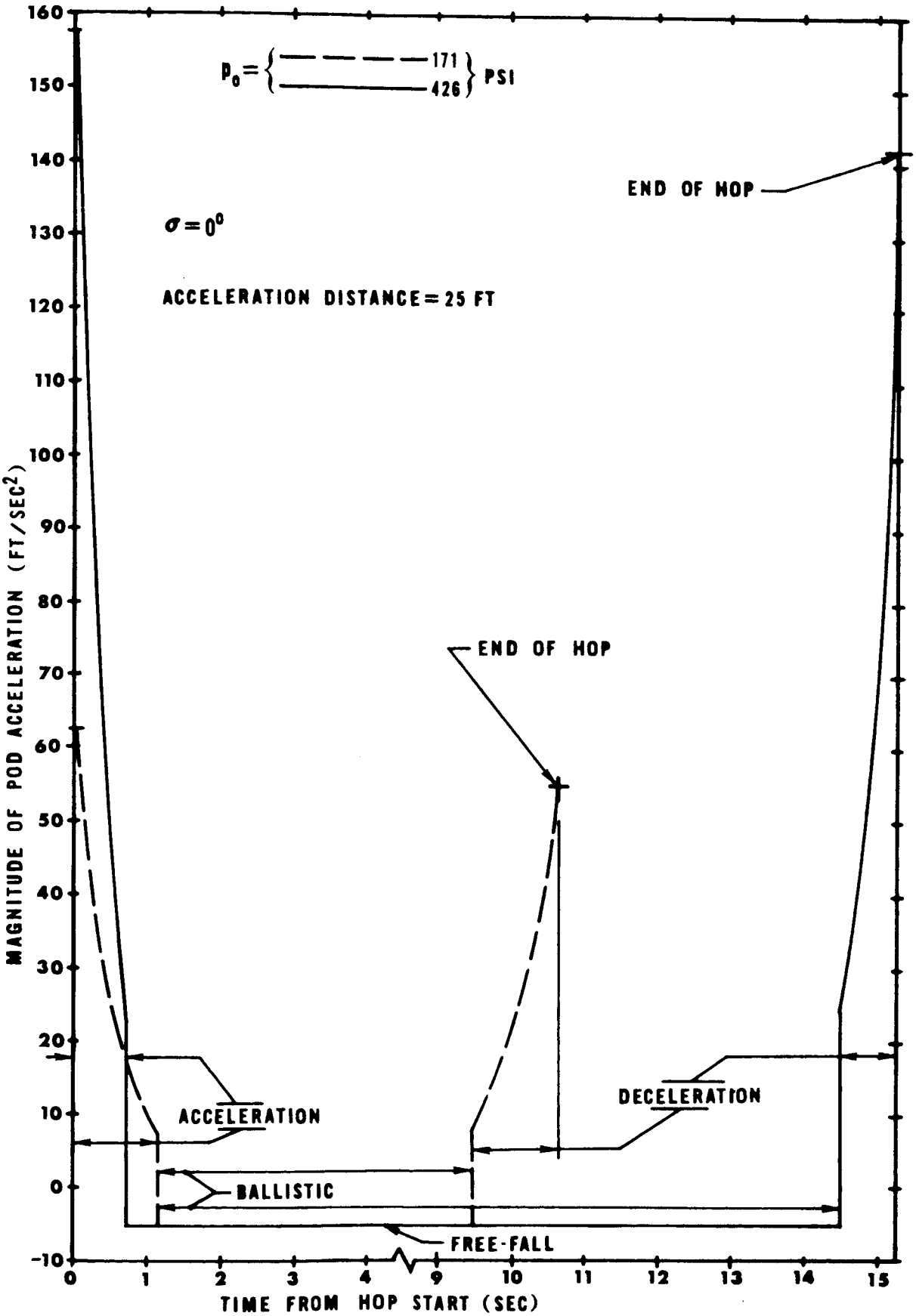

Figure 27. HOLAB Hop Profile Examples

G. Results of Plane Change Simulations

In order to demonstrate the ability of HOLAB to change its hopping plane without stopping between hops, the plane change simulation program was constructed and is listed in Appendix C. To apply this program the following parameter values are taken as constants:

$M = 229$ slugs

$m = 8$ slugs

$I_{L_{c_x}} = 864$ slug-ft^2

$I_{P_{c_x}} = 11{,}200$ slug-ft^2

$h = 4$ ft

$\gamma = 1.2$

$r = 5.0$

$A = 3.0$ ft^2

$g = 5.31$ ft/sec^2

In order to make this simulation compatible with that of the two-dimensional hop, p_d values were selected in such a way that maximum pressure and minimum displacement values attained in the plane change maneuver would approximate the p_o and d_o values of the hop calculations. Thus, the following relations were used to determine p_d:

$$p_d = p_o \left(\frac{d_o}{d_d}\right)^{\gamma} = p_o \left(\frac{1.5}{d_d}\right)^{1.2}$$

where

$$d_d = d_o + \frac{z_{P_d} - z_{P_o}}{r} = 1.5 + \frac{z_{P_d} - 6}{5} \quad .$$

In addition, to realistically simulate the effects of leg moments of inertia on dynamics, ℓ was determined from

$$\ell = \frac{z_{P_d} + 1}{2} \quad .$$

Once z_{P_d} and a corresponding value of p_o were selected, then d_d, p_d, and ℓ were uniquely specified. Initial values of the Euler angles and vehicle center of mass velocity components must also be selected. Without loss of generality the Y component of this velocity is assumed to be initially zero in all cases.

To simulate an actual plane change the following values were selected:

$z_{P_d} = 16$ ft

$p_o = 426$ psi.

These give

$d_d = 3.5$ ft

$p_d = 154$ psi

$\ell = 8.5$ ft.

Initial conditions were selected as

$\dot{X}_{cm}(t_d^-) = 29.1$ fps

$\dot{Z}_{cm}(t_d^-) = -29.1$ fps

$\varphi(t_d) = -90^\circ$

$\theta(t_d) = 45^\circ$

$\psi(t_d) = 105^\circ$

$\dot{\varphi}(t_d^-) = 0$

$\dot{\theta}(t_d^-) = -50^\circ/\text{sec}$

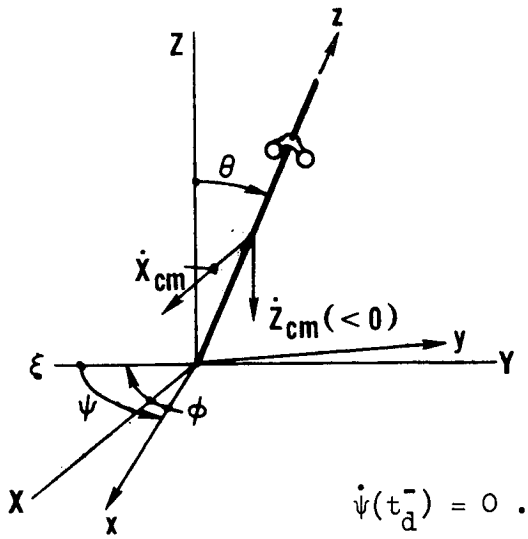

$\dot{\psi}(t_d^-) = 0$.

The variations of Euler angles and axial acceleration are illustrated in figure 28 as the maneuver is executed. Final angular orientation and rates are

$\varphi(t_e) = -188.6^\circ$

$\theta(t_e) = 7.2^\circ$

$\psi(t_e) = 205.0^\circ$

$\dot{\varphi}(t_e^+) = -1045.6^\circ/\text{sec}$

$\dot{\theta}(t_e^+) = 46.6^\circ/\text{sec}$

$\dot{\psi}(t_e^+) = 1053.7^\circ/\text{sec}$

$\dot{X}_{cm}(t_e^+) = 17.1$ fps

$\dot{Y}_{cm}(t_e^+) = 6.7$ fps

$\dot{Z}_{cm}(t_e^+) = 30.9$ fps

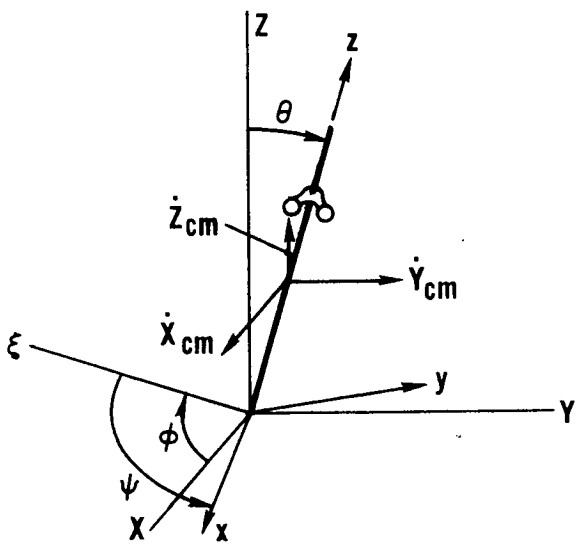

The plane of ballistic flight was changed by 21.5° during this maneuver.

This example demonstrates that a plane change can be accomplished by rotating the pod center of mass out of the hopping plane. In this case this angle was 15°. If $h = 0$, plane changes could be executed

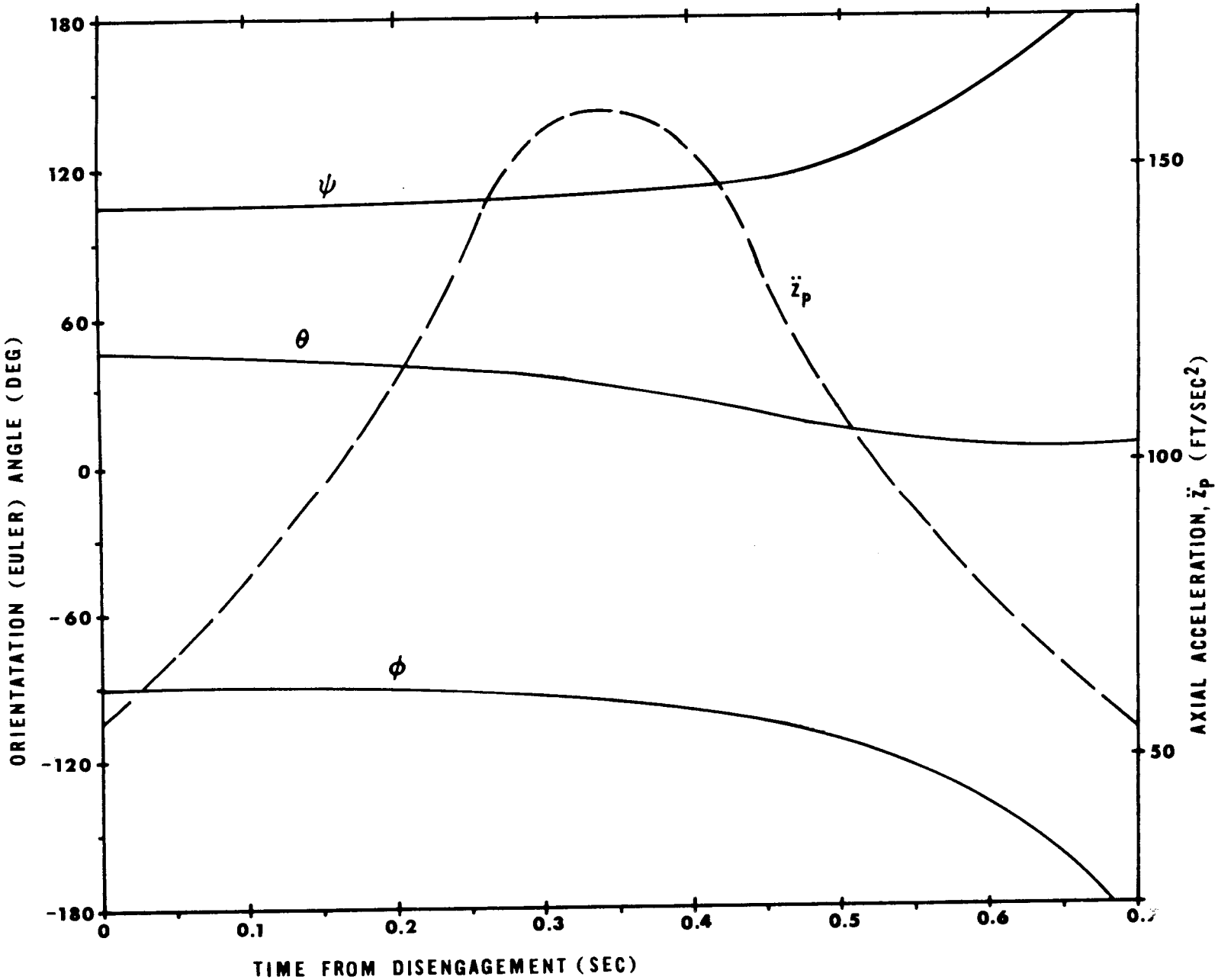

Figure 28. Example of HOLAB Plane Change Maneuver

by setting $\varphi(t_d) \neq \pm 90^{\circ}$. The example given here illustrates a need to optimize these maneuvers so that rotation rates at (t_e^+) are minimized or coordinated with succeeding disengagement events. This will reduce control system requirements. The general solution of plane change boundary relations requires a sophisticated and lengthy investigation of individual parameter sensitivities, because there are no less than nine critical dimensions and initial conditions.

V. CONCLUSIONS AND RECOMMENDATIONS

A. Primary Conclusions

The principal objective of this study is to present an investigation related to the feasibility of a hopping transporter concept. In particular, hop performance estimates are employed to demonstrate potential capabilities of such devices. These values were obtained only after making several relevant assumptions and considering factors which influence transporter design and operation. Two configurations were formulated to represent possible basic designs from which operational transporters might later be developed. Results of hop simulations of both vehicles indicate a significant improvement in performance over roving and flying transporters. Specifically, SHOT offers extended range to Apollo astronauts, up to and exceeding an operating radius of 10 km, recommended by the 1967 Santa Cruz Conference[1]. In addition, this vehicle enables lunar explorers to visit otherwise inaccessible topographic features. HOLAB appears to offer much larger ranges and speeds, for given vehicle mass, when compared to other proposed devices. The unique plane changing technique used by this transporter permits these high average speeds. Therefore, within the accuracies of assumptions applied in this study, hopping vehicles offer superior performance capabilities for lunar surface mobility.

B. Problems of Further Hopping Vehicle Development

The work presented here represents only a first-step in development of the hopping vehicle concept. Next, problems in several other technical areas must be addressed. A consideration of control techniques and

devices is essential to vehicle performance, stability, and maneuverability. SHOT will require an inertially stabilizing control system which allows plane changes to be executed between hops. HOLAB needs a much more sophisticated device because of its somewhat general three-dimensional motion during plane change maneuvers. The possibility of large disturbing moments resulting from foot slippage and leg misalignment indicates a need for large, stiff control systems. Optimization to minimize their weights is of major importance. Human limitations in a hopping acceleration environment will determine an upper bound on the performance envelope of such vehicles. Of primary importance is the response of man to repeated hop cycles. This must be investigated before serious consideration can be given to developing operational pogo transporters. Other factors to be studied include effects of g magnitude on the number of tolerable hop cycles, optimum frequency for comfort and endurance, seat design, and body orientation. Also of major importance is the design and operation of a propulsion system. This must be efficient, change modes quickly, and be inherently reliable. Such a device will, in effect, determine the attractiveness of hopping vehicles through the conservative use of fuel on lunar missions.

In order to design a navigational computer and plane change control system for HOLAB, the plane change problem must be completely solved. This will require much computation and data reduction time, and results may be most useful in parametric form, if possible. A certain amount of optimization may be achieved if take-off angular rates can be minimized or coordinated with subsequent engagement events, for given plane change values.

The structure of these vehicles must withstand many cycles at several Earth g's and have a minimum of weight. Of critical importance is the foot design. This must engage the lunar surface inelastically without appreciable slippage or sinking and be of minimum mass and moment of inertia. Reliability and safety should be designed into these vehicles. Failure modes must be considered and possibility of occurrence eliminated in each case.

C. Possible Experiments

Although vehicles considered here are designed for use on the Moon, initial experiments must be performed before sending such devices on lunar missions. To answer the very basic questions related to human tolerance in a hop cycle environment, acceleration profiles, similar to those expected in operation, should be simulated in test facilities. This type of experiment will indicate relationships between peak g and number of tolerable cycles, among other important data. Results may then be scaled to 1/6 g conditions.

Control and propulsion innovations can be tested by working models which operate in a 1 g environment. Various maneuvers and sequences may be studied and desirable operating modes determined. Foot designs might also be checked with such test devices.

APPENDIX A. OPTIMUM LAUNCH ANGLE

The following analysis is presented in a general form but is of major importance to the performance study of Chapter III. Consider the problem of maximizing the ballistic range of a constant mass projectile with given initial speed v, uniform gravitational vector $\vec{g}$, and linear surface slope σ. The objective is to determine launch angle, α such that range R is a maximum. (This is also the problem of finding α for a minimum initial velocity when R is fixed.)

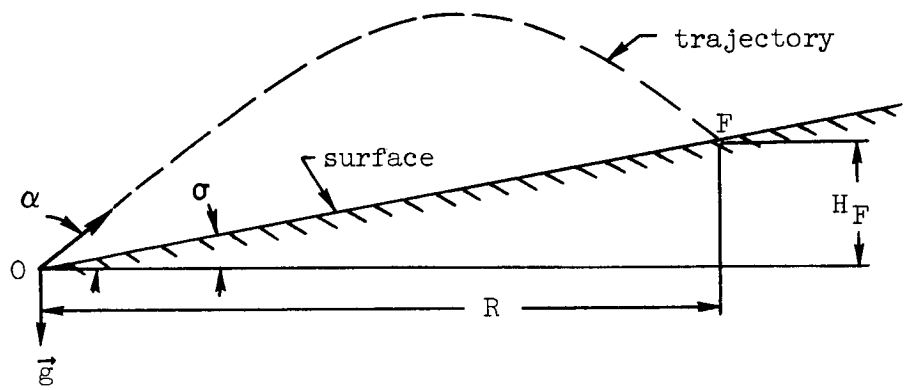

It is assumed that at time $t = 0$ the projectile is at point 0 with speed v. First, it is necessary to express R as a function of α, g, v, and σ. This is done by matching trajectory and surface equations at point F. Elevation, H_F of the surface at this point is

$$H_F = R \tan \sigma \quad . \tag{A-1}$$

From the classic equations of ballistic trajectories, the value of elevation of flight path at point F is

$$H_F = vt \sin \alpha - \frac{1}{2} gt^2 \quad . \tag{A-2}$$

To eliminate time the constant horizontal velocity phenomenon can be used,

$$t = \frac{R}{v \cos \alpha} \quad . \tag{A-3}$$

Combining (A-1), (A-2), and (A-3) to eliminate H_F and t leads to

$$R = \frac{2v^2}{g} \left(\frac{1}{2} \sin 2\alpha - \tan \sigma \cos^2 \alpha\right) \quad . \tag{A-4}$$

The condition for stationary value of R is

$$\frac{dR}{d\alpha} = 0 \quad . \tag{A-5}$$

Differentiating (A-4) with respect to α and applying (A-5) leads to the condition for optimum α,

$$\tan \sigma \sin 2\alpha_{opt} + \cos 2\alpha_{opt} = 0$$

or

$$\alpha_{opt} = \frac{1}{2} \tan^{-1}(-\cot \sigma) \tag{A-6}$$

The range of interest of α is 0 to 90°. Therefore, (A-6) indicates

$$\alpha_{opt} \begin{cases} > 45^\circ & \text{for} \quad \sigma > 0 \\ < 45^\circ & \text{for} \quad \sigma < 0 \end{cases} \quad .$$

From trigonemetry comes a useful identity:

$$- \cot \sigma = \tan\left(\frac{\pi}{2} + \sigma\right) \quad .$$

Applying this to (A-6) leads to a simple form of α_{opt},

$$\alpha_{opt} = \frac{\pi}{4} + \frac{\sigma}{2} \tag{A-7}$$

where the slope falls in the interval of $-90^{\circ} < \sigma < 90^{\circ}$.

Condition (A-5) leads to an extremum of range. It is easy to demonstrate that this is a maximum rather than a minimum. The condition for a maximum is

$$\frac{d^2R}{d\alpha^2} < 0$$

for the variable intervals of interest. Taking the second derivative of (A-4) yields

$$\frac{d^2R}{d\alpha^2} = -\frac{4v^2}{g}\left[\sin 2\alpha - \tan\sigma \cos 2\alpha\right] \quad .$$

Applying (A-7) to this results gives

$$\frac{d^2R}{d\alpha^2} = -\frac{4v^2}{g}\left[\cos\sigma + \frac{\sin^2\sigma}{\cos\sigma}\right] \quad .$$

For the interval of σ mentioned above, $d^2R/d\alpha^2 < 0$. Therefore, (A-7) leads to a maximum of range.

Substituting (A-7) into (A-4) gives R_{max},

$$R_{max} = \frac{2v^2}{g}\left[\frac{1}{2}\cos\sigma - \tan\sigma \cos^2\left(\frac{\pi}{4} + \frac{\sigma}{2}\right)\right] \quad . \qquad \text{(A-8)}$$

The corresponding time of ballistic flight is obtained by inserting (A-7) and (A-8) into (A-3),

$$t_{opt} = \frac{2v}{g}\left(\sin\alpha_{opt} - \tan\sigma \cos\alpha_{opt}\right) \quad .$$

APPENDIX B. EXPEDITIOUS METHOD FOR OBTAINING COMPUTER SOLUTIONS TO THE MOTION OF MECHANICAL SYSTEMS

I. INTRODUCTION

It is always desirable to obtain closed-form solutions to mechanics problems since they possess the general parametric relationships of the system. However, the tools of mathematical analysis have developed slowly and only to a point where such analytical solutions can be secured for a relatively small number of the interesting cases. Because of this limitation investigators have been and still are inventing analytical techniques for gaining insight into the motion of mechanical systems without actually solving the associated differential equations. These include searching for special soluble cases of a particular problem under more restrictive conditions and perturbation techniques which are useful when small variaions from a nominal configuration are of interest. A classic example of the former technique is the restricted three-body problem. If a complicated system is known to have periodic motion then it is sometimes possible to obtain the frequencies of its motion without actually performing a detailed analysis. Fortunately, in many cases these frequencies are the only quantities of interest to the investigator. The work presented here deals with determining the motion of certain classes of mechanical systems, especially those which cannot be analyzed by the above-mentioned techniques.

Development of modern high-speed digital computing devices has initiated a revolution in the general approach to solving technical, as well as other, problems. In principle, any properties of a physical system which can be reduced to a mathematical description can be analyzed and results obtained, either by closed-form or numerical methods. It is also conceivable that computers will soon be able to give pseudo-closed-

form solutions for given ranges of system parameters with specified accuracy. This type of solution is quite adequate for most engineering applications since accuracy can always be bought at the price of computing time. Of course, until these soft-ware systems have come of age, it will be desirable to obtain analytical solutions whenever possible. The work presented here might be thought of as a preliminary step toward the evolution of psuedo-closed-form solutions, at least in the area of mechanical system dynamics. Work of this type has already been done in another area of dynamics by Davids and Mehta[24].

Since the systems considered here do not lend themselves to the usual analytical methods of solution and are not necessarily periodic, such problems require a numerical approach. Therefore, it would be desirable to have the ability to quickly set these problems into digital computer programs while employing a minimum of mathematical manipulation and computer programming skills. This would give an investigator the ability to obtain desired solutions of motion shortly after being presented with a mechanical system to analyze. The procedure described below offers this capability and requires a minimum of work and time on the part of the investigator.

This technique is developed from the formalisms of analytical mechanics with the objective of making maximum use of existing computer subroutines which are written for general application of specific mathematical manipulations. The method presented here is applicable to frictionless mechanical systems which have holonomic constraints and whose kinetic energy is a quadratic form in the generalized velocities. Requirements and general characteristics of relevant subroutines are discussed.

Since analytical expressions must be tailored to these subroutines, it is of prime importance to investigate their formats and availability. The differential equations of motion may be obtained from Lagrange's method or from Hamilton's method. The two forms are compared for their merits in this application. A general computer program is outlined which makes use of the previously mentioned subroutines to actually numerically integrate the equations of motions from the initial conditions of the system to a final configuration determined either by specifying the integration interval of the independent variable, time, or by specifying a final value of one of the dependent variables, i.e., coordinate, velocity or acceleration. A step-by-step description of the application of this procedure is also given. Finally, to illustrate the mechanics and utility of this technique, a simple mechanical system is studied by applying these steps in sequence.

II. STATEMENT OF THE PROBLEM

The pertinent problem here is to devise a procedure for transforming a mechanical system of a certain class into a computer simulation with a minimum of effort. The general approach developed here does away with the usual two step method for obtaining a computer solution. Instead of first deriving the differential equations of motion and then transforming these into a convenient form for the computer program, the procedure presented here permits the differential equations to be derived directly in the desired form. This format for the differential equations is dictated because of the philosophy adopted in this work. In order to minimize computer program complexity and programming time, currently

available scientific subroutines will be used wherever possible. Numerical integration subroutines of the type required here are constructed so that they will accept differential equations only if presented in a strictly specified format. Thus, it is necessary to formulate the equations of motion such that they are compatible with these subroutines. It turns out that there is a significant savings of time and effort by deriving these equations in the desired format.

Discussion will be restricted to mechanical systems with holonomic kinematic constraints which do no virtual work (cause no internal friction) as defined by Goldstein[22] and ter Haar[25]. This will permit use of the basic formulations of analytical mechanics. Furthermore, the system kinetic energy is assumed to be a quadratic function of the generalized velocities with coefficients depending on time and the generalized coordinates. Thus, for a system with n degrees of freedom,

$$T = \frac{1}{2}\sum_{i,j}^{n} a_{ij}(t,q_1,q_2,\ldots,q_n)\dot{q}_i\dot{q}_j \ , \qquad \text{(B-1a)}$$

which is typical of systems containing particles and rigid bodies. Although certain types of non-conservative systems are considered here, of particular interest to many is the class of problems in which energy is conserved. This is a special case of the above outlined class of problems in which restrictions are increased and extended to the applied forces. Thus, for a conservative system in the usual sense the applied forces are derivable from a potential which depends on the generalized coordinates alone and the constraints are time independent. Then kinetic energy would have the form

$$T = \frac{1}{2}\sum_{i,j}^{n} a_{ij}(q_1, q_2, \ldots q_n)\dot{q}_i\dot{q}_j \quad . \tag{B-1b}$$

The procedure is separately described for this class of problems.

Consideration is further limited to systems in which initial values of the coordinates, velocities, and time are given. This restriction seems somewhat harsh, because many problems of interest require the determination of system parameter values which satisfy a given set of boundary conditions. However, standard subroutines which solve sets of non-linear differential equations with given boundary values are generally unavailable. Of course, one can always attempt solving such boundary value problems by using trial-and-error methods with initial value problem solutions as proposed here.

III. STANDARD SUBROUTINES

In general, the equations of motion of mechanical systems are second order ordinary non-linear differential equations when expressed in terms of generalized coordinates and their derivatives. These equations are to be numerically integrated. However, numerical solution of a system of second or higher order differential equations presents special programming problems which make the establishment of the corresponding standard subroutines a very difficult task. Thus, such subroutines are not readily available for general application. Fortunately, there is a large selection of subroutines which solve systems of first order ordinary non-linear differential equations (e.g., see ref. 26 and 27) provided these equations are presented in a prescribed form to the subroutine. This form is illustrated by

$$y_i' = f_i(x,y_1,y_2,\ldots,y_N) \qquad (i = 1,2,\ldots,N) \qquad \text{(B-2)}$$

where y_i $(i = 1,2,\ldots N)$ are the dependent variables, x is the independent variable and

$$y_i' = \frac{dy_i}{dx} .$$

Therefore, if the equations of motion can be reduced to first order and written in form (B-2), then standard subroutines can be used to solve these equations.

Any set of n second order ordinary differential equations can be reduced to a set of $2n$ first order ordinary differential equations by introducing

$$u_i = \dot{q}_i \qquad (i = 1,2,\ldots,n) , \qquad \text{(B-3)}$$

and eliminating second order derivatives with

$$\ddot{q}_i = \dot{u}_i \qquad (i = 1,2,\ldots,n) . \qquad \text{(B-4)}$$

It remains to be shown that the resulting $2n$ equations can be written in form (B-2). However, set (B-3) represents half of the new first order equations and this set is already in form (B-2). All that remains to satisfy the requirements of available subroutines is to show that the other n first order equations can be written as

$$\dot{u}_i = f_i(t,q_1,q_2,\ldots,q_n,u_1,u_2,\ldots,u_n) \qquad (i = 1,2,\ldots,n) \quad \text{(B-5)}$$

The ability to do this for all cases of interest will be demonstrated in the analysis of part IV in this appendix.

Another outcome of the analysis indicates the desirability of using another type of subroutine which solves a set of simultaneous linear algebraic equations. This will be employed to obtain equations (B-5) in numerical form at each step of the integration process. Fortunately, as in the above situation, there are several library subroutines available which perform this operation (e.g., see ref.26). Of particular interest are those subroutines specialized to handle sets of equations with a symmetric coefficient matrix. Of course, for simple mechanical systems with just a few degrees of freedom, these algebraic equations in $\dot{u}_i$ $(i = 1,2,\ldots,n)$ can be solved by any of the well known methods, e.g., Cramer's rule or Gauss-Jordan reduction.[28] These subroutines are discussed further in connection with the computer program development.

IV. DEVELOPMENTS FROM ANALYTICAL MECHANICS

It is well known that for a mechanical system with n degrees of freedom, and holonomic constraints, the Lagrangian formulation gives a set of n second order ordinary differential equations of the form[22]

$$\frac{d}{dt}\left(\frac{\partial T}{\partial \dot{q}_i}\right) - \frac{\partial T}{\partial q_i} = Q_i \qquad (i = 1,2,\ldots,n) , \qquad \text{(B-6a)}$$

where Q_i is the applied force associated with the q_i coordinate and may be a function of the coordinates, velocities, and time. Hamilton's formulation for conservative mechanical systems gives a set of $2n$ first order ordinary differential equations of form

$$\left.\begin{aligned} \dot{q}_i &= \dot{q}_i(t,q_1,q_2,\ldots,q_n,p_1,p_2,\ldots,p_n) \\ \dot{p}_i &= \dot{p}_i(t,q_1,q_2,\ldots,q_n,p_1,p_2,\ldots,p_n) \end{aligned}\right\} \qquad (B\text{-}7)$$

$$(i = 1,2,\ldots,n)$$

where the p_i's are the conjugate momenta defined by

$$p_i = \frac{\partial T}{\partial \dot{q}_i} \qquad (i = 1,2,\ldots,n) \qquad (B\text{-}8)$$

It would appear that Hamilton's equations (B-7) would be preferential for conservative systems, because they are already in the desired format (B-2) required by existing integration subroutines. However, the following development of these two formulations brings out a somewhat surprising point. In order to derive expressions (B-7) by Hamilton's method, there is generally required more algebraic manipulation and mathematical complexity than to reduce Lagrange's equations to form (B-5) by using relations (B-3) and (B-4). This result indicates a preference for the method supported here, over Hamilton's method.

A. Lagrangian Formulation

As mentioned above, Lagrange's equations for a mechanical system with holonomic constraints have the form given by (B-6a). The derivation of these equations is classic and discussed by Whittaker[29] and Goldstein[22] in detail. These differential equations are further specialized by introducing the kinetic energy given by (B-1a) into (B-6a). Then noting that

$$\frac{\partial T}{\partial \dot{q}_i} = \sum_j^n a_{ij}\dot{q}_j$$

$$\frac{\partial T}{\partial q_i} = \frac{1}{2} \sum_{j,k}^{n} \frac{\partial a_{jk}}{\partial q_i} \dot{q}_j \dot{q}_k$$

$$\frac{da_{ij}}{dt} = \sum_{k}^{n} \frac{\partial a_{ij}}{\partial q_k} \dot{q}_k + \frac{\partial a_{ij}}{\partial t}$$

leads to differential equations of the form

$$\sum_{j}^{n} \left[\left(\sum_{k}^{n} \frac{\partial a_{ij}}{\partial q_k} \dot{q}_k + \frac{\partial a_{ij}}{\partial t} \right) \dot{q}_j + a_{ij} \ddot{q}_j \right]$$

$$- \frac{1}{2} \sum_{j,k}^{n} \frac{\partial a_{jk}}{\partial q_i} \dot{q}_j \dot{q}_k = Q_i \qquad (i = 1,2,\ldots,n) \; . \qquad \text{(B-9)}$$

Set (B-9) represents the n second order ordinary differential equations which must be reduced to 2n first order equations. These are obtained[25] by applying definition (B-3) and relation (B-4) to set (B-9). This results in

$$\sum_{j}^{n} a_{ij} \dot{u}_j = \frac{1}{2} \sum_{j,k}^{n} \frac{\partial a_{jk}}{\partial q_i} u_j u_k - \sum_{j}^{n} \left(\sum_{k}^{n} \frac{\partial a_{ij}}{\partial q_k} u_k + \frac{\partial a_{ij}}{\partial t} \right) u_j + Q_i$$

$$(i = 1,2,\ldots,n)$$

which is rewritten for convenience as

$$\sum_{j}^{n} a_{ij} \dot{u}_j = C_i(t, q_1, q_2, \ldots, q_n, u_1, u_2, \ldots, u_n) \qquad (i = 1,2,\ldots,n) \qquad \text{(B-10a)}$$

where

$$C_i = \sum_{j,k}^{n} \left(\frac{1}{2} \frac{\partial a_{jk}}{\partial q_i} - \frac{\partial a_{ij}}{\partial q_k} \right) u_j u_k - \sum_{j}^{n} \frac{\partial a_{ij}}{\partial t} u_j + Q_i \ . \qquad \text{(B-11a)}$$

Set (B-10a) indicates that Lagrange's equations reduce to a system of simultaneous linear algebraic equations in the $\dot{u}_j$'s. In order to finally obtain a set of form (B-2), system (B-10a) must be solved for $\dot{u}_j$ $(j = 1,2,\ldots,n)$. As mentioned in part III, this may be accomplished either by algebraic methods before coding the equations into a computer program or by having the computer solve set (B-10a) numerically at each step of the integration process. It is important to note that, in general, each of equations (B-10a) is a non-linear differential equation and a linear algebraic equation in the $\dot{u}_j$'s. Since these expressions are generally non-homogeneous and linarly independent, a unique solution of form (B-5) can be expected.[28] Therefore, the ability to obtain a set of differential equations of form (B-5) from Lagrange's equations has been demonstrated and equations (B-3) and (B-10a) constitute the desired set of 2n first order ordinary differential equations.

As a further expedient, note that since the coefficient matrix of set (B-10a) has elements a_{ij} $(i,j = 1,2,\ldots,n)$ and

$$a_{ij} = \frac{\partial^2 T}{\partial \dot{q}_i \partial \dot{q}_j} = \frac{\partial^2 T}{\partial \dot{q}_j \partial \dot{q}_i} = a_{ji} \ , \qquad \text{(B-12)}$$

then this matrix is symmetric. Recognition of this fact will help to avoid the mistake of determining all a_{ij}'s separately from the kinetic energy expression. An additional savings in time may be realized when solving set (B-10a) for the $\dot{u}_j$'s. If one is solving by hand some early cancelling and/or combining of like terms may simplify the algebra. If a

subroutine is used, one which assumes a symmetric coefficient matrix should be selected to minimize program length and running time.

Summarizing developments to this point, it is apparent that for a given mechanical system of the class considered here, the mathematical manipulation required to solve for the motion on a digital computer is a minimum and consists of performing the following operations. Determine the generalized coordinates, corresponding applied force expressions, and system kinetic energy. Then determine forms of the a_{ij}'s using (B-12) and C_i's using (B-11a). Finally, code these expressions into a computer program which uses standard subroutines for numerical integration and, if desirable, for solving set (B-10a) at each step of integration.

If the given mechanical system has time independent constraints and the applied forces can be written as

$$Q_i = -\frac{\partial V}{\partial q_i} \qquad (i = 1,2,\ldots,n) \qquad \text{(B-13)}$$

where V is the system potential energy and is an explicit function of the generalized coordinates alone, then the system is conservative and its kinetic energy has form (B-1b). Relation (B-13) permits the definition of the Lagrangian, L as

$$L(q_1,q_2,\ldots,q_n,\dot{q}_1,\dot{q}_2,\ldots,\dot{q}_n) = T - V$$

and Lagrange's equations (B-6a) become[22]

$$\frac{d}{dt}\left(\frac{\partial L}{\partial \dot{q}_i}\right) - \frac{\partial L}{\partial q_i} = 0 \qquad (i = 1,2,\ldots,n)\ . \qquad \text{(B-6b)}$$

An analysis similar to the preceeding one can be performed with equations (B-6b) by applying the kinetic energy in form (B-1b) and using definition (B-3)

to reduce the order of these equations. This procedure again gives a system of simultaneous linear algebraic equations in $\dot{u}_j$'s of the same form as (B-10a). The results can be written directly as

$$\sum_j a_{ij}\dot{u}_j = C_i(q_1,q_2,\ldots,q_n,u_1,u_2,\ldots,u_n) \qquad \text{(B-10b)}$$

$$(i = 1,2,\ldots,n)$$

where a_{ij} is again given by equation (B-12) and

$$C_i = \frac{\partial L}{\partial q_i} - \sum_j^n \frac{\partial^2 T}{\partial \dot{q}_i \partial q_j} u_j \ . \qquad \text{(B-11b)}$$

Note that any $\dot{q}_i$'s which appear after the indicated differentiation in (B-11b) must be replaced by u_i's in the final expression for C_i. Of course, results (B-10b) and (B-11b) are used in the same way as are (B-10a) and (B-11a).

B. Hamiltonian Formulation

Consider a conservative mechanical system of the type discussed above. Hamilton's equations of motion can be written as[22]

$$\dot{q}_i = \frac{\partial H}{\partial p_i}, \qquad \dot{p}_i = -\frac{\partial H}{\partial q_i} \qquad (i = 1,2,\ldots,n) \qquad \text{(B-14)}$$

where p_i is given by (B-8) and H is the Hamiltonian defined by

$$H(q_1,q_2,\ldots,q_n,p_1,p_2,\ldots,p_n) = \sum_i^n p_i\dot{q}_i - L \ .$$

For this type of conservative system, H is the total energy,

$$H = T + V \ . \qquad \text{(B-15)}$$

Substituting (B-1b) into (B-15) gives

$$H = \frac{1}{2} \sum_{i,j}^{n} a_{ij}\dot{q}_i\dot{q}_j + V(q_1,q_2,\ldots,q_n) \ . \qquad \text{(B-16)}$$

Equations (B-14) represent a set of $2n$ first order ordinary differential equations in the form required for numerical integration by the methods preposed here. However, before carrying out the partial differentiation of H with respect to each q_i and p_i, the Hamiltonian (B-16) must be expressed as a function of coordinates and momenta only, i.e., the velocity terms, $\dot{q}_i$'s, must be replaced by their equivalent functions of the q_i's and p_i's. This can be accomplished by first substituting equation (B-1b) into (B-8), getting

$$p_i = \sum_{j}^{n} a_{ij}\dot{q}_j \qquad (i = 1,2,\ldots,n) \ . \qquad \text{(B-17)}$$

This is a set of n simultaneous linear algebraic equations in the $\dot{q}_j$'s. Since every a_{ij} is a function of the coordinates alone, solving system (B-17) for the $\dot{q}_j$'s yields the required expressions which are to be substituted into (B-16). This is a straightforward operation in principle. However, in general, each of equations (B-17) is lengthly and complicated. This indicates an extensive amount of algebraic manipulation to solve (B-17) and substitute the results into (B-16). The work involved is further magnified when performing the differentiation indicated in (B-14). As an alternative to executing this large amount of algebra and as part of the overall numerical solution of set (B-14), equations (B-17) may be solved numerically at each step of the integration sequence. The resulting

values of the $\dot{q}_j$'s would then be used to perform a numerical differentiation of (B-16) at each integration step. It is now evident that the analysis based on Hamilton's equations of a general conservative system using the proposed computer solution procedure entails the use of two standard subroutines: one for a set of n simultaneous linear algebraic equations with symmetric coefficient matrix and one for a set of 2n first order ordinary differential equations plus a sophisticated computer routine for differentiating a function with respect to 2n variables. This last routine is used to obtain values of $\dot{q}_i$'s and $\dot{p}_i$'s which are then funneled into the integration sequence at each step. Unfortunately, subroutines for partial differentiation of a function of several variables are not readily available. This means that such a routine might have to be individually constructed if set (B-17) is solved within the computer. Furthermore, the use of numerical differentiation is strongly discouraged whenever it can be avoided[30] by analytical means, primarily because of inherent inaccuracies and excessive programming complications.

In summary, the Hamiltonian approach is somewhat more elegant than that of Lagrange but is applicable only to conservative systems (although not necessarily mechanical systems). Furthermore, the practical application of Hamilton's equations to the problem considered here generally requires either an excessive amount of algebraic manipulation or an extremely complicated computer program, whereas Lagrange's equations lead to much less algebra and programming complexity. Based on these observations, it appears that the elegance and simplicity of Hamilton's equations (B-14) are far outweighed by the expeditious and straightforward nature of the procedure developed from Lagrange's equations.

V. COMPUTER PROGRAM

Implementation of the procedure presented in this work is largely dependent upon a computer program which makes optimum use of existing (library) subroutines so that minimum time and effort are required of an engineer-programmer team to obtain numerical solutions to the motion of mechanical systems. Minimization of computer running time is considered to be of little importance in these applications, because the number of runs of a finished program is usually relatively small, indicating that only a small savings in this time is possible. In order to accomplish the primary goals in constructing this program, two types of mathematical subroutines must be selected: one to solve a set of first order ordinary differential equations and one to solve a system of linear algebraic equations with symmetric coefficient matrix. A qualitative description of the computer program logic is presented in the following paragraphs. This is intended to demonstrate the mechanics of implementing the proposed procedure, but does not include all features of a working program. Only an experienced programmer can develop it to a running stage.

The construction of a meaningful flow chart for this type of program must be performed within the requirements and limitations of a specific computer language. Of most popular use today is FORTRAN IV[31], which is one of the primary languages of IBM computers and offers a large selection of library subroutines[26]. The following program description was developed with the logic of this language as a guide. However, the basic ideas are applicable to any compiler.

This program can be thought of as two operating units: a main program and a set of subroutines. Of course, two subroutines will be selected

from a library and the others will support and be used by these two. The main program has several functions: including reading and printing input and output data, initialization of several parameters used in subroutines, and starting the subroutine which solves differential equations. Figure B-1 schematically illustrates the flow of logic in the program. Although it is oversimplified, the primary operations are presented. The heart of this program is the differential equation subroutine. It supplies information to two other subroutines which operate on this data and return other data. When integration is completed the main program receives final values of the dependent and independent variables to be printed out. Primary job of the function subroutine is to compute first derivative values of dependent variables using the values of these dependent variables received from the differential equation subroutine. This is done at each integration step. Since half of these derivatives are imbedded in the system of linear equations given by set (B-10), the function subroutine calls on still another subroutine to solve equations (B-10) at each step. Another essential part of the program is the output subroutine, having two important jobs. If desired it can be written so that numerical integration steps are tabulated. Also, this subroutine is employed to check a specified dependent variable in order to stop the integration process in those cases where the time interval of interesting motion is not known a priori, but the final value of one dependent variable is given. It should be noted that the function and output subroutines must be supplied according to the problem being studied, but the information received from and sent to library subroutines is strictly specified in the instructions associated with these routines.

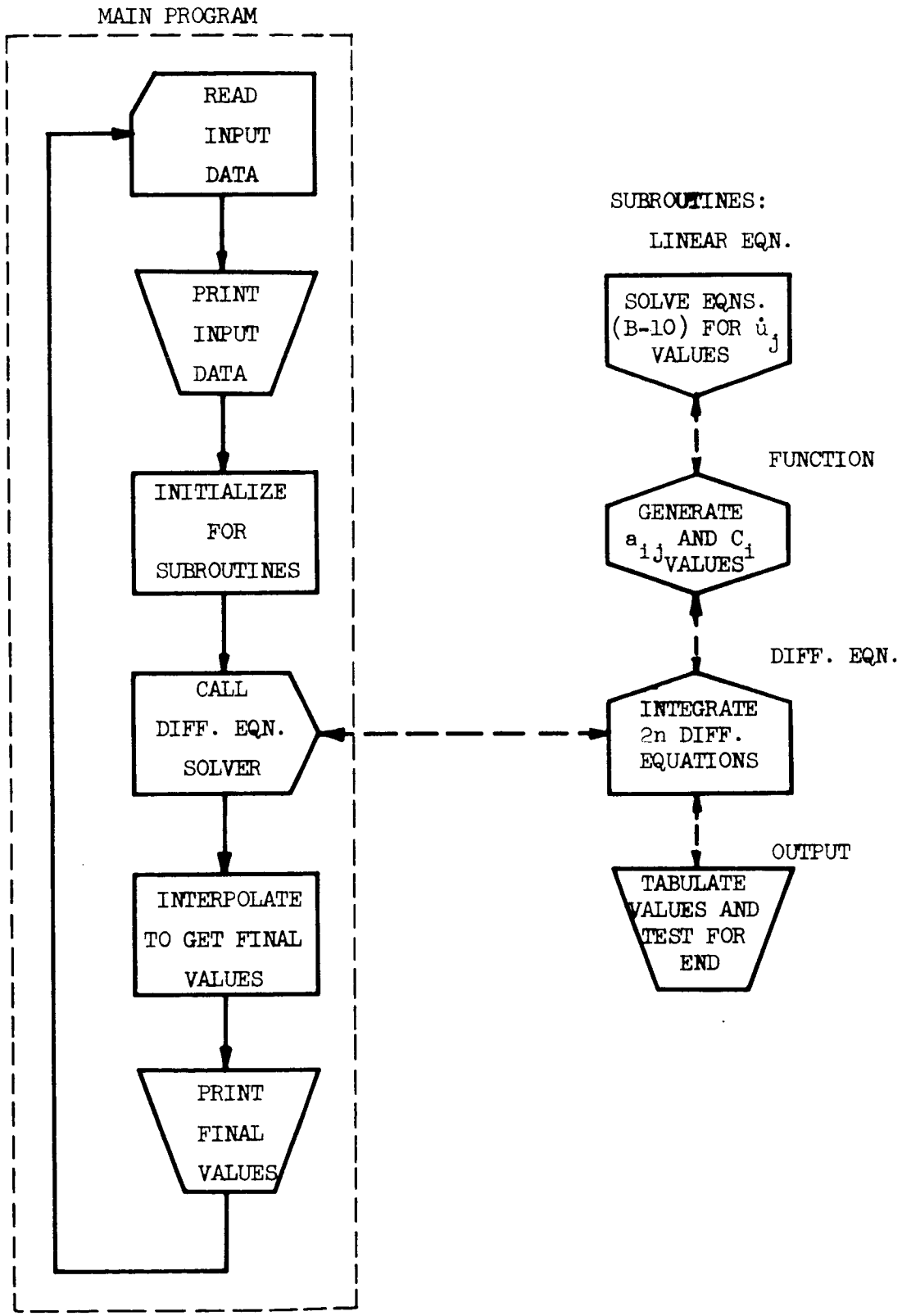

Figure B-1. Flow Chart for Computerization of Mechanical Systems

The logical sequence of this program in its simplest form may be described qualitatively as follows. Input data is read into the computer. This includes values of system mechanical properties, initial coordinates and velocities, and either an integration interval or terminal value of one dependent variable, whichever was decided upon when programming began. Then these values are printed on the output record to identify the problem being solved. Before integration is started, several program variables must be set to initial values. The differential equation subroutine is called and integration begins. At each step of this process function and output subroutines are called into operation, and each of these times the function subroutine calls on the algebraic equation solver. However, program control does not return to the main program until integration is terminated. Then if this process was stopped by a dependent variable value, integration probably proceeded to the step just beyond this value and interpolation is required to determine accurate values of time and other dependent variables corresponding to the given termination value. Finally, these values of time, coordinates, velocities, and acceleration may be printed on an output record. If there are more cases to be tried, program control returns to the beginning and repeats the run with new data.

The program just described contains only basic essentials for solving a problem of the type studied here. Much more may be done to analyze results before terminating a run. For example, one set of final variable values can be used in making a decision to change critical parameter values and repeat the run to obtain more desirable results. However, such specifications are largely dependent upon the particular problem at hand.

VI. APPLICATION OF THE PROCEDURE

It would be convenient at this point to outline the overall procedure in a manner that will make its application by an investigator, presented with a mechanical system, relatively easy. A step-by-step format for this outline is of most usefulness in quickly setting up the solution to system motion on a computer. The steps are presented in order of their application:

1. Determine whether or not the given mechanical system falls within the classes considered here. This is usually done by investigating kinematic constraints, internal forces, and system kinetic energy. If the constraints are holonomic and do no virtual work, and the kinetic energy has form (B-1), then this procedure is applicable to the problem at hand. It is helpful to note that a system whose inertia components consist of particles and rigid bodies will usually have a kinetic energy of this form.
2. Determine whether the system is conservative or non-conservative. If the forces are functions of coordinates only, then they are derivable from a potential function which depends on coordinates alone, i.e., $V(q_1, q_2, \ldots, q_n)$. The system is conservative if V exists and all applied forces can be derived from it, and if the constraints are scleronomous, i.e., independent of time.
3. Derive the expression for kinetic energy and either potential energy or applied generalized forces, depending upon the outcome of step 2. Then determine coefficients a_{ij} and constants C_i

using (B-12) and (B-11), respectively. Replace any $\dot{q}_i$'s by u_i's in the resulting expressions.

4. Select two library subroutines written in the computer language to be used for the program. One of these is used to solve a set of first order ordinary differential equations and the other to solve a system of linear algebraic equations with symmetric coefficient matrix. Mathematical library subroutines do not have provisions for reading or printing data.

5. Write a computer program which includes the selections of step 4 and provides input data and prints results, and includes other supporting subroutines, as shown in Figure B-1. Details of this program were presented in part V.

VII. EXAMPLE

To illustrate the application of this procedure, a simple mechanical system is presented for analysis. Consider the configuration shown in Figure B-2. A massless rod of length ℓ is supporting a slender uniform bar of mass m and length 2ℓ. Motion is frictionless and restricted to the vertical plane in which gravity acts downward. The problem is to determine the system motion for a given time interval and for a given set of initial coordinates and velocities. Following the procedure step-by-step gives:

1. The constraints here are plane motion, one end of the rod of length ℓ is fixed and ℓ is constant. These are all holonomic and scleronomous. There are two degrees of freedom and, therefore, two generalized coordinates which are selected to be

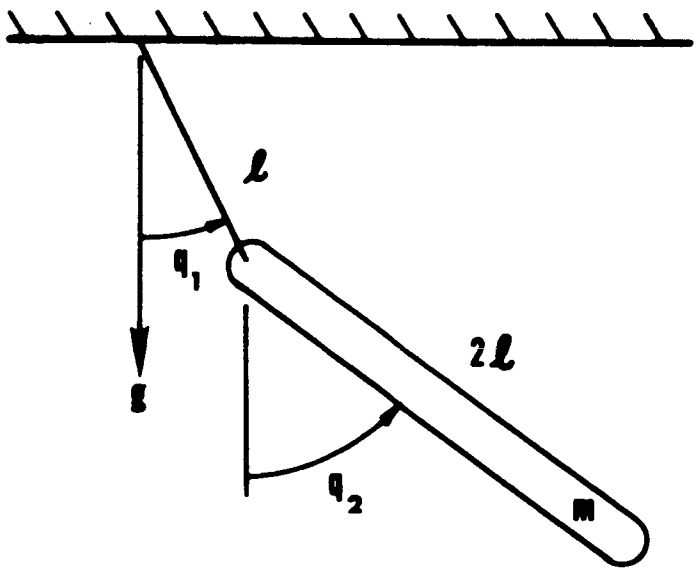

Figure B-2. Example System to Illustrate Procedure

q_1 and q_2, defined in Figure B-2. Assuming the moment of interia of the bar about its center of mass is $m\ell^2/3$, then the system kinetic energy can be written as

$$T = \frac{1}{2}(m\ell^2)\dot{q}_1^2 + \frac{1}{2}(\frac{4}{3}m\ell^2)\dot{q}_2^2 + [m\ell^2 \cos(q_1 - q_2)]\dot{q}_1\dot{q}_2 \ . \qquad \text{(B-18)}$$

Since T has form (B-1b) and the constraint conditions are satisfied, this system qualifies to be analyzed by the proposed procedure.

2. The only applied force experienced by this system is the gravitational force because of the potential energy,

$$V = - mg\ell(\cos q_1 + \cos q_2) \ .$$

Since $V(q_1,q_2,\ldots,q_n)$ exists and the constraints are scleronomous, this mechanical system is conservative.

3. By comparing (B-1b) and (B-18), the coefficients can immediately be written as

$$\left.\begin{aligned} a_{11} &= m\ell^2 \\ a_{12} &= a_{21} = m\ell^2 \cos(q_1 - q_2) \\ a_{22} &= \frac{4}{3} m\ell^2 \ . \end{aligned}\right\} \qquad \text{(B-19)}$$

Now applying definition (B-11b), and noting that $L = T - V$, results in the following expressions:

$$C_1 = - mg\ell \sin q_1 - m\ell^2 \sin(q_1 - q_2)u_2^2$$

$$C_2 = - mg\ell \sin q_2 + m\ell^2 \sin(q_1 - q_2)u_1^2$$

where $\dot{q}_1$ and $\dot{q}_2$ have been replaced by u_1 and u_2, respectively. The complete set of 4 differential equations for this problem are

$$\left.\begin{aligned} \dot{q}_1 &= u_1 \\ \dot{q}_2 &= u_2 \\ a_{11}\dot{u}_1 + a_{12}\dot{u}_2 &= C_1 \\ a_{21}\dot{u}_1 + a_{22}\dot{u}_2 &= C_2 \,. \end{aligned}\right\} \qquad \text{(B-20)}$$

4. If an IBM system/360 computer and the FORTRAN IV language are assumed, then the Scientific Subroutine Package[26] offers a large selection of library subroutines. For example, subroutines GELS and HPCG may be selected. The former solves a system of simultaneous linear algebraic equations with symmetric coefficient matrix and the latter solves a set of first order ordinary differential equations with given initial conditions.
5. Instead of displaying an actual listing of a computer program, it is more instructive to describe the application of the flow chart in Figure B-1 to this specific problem. Input data must include values of integration interval, $m, \ell, q_1(0)$, $q_2(0)$, $\dot{q}_1(0)$, and $\dot{q}_2(0)$, assuming different size rods and bars are to be investigated. These values would then be printed on an output sheet to identify following results. These data are also set equal to array elements which are required to start numerical integration. At each step of this process the function subroutine receives current values of q_1, q_2, u_1, u_2,

and t. These are used to calculate $a_{11}, a_{12}, a_{21}, a_{22}$ from (B-19). Then the function subroutine calls on the algebraic equation solver, GELS to calculate $\dot{u}_1$ and $\dot{u}_2$ by solving system (B-20) and send this information back. The differential equation subroutine, HPCG then receives values of $\dot{q}_1, \dot{q}_2, \dot{u}_1$, and $\dot{u}_2$ to be used in the next integration step. Also during each step, the output subroutine is called upon to tabulate data related to that step. However, this subroutine does not have to check a dependent variable value for integration termination, because the final value of the independent variable, time, is the criterion for stopping HPCG. This avoids the necessity of interpolating to get accurate final values, since termination will occur exactly at the end of the given time interval. Last operation of this program before re-cycling with new input data is to print final values of q_1, q_2, u_1, u_2, $\dot{u}_1$, and $\dot{u}_2$.

VIII. CONCLUDING REMARKS

Primary objective of this treatise is to introduce a step-by-step procedure for obtaining a computer solution to the motion of a mechanical system. This sequence of steps requires a minimum of time and effort by investigators, as compared with other methods of solving the same given problem by numerical techniques. Development of this procedure grew out of the formalisms of analytical mechanics with the availability of mathematical library subroutines as an influencing factor. This is done in such a way that advantages of both analytical and numerical

methods are employed in an optimum manner. Of course, the usual objection to numerical solutions is still present, in that only particular cases of any problem can be solved. This need not be a major drawback in engineering applications, because interesting ranges of values of important parameters are usually known a priori. Several particular cases with values in these ranges may be run, and the result can be a set of data which, in effect, makes a solution general enough for engineering use. In addition to this method of getting a somewhat general solution, a great deal can be done with computer programming techniques to analyze and reduce computed results and construct plots directly from computer output which give an accurate picture of variable dependence on important parameters and initial conditions. It would seem the maximum capabilities of this procedure for solving the motion of a mechanical system can best be realized through the combined efforts of analytical mechanicians and digital computer programmers. The next logical step in developing this procedure would be the construction of a library subroutine which incorporates all parts of the program outlined in part V, except the function subroutine which generates values of a_{ij} and C_i. Then an investigator would have to supply only expressions (B-12) and (B-11) for the particular problem at hand, provided, of course, that the problem qualifies for analysis by this procedure.

APPENDIX C. COMPUTER SIMULATION PROGRAMS

Computer programs constructed for this investigation are written in the FORTRAN IV language and were run on an IBM system 360/67 at the Stanford University Computation Center with the WATFOR (Waterloo Fast FORTRAN) compiler. These programs may also be run on other compilers which use this language.

Listings of these programs are presented on the following pages. Input data formats are also given for each. Since the same library subroutine, HPCG is used in all of these programs, it is not listed in each case, but is described in reference . Because WATFOR does not link edit, HPCG is renamed in these programs as HPMK to avoid confusion. This subroutine integrates a set of first order ordinary differential equations.

Programs are located as follows:

```
C TWO DIMENSIONAL HOP SIMULATION OF SHOT VEHICLE
C ***************************************************************
C INSTRUCTIONS FOR USING THIS PROGRAM:
C DATA CARD NO  1-- HEADING:
C                   THE FIRST 76 COLS. OF THIS CARD MAY CONTAIN ANYTHING
C                   THAT IS DESIRED FOR A HEADING ON THE OUTPUT.
C                   SINCE THIS PROGRAM WILL GIVE GOOD DATA WITH ANY
C                   CONSISTENT SET OF UNITS, THE HEADING SHOULD INCLUDE
C                   THE SYSTEM OF UNITS USED, E.G., MKS, FT/SLUG/SEC.
C                   USE OF COLS. 77-80 IS OPTIONAL.
C DATA CARD NO. 2-- GENERAL PARAMETERS:
C                   COL 1=ND,NO. OF DIMS. FOR THIS SET OF DATA.(=1 OR 2)
C                   COLS 2-10=GRAVITY CONST.(XXXXX.XXX)
C                   COLS 11-20=PRIMARY MASS,M(XXXXXX.XXX)
C                   COLS 21-30=LEG-PLUS-FOOT MASS.(XXXXXX.XXX)
C                   COLS 31-40=HOP STARTING TIME, TZERO.(XXXXXX.XXX)
C                   COLS 41-50=LMZERO.(XXXXXX.XXX)
C                   COLS 51-60=LMENGG.(XXXXXX.XXX)
C                   COLS 61-80=OPTIONAL.
C                   THESE PARAMETERS APPLY TO ALL CASES.
C DATA CARD NO. 3-- PROPULSION SPECIFICATIONS AND SLOPE:
C                   COLS 1-10=P0(INITIAL PRESS.)(XXXXXX.XXX)
C                   COLS 11-20=GAMMA(XXXXXX.XXX)(>OR=0.0)
C                   COLS 21-30=A,PISTON AREA(XXXXXX.XXX)
C                   COLS 31-40=DZERO (VZERO=A*DZERO) (XXXXXX.XXX)
C                   COLS 41-50=SLOPE(DEG)(XXXXXX.XXX)(NOT REQ'D IF ND=1)
C                   COLS 51-80=OPTIONAL
C DATA CARD NO. 4-- NUM. INTEGRATION PARAMETERS:
C                   THIS CARD IS BLANK IF GAMMA=0.0(CONST. PRESS.)
C                   OTHERWISE USE THE FOLLOWING FORMAT:
C                   COLS 1-10=TIME INCREMENT IN NUMERICAL INTEGRATION
C                   (XXXX.XXXXX)
C                   COLS 11-20=ERROR IN NUMERICAL INT. (XXXX.XXXXX)
C                   COLS 21-80=OPTIONAL
C***************************************************************
C MAIN PROGRAM FOLLOWS:
```

```
C*****************************************************************
      REAL HDNG(19),PARAM(7),DPT2(2),DDPT2(2),AUX1(16,2),TENMAX/100.0/,
     1ACO(2)/2*0.5/,LMZR,LMEN
      INTEGER ND
      EXTERNAL OUT1,FUNCT1,FUNCT2,OUT2
      COMMON/OUT/LMEN,TIME/FUN1/BMASS,EFGRAV,ZDUM,XDUM,CODUM
     1/FUN2/GAMMA,AREA/INT/NJUMP
   10 READ(5,15,END=999) HDNG
   15 FORMAT(19A4)
      READ(5,25) ND,GRAV,BMASS,SMASS,TZERO,LMZR,LMEN
   25 FORMAT(I1,F9.3,5F10.3)
      GO TO(20,100),ND
   20 READ(5,35) PZERO,GAMMA,AREA,DZERO
   35 FORMAT(4F10.3)
      READ(5,45) TINCRE,ERROR
   45 FORMAT(2F10.5)
      WRITE(6,55) HDNG
   55 FORMAT('1',19A4///)
      CONST=PZERO*(AREA*DZERO)**GAMMA
      WRITE(6,65) ND,PZERO,AREA,DZERO,TZERO,LMZR,LMEN,GAMMA,GRAV,BMASS,
     1SMASS,CONST
   65 FORMAT(3X,'THE PARAMETERS FOR THIS FLIGHT ARE AS FOLLOWS.'//5X,'TH
     1IS IS A ',I1,'-DIMENSIONAL HOP WITH INITIAL PRESSURE =',F10.3,5X
     2,'PISTON AREA =',F10.3,5X,'INIT. DISPLACEMENT =',F10.3//5X,'TO ='
     3,F10.3,5X,'LMZERO =',F10.3,5X,'LMENGG =',F10.3,5X,'GAMMA =',
     4F10.3,5X,'GRAVITY CONST. =',F9.3//5X,'MAIN BODY MASS =',F10.3,
     55X,'LEG MASS =',F10.3,5X,'PZERO*(A*DZERO)**GAMMA = KZERO =',F12.3)
      EFGRAV=GRAV
      DELLME=LMEN-LMZR
      ZDUM=LMZR
      XDUM=DZERO
      CODUM=CONST
      IF(DELLME) 70,70,80
   70 WRITE(6,75)
   75 FORMAT(//' ERROR: LMENGG MUST BE GREATER THAN LMZERO.')
      GO TO 10
```

```
 80 IF(GAMMA) 90,140,110
 90 WRITE(6,95)
 95 FORMAT(//' ERROR: EXPANSION EXPONENT MUST BE GRTER THAN OR=0.0')
    GO TO 10
110 WRITE(6,275) TINCRE,ERROR
275 FORMAT(//' THE NON-CONST. PRESSURE GASEXP CASES REQUIRE A NUMERICA
   1L INTEGRATION OF THE ACCEL. AND DECEL. PHASES.  HERE WE USE:'
   2// ' STEP SIZE =',F10.5,3X,'UPPER ERROR BOUND =',F10.5//
   3' ACCEL PHASE:')
    IF(GAMMA-1.0) 340,290,340
140 WRITE(6,175)
175 FORMAT(//' THE CONST. PRESSURE GASEXP CASES DO NOT REQUIRE ANY NUM
   1ERICAL INTEGRATIONS.')
    DDLMZR=(CONST*AREA)/BMASS-GRAV
    IF(DDLMZR) 200,200,210
200 WRITE(6,205) DDLMZR
205 FORMAT(//' THE PRESSURE IS TOO LOW.  THUS, WE HAVE AN ACCEL. OF',F
   110.3)
    GO TO 10
210 DUMM1=(2*DELLME)/DDLMZR
    TENGG=TZERO+SQRT(DUMM1)
    DLMEN=DDLMZR*(TENGG-TZERO)
220 DZENGG=(BMASS/(BMASS+SMASS))*DLMEN
    T2=TENGG+DZENGG/GRAV
    TASC=T2-TENGG
    ZMAXM=LMEN+DZENGG*TASC-0.5*GRAV*TASC*TASC
    TH=2*(T2-TZERO)
    WRITE(6,226)
226 FORMAT(//' BALLISTIC ASCENT:'//' ',5X,'TIME',6X,'ALTITUDE',2X,'VEL
   1OCITY')
    T=TENGG
    DELT=TASC*0.1
    DO 228 I=1,10
    T=T+DELT
    ALT=LMEN+DZENGG*(T-TENGG)-0.5*GRAV*(T-TENGG)*(T-TENGG)
    VEL=DZENGG-GRAV*(T-TENGG)
```

```
      WRITE(6,227) T,ALT,VEL
  227 FORMAT(' ',2X,F10.5,2F10.3)
  228 CONTINUE
      WRITE(6,225) DDLMZR,TENGG,TASC,TH,ZMAXM,DLMEN,DZENGG
  225 FORMAT(//' RESULTS:'//'  INITIAL ACCEL. =',F10.3,'   TIME OF ENGAG
     1EMENT, T1 =',F10.3,'   TIME OF BALLISTIC ASCENT =',F10.3//'  TOTAL
     2 HOP TIME =',F10.3,' MAX. ALT. OF MAIN BODY C. M. =',F10.3//'  VEL
     3OCITY JUST BEFORE ENGAGEMENT =',F10.3,', AND JUST AFTER =',F10.3)
      GO TO 10
  290 DDLMZR=CONST/(BMASS*DZERO)-EFGRAV
  295 PARAM(6)=0.0
      NJUMP= 0
      PARAM(1)=TZERO
      PARAM(7)=0.0
      PARAM(2)=TENMAX
      PARAM(3)=TINCRE
      PARAM(4)=ERROR
      DPT2(1)=LMZR
      DPT2(2)=0.0
      DDPT2(1)=ACO(1)
      DDPT2(2)=ACO(2)
      N2DIM=2
      CALL HPMK(PARAM,DPT2,DDPT2,N2DIM,NBIS,FUNCT1,OUT1,AUX1)
      IF(PARAM(6)) 300,310,10
  300 ERROR=10*ERROR
      WRITE(6,302)
  302 FORMAT(///' UPPER ERROR BOUND IS TOO SMALL.  RESTARTING HPMK WITH
     1ERROR =10(ERROR).')
      GO TO 295
  310 WRITE(6,315) ERROR
  315 FORMAT(//' THE ACTUAL ERROR BOUND USED =',F10.5)
      WRITE(6,317) AUX1
  317 FORMAT(//' AUX. ARRAY IS:' /(' ',16F8.3))
      DUMM7=DPT2(1)-AUX1(7,1)
      IF(DUMM7) 320,320,330
  320 WRITE(6,325)
```

```
325 FORMAT(//' NO INTERPOLATION REQUIRED')
    TENGG=TIME
    DLMEN=DDPT2(1)
    GO TO 222
330 FINCRE=TINCRE/(2.0**NBIS)
    TENGG=TIME-FINCRE*(DPT2(1)-LMEN)/DUMM7
    DLMEN=AUX1(14,1)+(DDPT2(1)-AUX1(14,1))*(LMEN-AUX1(7,1))/DUMM7
222 GO TO (220,224), ND
340 DDLMZR=((1.0/AREA)**(GAMMA-1.0))*CONST/(BMASS*DZERO**GAMMA)-EFGRAV
345 PARAM(6)=0.0
    NJUMP= 0
    PARAM(7)=0.0
    PARAM(1)=TZERO
    PARAM(2)=TENMAX
    PARAM(3)=TINCRE
    PARAM(4)=ERROR
    DPT2(1)=LMZR
    DPT2(2)=0.0
    DDPT2(1)=ACO(1)
    DDPT2(2)=ACO(2)
    N2DIM=2
    CALL HPMK(PARAM,DPT2,DDPT2,N2DIM,NBIS,FUNCT2,OUT1,AUX1)
    IF(PARAM(6)) 360,310,10
360 ERROR=10*ERROR
    WRITE(6,302)
    GO TO 345
100 READ(5,105) PZERO,GAMMA,AREA,DZERO,SLOPE
105 FORMAT(5F10.3)
    READ(5,45) TINCRE,ERROR
    WRITE(6,55) HDNG
    CONST=PZERO*(AREA*DZERO)**GAMMA
    WRITE(6,65) ND,PZERO,AREA,DZERO,TZERO,LMZR,LMEN,GAMMA,GRAV,BMASS,
   1SMASS,CONST
    WRITE(6,107) SLOPE
107 FORMAT(//5X,'SLOPE =',F7.3,' DEGREES.')
    DELLME=LMEN-LMZR
```

```
    IF(DELLME) 70,70,130
130 ALPHA=0.785398+0.872665E-2*SLOPE
    DALPHA=57.29578*ALPHA
    IF(GAMMA) 90,150,155
155 EFGRAV=GRAV*SIN(ALPHA)
    ZDUM=LMZR
    XDUM=DZERO
    CODUM=CONST
    GO TO 110
150 WRITE(6,175)
    DDLMZR=(CONST*AREA)/BMASS-GRAV*SIN(ALPHA)
    IF(DDLMZR) 200,200,152
152 DUMM1=(2*DELLME)/DDLMZR
    TENGG=TZERO+SQRT(DUMM1)
    DLMEN=DDLMZR*(TENGG-TZERO)
224 DX1T1B=DLMEN*COS(ALPHA)
    DZ1T1B=DLMEN*SIN(ALPHA)
    RMASS=BMASS/(BMASS+SMASS)
    V1=RMASS*DLMEN
    DX1T1A=RMASS*DX1T1B
    DZ1T1A=RMASS*DZ1T1B
    X1T1=LMEN*COS(ALPHA)
    Z1T1=LMEN*SIN(ALPHA)
    RSLP=0.017453*SLOPE
    TWOALF=2*ALPHA
    DELRNG=2*V1*V1*(0.5*SIN(TWOALF)-TAN(RSLP)*COS(ALPHA)**2)/GRAV
    TBAL=DELRNG/DX1T1A
    T3=TBAL+TENGG
    DZ1T3=DZ1T1A-GRAV*TBAL
    Z1T3=Z1T1+DELRNG*TAN(RSLP)
    X1T3=DELRNG+X1T1
    TNBETA=(-DZ1T3)/DX1T1A
    RBETA=ATAN(TNBETA)
    BETA=57.29578*RBETA
    ALMSLP=ALPHA-RSLP
    BETPSL=RBETA+RSLP
```

```
      Z4T3=LMEN*SIN(ALMSLP)/SIN(BETPSL)
      DZ4T3=DZ1T3/SIN(RBETA)
      T2=TENGG+DZ1T1A/GRAV
      TASC=T2-TENGG
      X1T2=DX1T1A*TASC+X1T1
      Z1T2=Z1T1+DZ1T1A*TASC-0.5*GRAV*TASC*TASC
      BLTIME=T3-TENGG
      WRITE(6,154) DX1T1A
  154 FORMAT(//' BALLISTIC PHASE:   HORIZ. VELOCITY =',F10.3//6X,'TIME',
     16X,'ALTITUDE',4X,'RANGE',4X,'VELOCITY')
      T=TENGG
      DELT=BLTIME*0.1
      DO 156 I=1,10
      T=T+DELT
      TDIF=T-TENGG
      ALT=Z1T1+DZ1T1A*TDIF-0.5*GRAV*TDIF*TDIF
      RANGE=X1T1+DX1T1A*TDIF
      ZVEL=DZ1T1A-GRAV*TDIF
      VELSQ=DX1T1A*DX1T1A+ZVEL*ZVEL
      VEL=SQRT(VELSQ)
      DERNGE=RANGE-LMZR*COS(ALPHA)
      WRITE(6,106) T,ALT,DERNGE,VEL
  106 FORMAT(3X,F10.5,3F10.3)
  156 CONTINUE
      IF(GAMMA.GT.0.0) GO TO 470
      XT1=DELLME+DZERO
      XD=Z4T3-LMEN+XT1
      DDZ4T3=DZ4T3*DZ4T3*0.5/(XD-DZERO)
      CONSTD=BMASS*(DDZ4T3+GRAV*SIN(RBETA))/AREA
      PT3=CONSTD
      T4=T3-DZ4T3/DDZ4T3
      TH=T4-TZERO
      X1T4=X1T3+(XD-DZERO)*COS(RBETA)
      Z1T4=Z1T3-(XD-DZERO)*SIN(RBETA)
      X1T0=LMZR*COS(ALPHA)
      RMAL=X1T2-X1T0
```

```
      RDIS=X1T3-X1T0
      FRNG=X1T4-X1T0
      WRITE(6,158) TZERO,TENGG,T2,T3,T4,TASC,TBAL,TH,DDLMZR,DLMEN,V1,
     1RMAL,Z1T2,RDIS,Z1T3,Z4T3,DZ4T3,DDZ4T3,FRNG,Z1T4,DALPHA,BETA,DZERO,
     2PT3
  158 FORMAT(//' RESULTS:'// ' HOP STARTING TIME =',F10.3,3X,'TIME OF EN
     1GAGEMENT =',F10.3,3X,'TIME OF MAX. ALT. =',F10.3,3X,'TIME OF DISEN
     2GAGEMENT =',F10.3//' END OF HOP TIME =',F10.3,3X,'TIME TO ASCEND =
     3',F10.3,3X,'TIME OF BALLISTIC FLIGHT =',F10.3,3X,'TOTAL HOP TIME =
     4',F10.3//' INITIAL ACCEL. =',F10.3,3X,'LMENGG DOT =',F10.3,3X,'VE+
     5=',F10.3,3X,'RANGE AT MAX  ALT. =',F10.3,3X,'MAX. ALT. =',F10.3//
     6' RANGE AT DISENG. =',F10.3,3X,'ALT. AT DISENG. =',F10.3,3X,'LM(TD
     7) =',F10.3,3X,'LM(TD) DOT =',F10.3//' FINAL ACCEL. =',F10.3,3X,'FI
     8NAL RANGE =',F10.3,3X,'FINAL ALT. =',F10.3,3X,'ALPHA =',F6.3,' DEG
     9.  BETA =',F6.3,' DEG.'//' FINAL DISPLACEMENT =',F8.3,3X,'DISENG
     APRESSURE =',F10.3)
      GO TO 10
  470 XT1=DELLME+DZERO
      XD=Z4T3-LMEN+XT1
      EFGRAV=GRAV*SIN(RBETA)
      XDUM=XD
      ZDUM=Z4T3
      PT1=CONST/(AREA*XT1)**GAMMA
      PT3=(1.0-SIN(RSLP)*SIN(RSLP))*PT1
      WRITE(6,550) PT3,PT1
  550 FORMAT(//' DECEL PHASE:'//' TRYING P(TD) =',F10.3,3X,'NOTE: P(TE)
     1=',F10.3)
  472 CONSTD=PT3*(AREA*XD)**GAMMA
      CODUM=CONSTD
      PARAM(6)=0.0
      NJUMP= 0
      PARAM(1)=T3
      PARAM(7)=0.0
      PARAM(2)=TENMAX
      PARAM(3)=TINCRE
      PARAM(4)=ERROR
```

```
      DPT2(1)=Z4T3
      DPT2(2)=BMASS*DZ4T3
      DDPT2(1)=ACO(1)
      DDPT2(2)=ACO(2)
      N2DIM=2
      CALL HPMK(PARAM,DPT2,DDPT2,N2DIM,NBIS,FUNCT2,OUT2,AUX1)
      IF(PARAM(6)) 480,490,10
  480 ERROR=10*ERROR
      WRITE(6,302)
      GO TO 472
  490 DUMM7=DDPT2(1)-AUX1(14,1)
      IF(DUMM7) 500,500,510
  500 WRITE(6,325)
      T4=TIME
      Z4T4=DPT2(1)
      XT4=XD-Z4T3+Z4T4
      GO TO 520
  510 FINCRE=TINCRE/(2.0**NBIS)
      T4=TIME-FINCRE*DDPT2(1)/DUMM7
      Z4T4=DPT2(1)
      XT4=XD-Z4T3+Z4T4
  520 IF(XT4-DZERO) 530,540,540
  530 PT3=1.10*PT3
      WRITE(6,560) PT3
  560 FORMAT(//' P(TD) WAS TOO LOW.  NOW TRYING P(TD) =',F10.3)
      GO TO 472
  540 PT4=CONSTD/(AREA*XT4)**GAMMA
      DDZ4T4=CONSTD/(BMASS*AREA**(GAMMA-1.0)*(Z4T4-Z4T3+XD)**GAMMA)
     1-GRAV*SIN(RBETA)
      WRITE(6,315) ERROR
      WRITE(6,317) AUX1
      TH=T4-TZERO
      X1T4=X1T3+(XD-XT4)*COS(RBETA)
      Z1T4=Z1T3-(XD-XT4)*SIN(RBETA)
      X1T0=LMZR*COS(ALPHA)
      RMAL=X1T2-X1T0
```

```
      RDIS=X1T3-X1T0
      FRNG=X1T4-X1T0
      WRITE(6,158) TZERO,TENGG,T2,T3,T4,TASC,TBAL,TH,DDLMZR,DLMEN,V1,
     1RMAL,Z1T2,RDIS,Z1T3,Z4T3,DZ4T3,DDZ4T4,FRNG,Z1T4,DALPHA,BETA,DZERO,
     2PT3
      WRITE(6,159) PT4
  159 FORMAT('+',63X,'FINAL PRESSURE =',F10.3)
      GO TO 10
  999 RETURN
      END
C*********************************************************************
C SUBROUTINES FOLLOW:
C*********************************************************************
      SUBROUTINE OUT1(T,DP,DDP,NB,N2D,PAR)
      REAL PAR(7),DP(2),DDP(2),T
      INTEGER N2D,NB
      COMMON/OUT/Z1,TIME/INT/NJUMP/FUN1/BIGM,BLK1,BLK2,BLK3,BLK4
      TIME=T
      NJUMP=NJUMP+1
      ACCEL=DDP(2)/BIGM
      IF(NB-11) 10,20,30
   20 PAR(6)=-1.0
      GO TO 99
   30 WRITE(6,35) NB
   35 FORMAT(//' HPMK ERROR CODE =',I2)
      PAR(6)=1.0
      GO TO 99
   10 IF(PAR(7)) 40,50,40
   50 WRITE(6,55) T,DP(1),DDP(1),ACCEL,NB
   55 FORMAT(//9X,'TIME',9X,'LM',6X,'LMDOT',6X,'ACCEL',3X,'IHLF'
     1//(' ',5X,F10.5,3F10.3,3X,I2))
      PAR(7)=1.0
   58 IF(Z1-DP(1)) 60,60,99
   60 PAR(5)=1.0
      WRITE(6,45) T,DP(1),DDP(1),ACCEL,NB
      GO TO 99
```

```
   40 IF(NJUMP-3 ) 58,70,70
   70 NJUMP=0
      WRITE(6,45) T,DP(1),DDP(1),ACCEL,NB
   45 FORMAT(' ',5X,F10.5,3F10.3,3X,I2)
      GO TO 58
   99 RETURN
      END
C*********************************************************************
      SUBROUTINE FUNCT1(T,DP,DDP)
      REAL DP(2),DDP(2),T,M,K
      COMMON/FUN1/M,GRAV,ZZ,XZ,K
      DUM=DP(1)-ZZ+XZ
      IF(DUM) 40,40,30
   40 WRITE(6,45) DUM
   45 FORMAT(//' ERROR: YOU ARE ABOUT TO WIPE-OUT. DUM MUST BE GT 0.0'
     1//' TRY SMALLER INTEGRATION INCREMENT.  NOTE: DUM =',F10.3)
      DUM=DUM**2.5
   30 DDP(1)=DP(2)/M
      DDP(2)=K/DUM-M*GRAV
      RETURN
      END
C*********************************************************************
      SUBROUTINE FUNCT2(T,DP,DDP)
      REAL DP(2),DDP(2),T,M,K
      COMMON/FUN1/M,GRAV,ZZ,XZ,K/FUN2/EX,A
      DUM=DP(1)-ZZ+XZ
      IF(DUM) 40,40,30
   40 WRITE(6,45) DUM
   45 FORMAT(//' ERROR: YOU ARE ABOUT TO WIPE-OUT  DUM MUST BE GT 0.0'
     1//' TRY SMALLER INTEGRATION INCREMENT.  NOTE: DUM =',F10.3)
   30 DDP(1)=DP(2)/M
      DDP(2)=(1.0/A)**(EX-1.0)*K/DUM**EX-M*GRAV
      RETURN
      END
C*********************************************************************
      SUBROUTINE OUT2(T,DP,DDP,NB,N2D,PAR)
```

```
      REAL PAR(7),DP(2),DDP(2),T
      INTEGER N2D,NB
      COMMON/OUT/BLK,TIME/INT/NJUMP/FUN1/BIGM,BLK1,BLK2,BLK3,BLK4
      TIME=T
      NJUMP=NJUMP+1
      ACCEL=DDP(2)/BIGM
      IF(NB-11) 10,20,30
   20 PAR(6)=-1.0
      GO TO 99
   30 WRITE(6,35) NB
   35 FORMAT(//' HPMK ERROR CODE =',I2)
      PAR(6)=1.0
      GO TO 99
   10 IF(PAR(7)) 40,50,40
   50 WRITE(6,55) T,DP(1),DDP(1),ACCEL,NB
   55 FORMAT(//9X,'TIME',9X,'LM',6X,'LMDOT',6X,'ACCEL',3X,'IHLF'
     1//(' ',5X,F10.5,3F10.3,3X,I2))
      PAR(7)=1.0
   58 IF(DDP(1)) 99,60,60
   60 PAR(5)=1.0
      WRITE(6,45) T,DP(1),DDP(1),ACCEL,NB
      GO TO 99
   40 IF(NJUMP-3 ) 58,70,70
   70 NJUMP=0
      WRITE(6,45) T,DP(1),DDP(1),ACCEL,NB
   45 FORMAT(' ',5X,F10.5,3F10.3,3X,I2)
      GO TO 58
   99 RETURN
      END
C THIS IS THE END OF THE PROGRAM PECULIAR TO SHOT.
C SUBROUTINE HPMK (HPCG) IS ADDED HERE WHEN RUNNING PROGRAM.
```

```
C TWO DIMENSIONAL HOP SIMULATION OF HOLAB VEHICLE
C ************************************************************
C INSTRUCTIONS FOR USING THIS PROGRAM:
C DATA CARD NO. 1-- HEADING:
C                   THE FIRST 76 COLS. OF THIS CARD MAY CONTAIN ANYTHING
C                   THAT IS DESIRED FOR A HEADING ON THE OUTPUT
C                   SINCE THIS PROGRAM WILL GIVE GOOD DATA WITH ANY
C                   CONSISTENT SET OF UNITS, THE HEADING SHOULD INCLUDE
C                   THE SYSTEM OF UNITS USED, E.G., MKS, FT/SLUG/SEC.
C                   USE OF COLS. 77-80 IS OPTIONAL.
C DATA CARD NO. 2-- GENERAL PARAMETERS:
C                   COL 1=ND,NO  OF DIMS. FOR THIS SET OF DATA.(=1 OR 2)
C                   COLS 2-10=GRAVITY CONST.(XXXXX.XXX)
C                   COLS 11-20=PRIMARY MASS,M(XXXXXX.XXX)
C                   COLS 21-30=LEG-PLUS-FOOT MASS.(XXXXXX.XXX)
C                   COLS 31-40=HOP STARTING TIME, TZERO.(XXXXXX.XXX)
C                   COLS 41-50=ZPZERO.(XXXXXX.XXX)
C                   COLS 51-60=ZPENGG.(XXXXXX.XXX)
C                   COLS 61-80=OPTIONAL.
C                   THESE PARAMETERS APPLY TO ALL CASES.
C DATA CARD NO  3-- PROPULSION SPECIFICATIONS AND SLOPE:
C                   COLS 1-10=P0(INITIAL PRESS.)(XXXXXX.XXX)
C                   COLS 11-20=GAMMA(XXXXXX.XXX)(>OR=0.0)
C                   COLS 21-30=A,PISTON AREA(XXXXXX.XXX)
C                   COLS 31-40=DZERO (VZERO=A*DZERO) (XXXXXX.XXX)
C                   COLS 41-50=GEAR RATIO(XXXXXX.XXX)
C                   COLS 51-60=SLOPE(DEG)(XXXXXX.XXX)(NOT REQ'D IF ND=1)
C                   COLS 61-80=OPTIONAL
C DATA CARD NO. 4-- NUM. INTEGRATION PARAMETERS:
C                   THIS CARD IS BLANK IF GAMMA=0.0(CONST. PRESS.)
C                   OTHERWISE USE THE FOLLOWING FORMAT:
C                   COLS 1-10=TIME INCREMENT IN NUMERICAL INTEGRATION.
C                   (XXXX.XXXXX)
C                   COLS 11-20=ERROR IN NUMERICAL INT. (XXXX.XXXXX)
C                   COLS 21-80=OPTIONAL
C************************************************************
```

```
C MAIN PROGRAM FOLLOWS:
C*****************************************************************
      REAL HDNG(19),PARAM(7),DPT2(2),DDPT2(2),AUX1(16,2),TENMAX/100.0/,
     1ACO(2)/2*0.5/,ZPZR,ZPEN
      INTEGER ND
      EXTERNAL OUT1,FUNCT1,FUNCT2,OUT2
      COMMON/OUT/ZPEN,TIME/FUN1/BMASS,EFGRAV,ZDUM,XDUM,CODUM,GRAT
     1/FUN2/GAMMA,AREA/INT/NJUMP
   10 READ(5,15,END=999) HDNG
   15 FORMAT(19A4)
      READ(5,25) ND,GRAV,BMASS,SMASS,TZERO,ZPZR,ZPEN
   25 FORMAT(I1,F9.3,5F10.3)
      GO TO(20,100),ND
   20 READ(5,35) PZERO,GAMMA,AREA,DZERO,GRAT
   35 FORMAT(5F10.3)
      READ(5,45) TINCRE,ERROR
   45 FORMAT(2F10.5)
      WRITE(6,55) HDNG
   55 FORMAT('1',19A4///)
      CONST=PZERO*(AREA*DZERO)**GAMMA
      WRITE(6,65) ND,PZERO,AREA,DZERO,TZERO,ZPZR,ZPEN,GAMMA,GRAV,BMASS,
     1SMASS,CONST,GRAT
   65 FORMAT(3X,'THE PARAMETERS FOR THIS FLIGHT ARE AS FOLLOWS.'//5X,'TH
     1IS IS A ',I1,'-DIMENSIONAL HOP WITH INITIAL PRESSURE =',F10.3,5X
     2,'PISTON AREA =',F10.3,5X,'INIT. DISPLACEMENT =',F10.3//5X,'TO ='
     3,F10.3,5X,'ZPZERO =',F10.3,5X,'ZPENGG =',F10.3,5X,'GAMMA =',
     4F10.3,5X,'GRAVITY CONST. =',F9.3//5X,'MAIN BODY MASS =',F10.3,
     55X,'LEG MASS =',F10.3,5X,'PZERO*(A*DZERO)**GAMMA = KZERO =',F12.3/
     6/5X,'GEAR RATIO =',F10.3)
      EFGRAV=GRAV
      DELZPE=ZPEN-ZPZR
      ZDUM=ZPZR
      XDUM=DZERO
      CODUM=CONST
      IF(DELZPE) 70,70,80
   70 WRITE(6,75)
```

```
 75 FORMAT(//' ERROR: ZPENGG MUST BE GREATER THAN ZPZERO.')
    GO TO 10
 80 IF(GAMMA) 90,140,110
 90 WRITE(6,95)
 95 FORMAT(//' ERROR: EXPANSION EXPONENT MUST BE GRTER THAN OR=0.0')
    GO TO 10
110 WRITE(6,275) TINCRE,ERROR
275 FORMAT(//' THE NON-CONST. PRESSURE GASEXP CASES REQUIRE A NUMERICA
   1L INTEGRATION OF THE ACCEL. AND DECEL. PHASES.  HERE WE USE:'
   2// ' STEP SIZE =',F10.5,3X,'UPPER ERROR BOUND =',F10.5//
   3' ACCEL PHASE:')
    IF(GAMMA-1.0) 340,290,340
140 WRITE(6,175)
175 FORMAT(//' THE CONST. PRESSURE GASEXP CASES DO NOT REQUIRE ANY NUM
   1ERICAL INTEGRATIONS.')
    DDZPZR=(CONST*AREA)/(BMASS*GRAT)-GRAV
    IF(DDZPZR) 200,200,210
200 WRITE(6,205) DDZPZR
205 FORMAT(//' THE PRESSURE IS TOO LOW.  THUS, WE HAVE AN ACCEL. OF',F
   110.3)
    GO TO 10
210 DUMM1=(2*DELZPE)/DDZPZR
    TENGG=TZERO+SQRT(DUMM1)
    DZPEN=DDZPZR*(TENGG-TZERO)
220 DZENGG=(BMASS/(BMASS+SMASS))*DZPEN
    T2=TENGG+DZENGG/GRAV
    TASC=T2-TENGG
    ZMAXM=ZPEN+DZENGG*TASC-0.5*GRAV*TASC*TASC
    TH=2*(T2-TZERO)
    WRITE(6,226)
226 FORMAT(//' BALLISTIC ASCENT:'//' ',5X,'TIME',6X,'ALTITUDE',2X,'VEL
   10CITY')
    T=TENGG
    DELT=TASC*0.1
    DO 228 I=1,10
    T=T+DELT
```

```
      ALT=ZPEN+DZENGG*(T-TENGG)-0.5*GRAV*(T-TENGG)*(T-TENGG)
      VEL=DZENGG-GRAV*(T-TENGG)
      WRITE(6,227) T,ALT,VEL
  227 FORMAT(' ',2X,F10.5,2F10.3)
  228 CONTINUE
      WRITE(6,225) DDZPZR,TENGG,TASC,TH,ZMAXM,DZPEN,DZENGG
  225 FORMAT(//' RESULTS:'//'  INITIAL ACCEL. =',F10.3,'   TIME OF ENGAG
     1EMENT, T1 =',F10.3,'   TIME OF BALLISTIC ASCENT =',F10.3//'  TOTAL
     2 HOP TIME =',F10.3,' MAX. ALT. OF MAIN BODY C. M. =',F10.3//'  VEL
     3OCITY JUST BEFORE ENGAGEMENT =',F10.3,', AND JUST AFTER =',F10.3)
      GO TO 10
  290 DDZPZR=CONST/(BMASS*DZERO*GRAT)-EFGRAV
  295 PARAM(6)=0.0
      NJUMP= 0
      PARAM(1)=TZERO
      PARAM(7)=0.0
      PARAM(2)=TENMAX
      PARAM(3)=TINCRE
      PARAM(4)=ERROR
      DPT2(1)=ZPZR
      DPT2(2)=0.0
      DDPT2(1)=ACO(1)
      DDPT2(2)=ACO(2)
      N2DIM=2
      CALL HPMK(PARAM,DPT2,DDPT2,N2DIM,NBIS,FUNCT1,OUT1,AUX1)
      IF(PARAM(6)) 300,310,10
  300 ERROR=10*ERROR
      WRITE(6,302)
  302 FORMAT(///' UPPER ERROR BOUND IS TOO SMALL   RESTARTING HPMK WITH
     1ERROR =10(ERROR).')
      GO TO 295
  310 WRITE(6,315) ERROR
  315 FORMAT(//' THE ACTUAL ERROR BOUND USED =',F10.5)
      WRITE(6,317) AUX1
  317 FORMAT(//' AUX. ARRAY IS:' /(' ',16F8.3))
      DUMM7=DPT2(1)-AUX1(7,1)
```

```
      IF(DUMM7) 320,320,330
  320 WRITE(6,325)
  325 FORMAT(//' NO INTERPOLATION REQUIRED')
      TENGG=TIME
      DZPEN=DDPT2(1)
      GO TO 222
  330 FINCRE=TINCRE/(2.0**NBIS)
      TENGG=TIME-FINCRE*(DPT2(1)-ZPEN)/DUMM7
      DZPEN=AUX1(14,1)+(DDPT2(1)-AUX1(14,1))*(ZPEN-AUX1(7,1))/DUMM7
  222 GO TO (220,224), ND
  340 DDZPZR=((GRAT/AREA)**(GAMMA-1.0))*CONST/(BMASS*(DZERO*GRAT)**GAMMA
     1)-EFGRAV
  345 PARAM(6)=0.0
      NJUMP= 0
      PARAM(7)=0.0
      PARAM(1)=TZERO
      PARAM(2)=TENMAX
      PARAM(3)=TINCRE
      PARAM(4)=ERROR
      DPT2(1)=ZPZR
      DPT2(2)=0.0
      DDPT2(1)=ACO(1)
      DDPT2(2)=ACO(2)
      N2DIM=2
      CALL HPMK(PARAM,DPT2,DDPT2,N2DIM,NBIS,FUNCT2,OUT1,AUX1)
      IF(PARAM(6)) 360,310,10
  360 ERROR=10*ERROR
      WRITE(6,302)
      GO TO 345
  100 READ(5,105) PZERO,GAMMA,AREA,DZERO,GRAT,SLOPE
  105 FORMAT(6F10.3)
      READ(5,45) TINCRE,ERROR
      WRITE(6,55) HDNG
      CONST=PZERO*(AREA*DZERO)**GAMMA
      WRITE(6,65) ND,PZERO,AREA,DZERO,TZERO,ZPZR,ZPEN,GAMMA,GRAV,BMASS,
     1SMASS,CONST,GRAT
```

```
      WRITE(6,107) SLOPE
  107 FORMAT(//5X,'SLOPE =',F7.3,' DEGREES.')
      DELZPE=ZPEN-ZPZR
      IF(DELZPE) 70,70,130
  130 ALPHA=0.785398+0.872665E-2*SLOPE
      DALPHA=57.29578*ALPHA
      IF(GAMMA) 90,150,155
  155 EFGRAV=GRAV*SIN(ALPHA)
      ZDUM=ZPZR
      XDUM=DZERO
      CODUM=CONST
      GO TO 110
  150 WRITE(6,175)
      DDZPZR=(CONST*AREA)/(BMASS*GRAT)-GRAV*SIN(ALPHA)
      IF(DDZPZR) 200,200,152
  152 DUMM1=(2*DELZPE)/DDZPZR
      TENGG=TZERO+SQRT(DUMM1)
      DZPEN=DDZPZR*(TENGG-TZERO)
  224 DX1T1B=DZPEN*COS(ALPHA)
      DZ1T1B=DZPEN*SIN(ALPHA)
      RMASS=BMASS/(BMASS+SMASS)
      V1=RMASS*DZPEN
      DX1T1A=RMASS*DX1T1B
      DZ1T1A=RMASS*DZ1T1B
      X1T1=ZPEN*COS(ALPHA)
      Z1T1=ZPEN*SIN(ALPHA)
      RSLP=0.017453*SLOPE
      TWOALF=2*ALPHA
      DELRNG=2*V1*V1*(0.5*SIN(TWOALF)-TAN(RSLP)*COS(ALPHA)**2)/GRAV
      TBAL=DELRNG/DX1T1A
      T3=TBAL+TENGG
      DZ1T3=DZ1T1A-GRAV*TBAL
      Z1T3=Z1T1+DELRNG*TAN(RSLP)
      X1T3=DELRNG+X1T1
      TNBETA=(-DZ1T3)/DX1T1A
      RBETA=ATAN(TNBETA)
```

```
      BETA=57.29578*RBETA
      ALMSLP=ALPHA-RSLP
      BETPSL=RBETA+RSLP
      Z4T3=ZPEN*SIN(ALMSLP)/SIN(BETPSL)
      DZ4T3=DZ1T3/SIN(RBETA)
      T2=TENGG+DZ1T1A/GRAV
      TASC=T2-TENGG
      X1T2=DX1T1A*TASC+X1T1
      Z1T2=Z1T1+DZ1T1A*TASC-0.5*GRAV*TASC*TASC
      BLTIME=T3-TENGG
      WRITE(6,154) DX1T1A
  154 FORMAT(//' BALLISTIC PHASE:   HORIZ. VELOCITY =',F10.3//6X,'TIME',
     16X,'ALTITUDE',4X,'RANGE',4X,'VELOCITY')
      T=TENGG
      DELT=BLTIME*0.1
      DO 156 I=1,10
      T=T+DELT
      TDIF=T-TENGG
      ALT=Z1T1+DZ1T1A*TDIF-0.5*GRAV*TDIF*TDIF
      RANGE=X1T1+DX1T1A*TDIF
      ZVEL=DZ1T1A-GRAV*TDIF
      VELSQ=DX1T1A*DX1T1A+ZVEL*ZVEL
      VEL=SQRT(VELSQ)
      DERNGE=RANGE-ZPZR*COS(ALPHA)
      WRITE(6,106) T,ALT,DERNGE,VEL
  106 FORMAT(3X,F10.5,3F10.3)
  156 CONTINUE
      IF(GAMMA.GT.0.0) GO TO 470
      XT1=DELZPE+DZERO
      XD=Z4T3-ZPEN+XT1
      DDZ4T3=DZ4T3*DZ4T3*0.5/(GRAT*(XD-DZERO))
      CONSTD=BMASS*GRAT*(DDZ4T3+GRAV*SIN(RBETA))/AREA
      PT3=CONSTD
      T4=T3-DZ4T3/DDZ4T3
      TH=T4-TZERO
      X1T4=X1T3+(XD-DZERO)*COS(RBETA)*GRAT
```

```
      Z1T4=Z1T3-(XD-DZERO)*SIN(RBETA)*GRAT
      X1T0=ZPZR*COS(ALPHA)
      RMAL=X1T2-X1T0
      RDIS=X1T3-X1T0
      FRNG=X1T4-X1T0
      WRITE(6,158) TZERO,TENGG,T2,T3,T4,TASC,TBAL,TH,DDZPZR,DZPEN,V1,
     1RMAL,Z1T2,RDIS,Z1T3,Z4T3,DZ4T3,DDZ4T3,FRNG,Z1T4,DALPHA,BETA,DZERO,
     2PT3
  158 FORMAT(//' RESULTS:'// ' HOP STARTING TIME =',F10.3,3X,'TIME OF EN
     1GAGEMENT =',F10.3,3X,'TIME OF MAX. ALT. =',F10.3,3X,'TIME OF DISEN
     2GAGEMENT =',F10.3//' END OF HOP TIME =',F10.3,3X,'TIME TO ASCEND =
     3',F10.3,3X,'TIME OF BALLISTIC FLIGHT =',F10.3,3X,'TOTAL HOP TIME =
     4',F10.3//' INITIAL ACCEL. =',F10.3,3X,'ZPENGG DOT =',F10.3,3X,'VE+
     5=',F10.3,3X,'RANGE AT MAX. ALT. =',F10.3,3X,'MAX. ALT. =',F10.3//
     6' RANGE AT DISENG. =',F10.3,3X,'ALT. AT DISENG. =',F10.3,3X,'ZP(TD
     7) =',F10.3,3X,'ZP(TD) DOT =',F10.3//' FINAL ACCEL. =',F10.3,3X,'FI
     8NAL RANGE =',F10.3,3X,'FINAL ALT. =',F10.3,3X,'ALPHA =',F6.3,' DEG
     9.  BETA =',F6.3,' DEG.'//' FINAL DISPLACEMENT =',F8.3,3X,'DISENG.
     APRESSURE =',F10.3)
      GO TO 10
  470 XT1=DELZPE/GRAT+DZERO
      XD=(Z4T3-ZPEN)/GRAT+XT1
      EFGRAV=GRAV*SIN(RBETA)
      XDUM=XD
      ZDUM=Z4T3
      PT1=CONST/(AREA*XT1)**GAMMA
      PT3=(1.0-SIN(RSLP)*SIN(RSLP))*PT1
      WRITE(6,550) PT3,PT1
  550 FORMAT(//' DECEL PHASE:'//' TRYING P(TD) =',F10.3,3X,'NOTE: P(TE)
     1=',F10.3)
  472 CONSTD=PT3*(AREA*XD)**GAMMA
      CODUM=CONSTD
      PARAM(6)=0.0
      NJUMP= 0
      PARAM(1)=T3
      PARAM(7)=0.0
```

```
      PARAM(2)=TENMAX
      PARAM(3)=TINCRE
      PARAM(4)=ERROR
      DPT2(1)=Z4T3
      DPT2(2)=BMASS*DZ4T3
      DDPT2(1)=ACO(1)
      DDPT2(2)=ACO(2)
      N2DIM=2
      CALL HPMK(PARAM,DPT2,DDPT2,N2DIM,NBIS,FUNCT2,OUT2,AUX1)
      IF(PARAM(6)) 480,490,10
  480 ERROR=10*ERROR
      WRITE(6,302)
      GO TO 472
  490 DUMM7=DDPT2(1)-AUX1(14,1)
      IF(DUMM7) 500,500,510
  500 WRITE(6,325)
      T4=TIME
      Z4T4=DPT2(1)
      XT4=XD-(Z4T3-Z4T4)/GRAT
      GO TO 520
  510 FINCRE=TINCRE/(2.0**NBIS)
      T4=TIME-FINCRE*DDPT2(1)/DUMM7
      Z4T4=DPT2(1)
      XT4=XD-(Z4T3-Z4T4)/GRAT
  520 IF(XT4-DZERO) 530,540,540
  530 PT3=1.10*PT3
      WRITE(6,560) PT3
  560 FORMAT(//' P(TD) WAS TOO LOW.  NOW TRYING P(TD) =',F10.3)
      GO TO 472
  540 PT4=CONSTD/(AREA*XT4)**GAMMA
      DDZ4T4=(GRAT/AREA)**(GAMMA-1.0)*CONSTD/(BMASS*(Z4T4-Z4T3+(XD*GRAT
     1))**GAMMA)-GRAV*SIN(RBETA)
      WRITE(6,315) ERROR
      WRITE(6,317) AUX1
      TH=T4-TZERO
      X1T4=X1T3+(XD-XT4)*COS(RBETA)*GRAT
```

```
      Z1T4=Z1T3-(XD-XT4)*SIN(RBETA)*GRAT
      X1T0=ZPZR*COS(ALPHA)
      RMAL=X1T2-X1T0
      RDIS=X1T3-X1T0
      FRNG=X1T4-X1T0
      WRITE(6,158) TZERO,TENGG,T2,T3,T4,TASC,TBAL,TH,DDZPZR,DZPEN,V1,
     1RMAL,Z1T2,RDIS,Z1T3,Z4T3,DZ4T3,DDZ4T4,FRNG,Z1T4,DALPHA,BETA,DZERO,
     2PT3
      WRITE(6,159) PT4
  159 FORMAT('+',63X,'FINAL PRESSURE =',F10.3)
      GO TO 10
  999 RETURN
      END
C*********************************************************************
C SUBROUTINES FOLLOW:
C*********************************************************************
      SUBROUTINE OUT1(T,DP,DDP,NB,N2D,PAR)
      REAL PAR(7),DP(2),DDP(2),T
      INTEGER N2D,NB
      COMMON/OUT/Z1,TIME/INT/NJUMP/FUN1/BIGM,BLK1,BLK2,BLK3,BLK4,BLK5
      TIME=T
      NJUMP=NJUMP+1
      ACCEL=DDP(2)/BIGM
      IF(NB-11) 10,20,30
   20 PAR(6)=-1.0
      GO TO 99
   30 WRITE(6,35) NB
   35 FORMAT(//' HPMK ERROR CODE =',I2)
      PAR(6)=1.0
      GO TO 99
   10 IF(PAR(7)) 40,50,40
   50 WRITE(6,55) T,DP(1),DDP(1),ACCEL,NB
   55 FORMAT(//9X,'TIME',9X,'ZP',6X,'ZPDOT',6X,'ACCEL',3X,'IHLF'
     1//(' ',5X,F10.5,3F10.3,3X,I2))
      PAR(7)=1.0
   58 IF(Z1-DP(1)) 60,60,99
```

```
   60 PAR(5)=1.0
      WRITE(6,45) T,DP(1),DDP(1),ACCEL,NB
      GO TO 99
   40 IF(NJUMP-3 ) 58,70,70
   70 NJUMP=0
      WRITE(6,45) T,DP(1),DDP(1),ACCEL,NB
   45 FORMAT(' ',5X,F10.5,3F10.3,3X,I2)
      GO TO 58
   99 RETURN
      END
C*****************************************************************
      SUBROUTINE FUNCT1(T,DP,DDP)
      REAL DP(2),DDP(2),T,M,K
      COMMON/FUN1/M,GRAV,ZZ,XZ,K,GR
      DUM=DP(1)-ZZ+XZ*GR
      IF(DUM) 40,40,30
   40 WRITE(6,45) DUM
   45 FORMAT(//' ERROR: YOU ARE ABOUT TO WIPE-OUT. DUM MUST BE GT 0.0'
     1//' TRY SMALLER INTEGRATION INCREMENT.  NOTE: DUM =',F10.3)
      DUM=DUM**2.5
   30 DDP(1)=DP(2)/M
      DDP(2)=K/DUM-M*GRAV
      RETURN
      END
C*****************************************************************
      SUBROUTINE FUNCT2(T,DP,DDP)
      REAL DP(2),DDP(2),T,M,K
      COMMON/FUN1/M,GRAV,ZZ,XZ,K,GR/FUN2/EX,A
      DUM=DP(1)-ZZ+XZ*GR
      IF(DUM) 40,40,30
   40 WRITE(6,45) DUM
   45 FORMAT(//' ERROR: YOU ARE ABOUT TO WIPE-OUT. DUM MUST BE GT 0.0'
     1//' TRY SMALLER INTEGRATION INCREMENT.  NOTE: DUM =',F10.3)
   30 DDP(1)=DP(2)/M
      DDP(2)=(GR/A)**(EX-1.0)*K/DUM**EX-M*GRAV
      RETURN
```

```
      END
C*****************************************************************
      SUBROUTINE OUT2(T,DP,DDP,NB,N2D,PAR)
      REAL PAR(7),DP(2),DDP(2),T
      INTEGER N2D,NB
      COMMON/OUT/BLK,TIME/INT/NJUMP/FUN1/BIGM,BLK1,BLK2,BLK3,BLK4,BLK5
      TIME=T
      NJUMP=NJUMP+1
      ACCEL=DDP(2)/BIGM
      IF(NB-11) 10,20,30
   20 PAR(6)=-1.0
      GO TO 99
   30 WRITE(6,35) NB
   35 FORMAT(//' HPMK ERROR CODE =',I2)
      PAR(6)=1.0
      GO TO 99
   10 IF(PAR(7)) 40,50,40
   50 WRITE(6,55) T,DP(1),DDP(1),ACCEL,NB
   55 FORMAT(//9X,'TIME',9X,'ZP',6X,'ZPDOT',6X,'ACCEL',3X,'IHLF'
     1//(' ',5X,F10.5,3F10.3,3X,I2))
      PAR(7)=1.0
   58 IF(DDP(1)) 99,60,60
   60 PAR(5)=1.0
      WRITE(6,45) T,DP(1),DDP(1),ACCEL,NB
      GO TO 99
   40 IF(NJUMP-3 ) 58,70,70
   70 NJUMP=0
      WRITE(6,45) T,DP(1),DDP(1),ACCEL,NB
   45 FORMAT(' ',5X,F10.5,3F10.3,3X,I2)
      GO TO 58
   99 RETURN
      END
C THIS IS THE END OF THE PROGRAM PECULIAR TO SHOT.
C SUBROUTINE HPMK (HPCG) IS ADDED HERE WHEN RUNNING PROGRAM.
```

```
C PLANE CHANGE MANEUVER PROGRAM FOR HOLAB VEHICLE
C ************************************************************
C INSTRUCTIONS FOR USING THIS PROGRAM:
C THERE ARE AT LEAST FOUR DATA CARDS REQUIRED FOR EACH CONFIGURATION.
C DATA CARD 1- NUM. INT. PARAMETERS AND HEADING:
C              COLS 1-10=TINCRE(INIT. INCREMENT OF TIME)(DEC.NO.)
C              COLS 11-20=ERROR(UPPER ERROR BOUND OF NUM. INT.)(DEC.NO.)
C              COLS 21-72=HDNG(ANY DESIRED OUTPUT HEADING FOR THIS CONFI
C                         GURATION. ANY MASS AND LENGTH UNITS MAY BE
C                         USED IN THIS PROGRAM, BUT TIME MUST BE IN SEC.
C                         UNITS USED SHOULD APPEAR IN HDNG.
C              COLS 73-80=OPTIONAL
C DATA CARD 2- CONFIGURATION PARAMETERS:
C              COLS 1-10=BM(POD MASS)(DEC.NO.)
C              COLS 11-20=SM(LEG MASS)(DEC.NO.)
C              COLS 21-30=ILCX(DEC.NO.)
C              COLS 31-40=IPCX(DEC.NO.)
C              COLS 41-50=H(DEC.NO.)
C              COLS 51-60=L (DEC.NO.)
C              COLS 61-70=ZPD(ZP AT TD)(DEC.NO.)
C              COLS 71-80=OPTIONAL
C DATA CARD 3- PROPULSION AND ENVIRONMENTAL PARAMETERS:
C              COLS 1-10=PD(CYL. PRESS. AT TD)(DEC.NO.)
C              COLS 11-20=DD( CYL. DISPLACEMENT AT TD. TO AVOID ZP GOING
C                         THRU 0.0 MAKE DD.LE.ZPD/GR)(DEC.NO.)
C              COLS 21-30=A(PISTON AREA)(DEC.NO.)
C              COLS 31-40=GR(GEAR RATIO)(DEC.NO.)
C              COLS 41-50=GAMA(SPEC. HEAT RATIO)(DEC.NO.)
C              COLS 51-60=G,GRAVITY CONSTANT(DEC.NO.)
C              COLS 61-80=OPTIONAL
C DATA CARD 4- INITIAL CONDITIONS:
C              COL 1=ICD(THIS MUST BE= 1 IF ANOTHER CARD 4 FOLLOWS THIS
C                    ONE SO THAT THE I.C. CAN BE CHANGED FOR THE SAME
C                    CONFIGURATION. THE LAST CARD OF INITIAL CONDITIONS
C                    MUST NOT HAVE A 1 IN COL 1.)
C              COLS 2-8=DXCMDM(VX OF VEH. C.M. AT TD. MUST BE .GE. 0.0)
```

```
C                        (DEC.NO.)
C              COLS 9-16=DZCMDM(VZ OF VEH. C.M. AT TD. MUST BE .LT. 0.0)
C                        (DEC.NO.)
C              COLS 17-24=PHID(IN DEG )(DEC.NO.)
C              COLS 25-32=THTD(IN DEG.)(DEC.NO.)
C              COLS 33-40=PSID(IN DEG.)(DEC.NO.)
C              COLS 41-48=DPHIDM(IN DEG/SEC)(DEC.NO.)
C              COLS 49-56=DTHTDM(IN DEG/SEC)(DEC.NO.)
C              COLS 57-64=DPSIDM(IN DEG/SEC)(DEC NO.)
C              COLS 65-80=OPTIONAL
C*****************************************************************
C MAIN PROGRAM FOLLOWS:
C*****************************************************************
      REAL HDNG(13),L,ILCX,IPCX,IX,IY,TD/0.0/,LXD,LYD,LZD,LXE,LYE,LZE
      COMMON/MFUN/BMASS,SMASS,SIX,SIY,SIZ,SL,HOF,XZ,AREA,GRAT,GAM,GRAV,
     1CONST/MNSL/TZ,TIN,ERR,ZZ,PRM6
   10 READ(5,15,END=999) TINCRE,ERROR,HDNG
   15 FORMAT(2F10.4,13A4)
      READ(5,25) BM,SM,ILCX,IPCX,H,L,ZPD,PD,DD,A,GR,GAMA,G
   25 FORMAT(7F10.3/6F10.3)
      WRITE(6,35)HDNG,TINCRE,ERROR,BM,SM,ILCX,IPCX,H,L,ZPD,PD,DD,A,GR,GA
     1MA,G
   35 FORMAT('1',5X,13A4//5X,'NUM. INTEG. PARAMETERS FOR HPMK ARE:'/8X,'
     1INIT. INCREMENT OF TIME =',F8.4,6X,'UPPER ERROR BOUND =',F8.4//5X,
     2'CONFIGURATION PARAMETERS ARE:'/8X,'POD MASS=',F10.3,6X,'LEG MASS=
     3',F10.3,6X,'ILCX =',F10.3,6X,'IPCX =',F10.3,6X,'H =',F10.3/8X,'L =
     4',F10.3,6X,'ZPD =',F10.3//5X,'PROPUSION PARAMETERS ARE:'/8X,'PD ='
     5,F10.3,6X,'DD =',F7.3,6X,'A =',F7.3,6X,'GEAR RATIO =',F7.3,6X,'GAM
     6MA =',F7.3,6X,'GRAVITY CONST. =',F8.3)
      IX=ILCX+SM*L*L+IPCX
      IY=ILCX+SM*L*L
      IZ=IPCX
   20 READ(5,45) ICD,DXCMDM,DZCMDM,PHID,THTD,PSID,DPHIDM,DTHTDM,DPSIDM
   45 FORMAT(I1,F7.2,7F8.2)
      WRITE(6,55)PHID,THTD,PSID,DPHIDM,DTHTDM,DPSIDM,DXCMDM,DZCMDM
   55 FORMAT(///5X,'INITIAL CONDITIONS:'/8X,'PHI(TD) =',F6.2,'DEG.  THET
```

```
     1A(TD) =',F6.2,'DEG.  PSI(TD) =',F6.2,'DEG.  DPHI(TD-) =',F7.3,'DEG
     2/SEC.  DTHETA(TD-) =',F7.3,'DEG/SEC.'/8X,'DPSI(TD-) =',F7.3,'DEG/S
     3EC.  DXCM(TD-) =',F8.3,5X,'DZCM(TD-) =',F8.3)
      IF(DXCMDM) 30,50,50
  30  WRITE(6,32)
  32  FORMAT(//' ***ERROR: DXCM(TD-) CANNOT BE NEGATIVE.')
  40  IF(ICD-1) 10,20,10
  50  IF(DZCMDM) 70,60,60
  60  WRITE(6,65)
  65  FORMAT(//' ***ERROR: DZCM(TD-) MUST BE NEGATIVE.')
      GO TO 40
  70  IF(THTD) 80,80,90
  80  WRITE(6,85)
  85  FORMAT(//' ***ERROR: THETA(TD) MUST BE POSITIVE AND LESS THAN 90 D
     1EG.')
  90  IF(THTD-90.0) 110,80,80
 110  RPD=1.745329E-2
      DPR=57.29578
      RPHID=PHID*RPD
      RTHTD=THTD*RPD
      RPSID=PSID*RPD
      SPH=SIN(RPHID)
      CPH=COS(RPHID)
      STH=SIN(RTHTD)
      CTH=COS(RTHTD)
      SPS=SIN(RPSID)
      CPS=COS(RPSID)
      VCMX=(CPS*CPH-CTH*SPH*SPS)*DXCMDM+STH*SPS*DZCMDM
      VCMY=(-SPS*CPH-CTH*SPH*CPS)*DXCMDM+STH*CPS*DZCMDM
      VCMZ=STH*SPH*DXCMDM+CTH*DZCMDM
      ETA=((ZPD-L)*(ZPD-L)+H*H)**0.5
      ZETA=BM*ETA/(BM+SM)
      XC=ZETA*H/ETA
      ZC=ZETA*(ZPD-L)/ETA+L
      WX=(DPHIDM*STH*SPS+DTHTDM*CPS)*RPD
      WY=(DPHIDM*STH*CPS-DTHTDM*SPS)*RPD
```

```
WZ=(DPHIDM*CTH+DPSIDM)*RPD
VLCX=VCMX-(ZC-L)*WY
VLCY=VCMY-XC*WZ+(ZC-L)*WX
VLCZ=VCMZ+XC*WY
VPCX=VLCX+(ZPD-L)*WY
VPCY=VLCY-(ZPD-L)*WX+H*WZ
VPCZ=VLCZ-H*WY
HSQ=H*H
ZPDSQ=ZPD*ZPD
DEN1=IY+BM*ZPDSQ+BM*HSQ
LXD=(ILCX+IPCX)*WX-SM*L*VLCY-BM*ZPD*VPCY
LYD=ILCX*WY+SM*L*VLCX+BM*(ZPD*VPCX-H*VPCZ)
LZD=IPCX*WZ+BM*H*VPCY
WYDP=(LYD+BM*H*VLCZ)/DEN1
DUM1=IX+BM*ZPDSQ
DUM2=IZ+BM*HSQ
DEN2=DUM1*DUM2-BM*BM*ZPDSQ*HSQ
WXDP=(DUM2*LXD+BM*ZPD*H*LZD)/DEN2
WZDP=(LZD+BM*H*ZPD*WXDP)/DUM2
DZPDP=VLCZ
VLCXDP=L*WYDP
VLCYDP=-L*WXDP
VPCXDP=ZPD*WYDP
VPCYDP=H*WZDP-ZPD*WXDP
VPCZDP=VLCZ-H*WYDP
DPHIDP=SPS*WXDP/STH+CPS*WYDP/STH
DTHTDP=CPS*WXDP-SPS*WYDP
DPSIDP=WZDP-CTH*(CPS*WYDP+SPS*WXDP)/STH
TZ=TD
TIN=TINCRE
ERR=ERROR
BMASS=BM
SMASS=SM
SIX=IX
SIY=IY
SIZ=IZ
```

```
      SL=L
      ZZ=ZPD
      HOF=H
      XZ=DD
      AREA=A
      GRAT=GR
      GAM=GAMA
      GRAV=G
      PZ=PD
      DZZ=DZPDP
      PHIZ=PHID
      THETZ=THTD
      PSIZ=PSID
      DPHIZ=DPHIDP
      DTHETZ=DTHTDP
      DPSIZ=DPSIDP
      CALL SLRSLP(PZ,DZZ,PHIZ,THETZ,PSIZ,DPHIZ,DTHETZ,DPSIZ,PM,ZMIN,DMIN
     1,AXMAX,TE,PHIE,THTE,PSIE,DPHIEM,DTHTEM,DPSIEM,DZPEM,DWPHEM,DWTHEM,
     2DWPSEM,DVZEM)
      IF(PRM6) 150,150,10
  150 SPHE=SIN(PHIE)
      CPHE=COS(PHIE)
      STHE=SIN(THTE)
      CTHE=COS(THTE)
      SPSE=SIN(PSIE)
      CPSE=COS(PSIE)
      ZPE=ZPD
      WXEM=DPHIEM*STHE*SPSE+DTHTEM*CPSE
      WYEM=DPHIEM*STHE*CPSE-DTHTEM*SPSE
      WZEM=DPHIEM*CTHE+DPSIEM
      VLCXEM=L*WYEM
      VLCYEM=-L*WXEM
      VPCXEM=ZPE*WYEM
      VPCYEM=H*WZEM-ZPE*WXEM
      VPCZEM=DZPEM-H*WYEM
      LXE=(ILCX+IPCX)*WXEM-SM*L*VLCYEM-BM*ZPE*VPCYEM
```

```
      LYE=ILCX*WYEM+SM*L*VLCXEM+BM*ZPE*VPCXEM-BM*H*VPCZEM
      LZE=IZ*WZEM+BM*H*VPCYEM
      PXE=SM*VLCXEM+BM*VPCXEM
      PYE=SM*VLCYEM+BM*VPCYEM
      PZE=BM*VPCZEM
      MU=(SM*L+BM*ZPE)/(SM+BM)
      DEN3=IY-SM*L*ZPE+MU*SM*(ZPE-L)+BM*SM*HSQ/(SM+BM)
      WYEP=(LYE+BM*H*PZE/(SM+BM)-MU*PXE)/DEN3
      AXX=IX-SM*L*ZPE+MU*SM*(ZPE-L)
      AXZ=SM*L*H-MU*SM*H
      CLX=LXE+MU*PYE
      AZZ=IZ+SM*BM*HSQ/(SM+BM)
      AZX=SM*BM*H*(ZPE-L)/(SM+BM)
      CLZ=LZE-BM*H*PYE/(SM+BM)
      DEN4=AXX*AZZ+AXZ*AZX
      WXEP=(AZZ*CLX-AXZ*CLZ)/DEN4
      WZEP=(AXX*CLZ+AZX*CLX)/DEN4
      VPCXEP=(PXE+SM*(ZPE-L)*WYEP)/(SM+BM)
      VPCYEP=(PYE+SM*H*WZEP-SM*(ZPE-L)*WXEP)/(SM+BM)
      VPCZEP=(PZE-SM*H*WYEP)/(SM+BM)
      VLCXEP=VPCXEP-(ZPE-L)*WYEP
      VLCYEP=VPCYEP+(ZPE-L)*WXEP-H*WZEP
      VLCZEP=VPCZEP+H*WYEP
      VCMXEP=VLCXEP+(ZC-L)*WYEP
      VCMYEP=VLCYEP+XC*WZEP-(ZC-L)*WXEP
      VCMZEP=VLCZEP-XC*WYEP
      DXCMEP=(CPSE*CPHE-CTHE*SPHE*SPSE)*VCMXEP-(SPSE*CPHE+CTHE*SPHE*CPSE
     1)*VCMYEP+STHE*SPHE*VCMZEP
      DYCMEP=(CPSE*SPHE+CTHE*CPHE*SPSE)*VCMXEP-(SPSE*SPHE-CTHE*CPHE*CPSE
     1)*VCMYEP-STHE*CPHE*VCMZEP
      DZCMEP=STHE*SPSE*VCMXEP+STHE*CPSE*VCMYEP+CTHE*VCMZEP
      DELTA=ATAN2(DYCMEP,DXCMEP)*DPR
      PHIF=PHIE*DPR
      THTF=THTE*DPR
      PSIF=PSIE*DPR
      DPHIF=(SPSE*WXEP/STHE+CPSE*WYEP/STHE)*DPR
```

```
      DTHTF=(CPSE*WXEP-SPSE*WYEP)*DPR
      DPSIF=(WZEP-CTHE*(CPSE*WYEP+SPSE*WXEP)/STHE)*DPR
      WRITE(6,305)TE,DELTA,PHIF,THTF,PSIF,DPHIF,DTHTF,DPSIF,DXCMEP,DYCME
     1P,DZCMEP
  305 FORMAT(///8X,'MANEUVERING TIME =',F8.3,'SEC.  PLANE CHANGE =',F8.3
     1,'DEG.'//10X,'PHI(TE) =',F8.3,'DEG  THETA(TE) =',F8.3,'DEG  PSI(TE
     2) =',F8.3,'DEG.'/10X,'DPHI(TE) =',F7.3,'D/S  DTHETA(TE) =',F7.3,
     3'D/S  DPSI(TE) =',F7.3,'D/S.'/10X,'C. M. VEL. COMPONENTS AT TE+:
     4VX=',F8.3,5X,'VY =',F8.3,5X,'VZ =',F8.3)
      WRITE(6,355) AXMAX,ZMIN,DMIN,PM
  355 FORMAT(/' MAX AXIAL ACCEL=',F10.3,3X,'ZMIN=',F10.3,3X,'DMIN=',
     1F10.3,3X,'PMAX=',F12.3)
      GO TO 40
  999 RETURN
      END
C*********************************************************************
C SUBROUTINES FOLLOW:
C*********************************************************************
      SUBROUTINE SLRSLP(PZ,DZZ,PHIZ,THETZ,PSIZ,DPHIZ,DTHETZ,DPSIZ,
     1PMAX,ZPMN,XMIN,AXMAX,T2,PHI2,THET2,PSI2,DPHI2,DTHET2,DPSI2,DZP2,DW
     2PH2,DWTH2,DWPS2,DVZ2)
      REAL ACO(8)/8*0.125/,PRMT(7),DPT(8),DDPT(8),AUX(16,8),
     1TMAX/1000.0/,L,IX,IY,IZ
      EXTERNAL FUNCT,OUT
      COMMON/MOUT/TIME,NJUMP,ZPMIN,DVZMAX/MFUN/BM,SM,IX,IY,IZ,L,H,XZ,A,G
     1R,GAMA,GRAV,CONST/MOUFUN/ZZ/MNSL/TZERO,TINCRE,ERROR,ZZZ,PM6
      RPD=1.745329E-2
      ZZ=ZZZ
      ER=ERROR
      CONST=PZ*(A*XZ)**GAMA
   80 NJUMP=0
      PRMT(1)=TZERO
      PRMT(2)=TMAX
      PRMT(3)=TINCRE
      PRMT(4)=ER
      PRMT(6)=0.0
```

```
      PRMT(7)=0.0
      DO 90 I=1,8
   90 DDPT(I)=ACO(I)
      DPT(1)=PHIZ*RPD
      DPT(2)=THETZ*RPD
      DPT(3)=PSIZ*RPD
      DPT(4)=ZZ
      DPT(5)=DPHIZ
      DPT(6)=DTHETZ
      DPT(7)=DPSIZ
      DPT(8)=DZZ
      NDIM=8
      CALL HPMK(PRMT,DPT,DDPT,NDIM,NBIS,FUNCT,OUT,AUX)
      PM6=PRMT(6)
      IF(PRMT(6)) 100,240,999
  100 ER=10*ER
      WRITE(6,105)
  105 FORMAT(///' *UPPER ERROR BOUND IS TOO SMALL.  RESTARTING HPMK WITH
     1 ERROR =10(ERROR).')
      GO TO 80
  240 WRITE(6,245) ER
  245 FORMAT(// '  THE ACTUAL ERROR BOUND USED =' ,F6.4)
      DPR=57.29578
      DIFFZ=DPT(4)-AUX(7,4)
      IF(DIFFZ) 280,260,280
  260 WRITE(6,265)
  265 FORMAT(// ' NO INTERPOLATION REQUIRED.')
      T2=TIME
      PHI2=DPT(1)
      THET2=DPT(2)
      PSI2=DPT(3)
      DPHI2=DPT(5)
      DTHET2=DPT(6)
      DPSI2=DPT(7)
      DZP2=DPT(8)
      DWPH2=DDPT(5)
```

```
      DWTH2=DDPT(6)
      DWPS2=DDPT(7)
      DVZ2=DDPT(8)
      GO TO 300
  280 FINCRE=TINCRE/(2.0**NBIS)
      RDIFFZ=(DPT(4)-ZZ)/DIFFZ
      T2=TIME-FINCRE*RDIFFZ
      PHI2=DPT(1)-(DPT(1)-AUX(7,1))*RDIFFZ
      THET2=DPT(2)-(DPT(2)-AUX(7,2))*RDIFFZ
      PSI2=DPT(3)-(DPT(3)-AUX(7,3))*RDIFFZ
      DPHI2=DPT(5)-(DPT(5)-AUX(7,5))*RDIFFZ
      DTHET2=DPT(6)-(DPT(6)-AUX(7,6))*RDIFFZ
      DPSI2=DPT(7)-(DPT(7)-AUX(7,7))*RDIFFZ
      DZP2=DPT(8)-(DPT(8)-AUX(7,8))*RDIFFZ
      DWPH2=DDPT(5)-(DDPT(5)-AUX(14,5))*RDIFFZ
      DWTH2=DDPT(6)-(DDPT(6)-AUX(14,6))*RDIFFZ
      DWPS2=DDPT(7)-(DDPT(7)-AUX(14,7))*RDIFFZ
      DVZ2=DDPT(8)-(DDPT(8)-AUX(14,8))*RDIFFZ
  300 XMIN=XZ-(ZZ-ZPMIN)/GR
      ZPMN=ZPMIN
      AXMAX=DVZMAX
      PMAX=CONST/(XMIN*A)**GAMA
  999 RETURN
      END
C*****************************************************************
      SUBROUTINE OUT(T,DP,DDP,NB,ND,PAR)
      REAL PAR(7),DP(8),DDP(8),T,DQ(7),DDQ(7)
      COMMON/MOUT/TIME,NJUMP,ZPMIN,DVZMAX/MOUFUN/ZZ
      TIME=T
      DPR=57.29578
      NJUMP=NJUMP+1
      IF(NB-11) 10,20,30
   20 PAR(6)=-1.0
      RETURN
   30 WRITE(6,35) NB
   35 FORMAT(//' **HPMK ERROR CODE = ',I2)
```

```
      PAR(6)=1.0
      RETURN
   10 DO 51 I=1,3
   51 DQ(I)=DP(I)*DPR
      DO 52 I=5,7
   52 DQ(I)=DP(I)*DPR
      DO 53 I=5,7
   53 DDQ(I)=DDP(I)*DPR
      IF(PAR(7)) 12,50,12
   50 WRITE(6,55) T,DP(4),DQ(1),DQ(2),DQ(3),DP(8),DQ(5),DQ(6),DQ(7),
     1DDP(8),DDQ(5),DDQ(6),DDQ(7),NB
   55 FORMAT(//3X, 'TIME' ,7X, 'ZP',7X, 'PHI' ,4X,'THETA',4X, 'PSI',5X,
     1'DZP',6X, 'DPHI' ,5X,'DTHETA' ,5X, 'DPSI' ,6X, 'DDZP' ,6X,'DDPHI',
     24X,'DDTHETA',4X,'DDPSI' ,3X, 'IHLF' //' ' ,2(F9.3,1X),3(F7.3,1X),4
     3(F9.3,1X),4(F8.3,1X),2X,I2)
      PAR(7)=1.0
      MIN=0
      RETURN
   12 IF(MIN-1) 40,60,40
   40 IF(DP(8)) 60,70,70
   70 MIN=1
      ZPMIN=DP(4)
      DVZMAX=DDP(8)
   60 IF(NJUMP-15) 90,80,80
   80 NJUMP=0
      WRITE(6,85) T,DP(4),DQ(1),DQ(2),DQ(3),DP(8),DQ(5),DQ(6),DQ(7),
     1DDP(8),DDQ(5),DDQ(6),DDQ(7),NB
   85 FORMAT(' ' ,2(F9.3,1X),3(F7.3,1X),4(F9.3,1X),4(F8.3,1X),2X,I2)
   90 IF(DP(4)-ZZ) 99,92,92
   92 PAR(5)=1.0
      WRITE(6,85) T,DP(4),DQ(1),DQ(2),DQ(3),DP(8),DQ(5),DQ(6),DQ(7),
     1DDP(8),DDQ(5),DDQ(6),DDQ(7),NB
   99 RETURN
      END
C*****************************************************************
      SUBROUTINE FUNCT(T,DP,DDP)
```

```
      REAL DP(8),DDP(8),T,IX,IY,IZ,L,K
      COMMON/MOUFUN/ZZ/MFUN/BM,SM,IX,IY,IZ,L,H,XZ,A,GR,GAMA,GRAV,K
      DUM=DP(4)-ZZ+XZ*GR
      IF(DUM) 40,40,30
   40 WRITE(6,45)
   45 FORMAT(//' ***ERROR: YOU ARE ABOUT TO WIPE-OUT BECAUSE OF THE INIT
     1IALIZATION OF HPMK. THIS CAUSED DUM TO BE .LE. 0.0' / '  AVOID THI
     2S BY TRYING A SMALLER VALUE FOR INIT. TIME INCREMENT, TINCRE.')
      DUM=DUM**2.5
   30 STH=SIN(DP(2))
      SPS=SIN(DP(3))
      CTH=COS(DP(2))
      CPS=COS(DP(3))
      SSTH=STH*STH
      SSPS=SPS*SPS
      CSTH=CTH*CTH
      CSPS=CPS*CPS
      WPH=DP(5)
      WTH=DP(6)
      WPS=DP(7)
      ZP=DP(4)
      VZ=DP(8)
      PHPH=SSTH*(IX*SSPS+IY*CSPS)+IZ*CSTH+BM*(H*H*CSPS+(ZP*STH-H*CTH*SPS
     1)**2)
      PHTH=(IX-IY)*STH*SPS*CPS-BM*H*CPS*(H*STH*SPS+ZP*CTH)
      PHPS=IZ*CTH+BM*H*(H*CTH-ZP*STH*SPS)
      PHZP=-(BM*H*STH*CPS)
      CPHI=(IX-IY)*(WTH*WPS*STH*(SSPS-CSPS)-SPS*CPS*(2*WPH*WPS*SSTH+WTH*
     1WTH*CTH)) -2*(IX*SSPS+IY*CSPS)*WPH*WTH*STH*CTH+IZ*WTH*STH*(2*WPH*C
     2TH+WPS)-BM*(2*ZP*WPH*STH*(VZ*STH+ZP*WTH*CTH) -2*H*VZ*CTH*(WPH*STH*
     3SPS+WTH*CPS) -H*H*(2*WPH*(WPS*STH*CPS+WTH*CTH*SPS)*STH*SPS +2*WTH*
     4WPS*STH*CSPS -WTH*WTH*CTH*SPS*CPS) -H*ZP*(2*WPH*WTH*SPS*(CSTH-SSTH
     5) +STH*CPS*(2*WPH*WPS*CTH+WPS*WPS-WTH*WTH)))
      THTH=IX*CSPS+IY*SSPS+BM*(ZP*ZP+H*H*SSPS)
      THPS=-(BM*H*ZP*CPS)
      THZP=BM*H*SPS
```

```
 CTHT=(IX-IY)*WPS*(2*WTH*SPS*CPS-WPH*STH*(CSPS-SSPS)) +(IX*SSPS+IY*
1CSPS)*WPH*WPH*STH*CTH -IZ*WPH*STH*(WPH*CTH+WPS) -BM*(ZP*(2*VZ*WTH-
2ZP*WPH*WPH*STH*CTH) +H*H*SPS*(2*WPS*(WTH*CPS+WPH*STH*SPS) +WPH*WPH
3*STH*CTH*SPS) +H*ZP*SPS*((WPS+WPH*CTH)**2 -WPH*WPH*SSTH)) +SM*GRAV
4*L*STH +BM*GRAV*(ZP*STH-H*CTH*SPS)
 PSPS=IZ+BM*H*H
 CPSI=(IX-IY)*(SPS*CPS*(WPH*WPH*SSTH-WTH*WTH) +WPH*WTH*STH*(CSPS-SS
1PS)) +IZ*WPH*WTH*STH -BM*(H*H*SPS*(CPS*(WPH*WPH*SSTH-WTH*WTH)-2*WP
2H*WTH*STH*SPS) -2*H*VZ*(WTH*CPS+WPH*STH*SPS) -H*ZP*WPH*CTH*(2*WTH*
3SPS-WPH*STH*CPS)) -BM*GRAV*H*STH*CPS
 VZZP=BM
 CVZP=BM*(ZP*(WPH*WPH*SSTH+WTH*WTH) -H*(WPH*STH*SPS*(WPH*CTH+2*WPS)
1+2*WTH*WPS*CPS)) -BM*GRAV*CTH +(GR/A)**(GAMA-1.0)*K/DUM**GAMA
 DEL= PHZP*(2*THZP*(PHTH*PSPS-PHPS*THPS) +PHZP*(THPS*THPS-THTH*PSPS
1)) +THZP*THZP*(PHPS*PHPS-PHPH*PSPS) +VZZP*(THTH*(PHPH*PSPS-PHPS*PH
2PS) +THPS*(2*PHTH*PHPS-PHPH*THPS)-PHTH*PHTH*PSPS)
 DELPHI=PHZP*(CVZP*(THPS*THPS-THTH*PSPS) +THZP*(CTHT*PSPS-THPS*CPSI
1)) +THZP*(CVZP*(PHTH*PSPS-PHPS*THPS) +THZP*(PHPS*CPSI-CPHI*PSPS))
2+VZZP*(CPHI*(THTH*PSPS-THPS*THPS) +CTHT*(PHPS*THPS-PHTH*PSPS) +CPS
3I*(PHTH*THPS-PHPS*THTH))
 DELTHT=PHZP*(PHZP*(THPS*CPSI-CTHT*PSPS) +CVZP*(PHTH*PSPS-PHPS*THPS
1)) +THZP*(CVZP*(PHPS*PHPS-PHPH*PSPS) +PHZP*(CPHI*PSPS-PHPS*CPSI))
2+VZZP*(PHPH*(CTHT*PSPS-THPS*CPSI) +PHTH*(PHPS*CPSI-CPHI*PSPS) +PHP
3S*(CPHI*THPS-PHPS*CTHT))
 DELPSI=PHZP*(CTHT*(PHZP*THPS-PHPS*THZP) +CPSI*(PHTH*THZP-PHZP*THTH
1) +CVZP*(PHPS*THTH-PHTH*THPS)) +THZP*(CPHI*(PHPS*THZP-PHZP*THPS) +
2CPSI*(PHTH*PHZP-PHPH*THZP) +CVZP*(PHPH*THPS-PHTH*PHPS)) +VZZP*(CPH
3I*(PHTH*THPS-PHPS*THTH) +CPSI*(PHPH*THTH-PHTH*PHTH) +CTHT*(PHTH*PH
4PS-PHPH*THPS))
 DELZP=PHZP*(CPHI*(THPS*THPS-THTH*PSPS) +CPSI*(PHPS*THTH-PHTH*THPS)
1 +CTHT*(PHTH*PSPS-PHPS*THPS)) +THZP*(CPHI*(PHTH*PSPS-PHPS*THPS) +C
2PSI*(PHPH*THPS-PHTH*PHPS) +CTHT*(PHPS*PHPS-PHPH*PSPS)) +CVZP*(THTH
3*(PHPH*PSPS-PHPS*PHPS) +THPS*(2*PHTH*PHPS-PHPH*THPS) -PHTH*PHTH*PS
4PS)
 DDP(1)=DP(5)
 DDP(2)=DP(6)
```

```
      DDP(3)=DP(7)
      DDP(4)=DP(8)
      DDP(5)=DELPHI/DEL
      DDP(6)=DELTHT/DEL
      DDP(7)=DELPSI/DEL
      DDP(8)=DELZP/DEL
      RETURN
      END
C THIS IS THE END OF THE PROGRAM PECULIAR TO HOLAB PLANE CHANGE
C SUBROUTINE HPMK (HPCG) IS ADDED HERE WHEN RUNNING PROGRAM.
```

REFERENCES

1. "1967 Summer Study of Lunar Science and Exploration," NASA SP-157, 1967.

2. Wong, R. E., "Lunar Surface Mobility Systems," Astronautica Acta, 12, 1966, pp. 394-404.

3. Oberth, H., Man Into Space, Harper & Bros., New York, 1954.

4. Oberth, H., The Moon Car, Harper & Bros., New York, 1959.

5. "Study of Manned Flying Systems," (Mid-Term Report) Bell Aerosystems Report No. 7243-950001, Textron's Bell Aerosystems Company, Buffalo, New York, Nov. 1965.

6. Seifert, H. S., "The Lunar Pogo Stick," Journal of Spacecraft and Rockets, 4, 1967, pp. 941-43.

7. Weil, N. A., Lunar and Planetary Surface Conditions, Academic Press, New York, 1965, pp. 28-94.

8. Singer, S. F., "Atmosphere Near the Moon," Astronautica Acta, 7, 1961, pp. 135-40.

9. Baldwin, R. D., "The Nature of the Lunar Surface and Major Structural Features," Proceedings of the Conference on Lunar Exploration, Part A, Paper No. VII, Engineering Experiment Station Series No. 152, Virginia Polytechnic Institute, Blacksburg, Virginia, Aug. 1962.

10. Johnson, R. W., "The Lunar Surface According to Luna IX and Surveyor I," Astronautica Acta, 12, 1966, pp. 370-83.

11. "Surveyor III Mission Report, Part II. Scientific Results," JPL TR-32-1177, Jet Propulsion Labs., Pasadena, California, June 1967, pp. 3-7.

12. "Surveyor V Mission Report, Part II: Science Results," JPL TR-32-1246, Jet Propulsion Labs., Pasadena, California, Nov. 1967, pp. 5-6, 43-60.

13. Sears, F. W., An Introduction to Thermodynamics, the Kinetic Theory of Gases, and Statistical Mechanics, 2nd ed., Addison-Wesley, Reading, Massachusetts, 1953, pp. 153-4.

14. Fraser, T. M., "Human Response to Sustained Acceleration," NASA SP-103, 1966, pp. 1-9.

15. Gaume, J. G. and Kuehnegger, W., "Effects of Chronic Lunar Gravity on Human Physiology," Progress in Astronautics, 10, ed. by C. I. Cummings and H. R. Lawrence, Academic Press, New York, 1963, pp. 381-412.

16. Damon, A., Stoudt, H. W., McFarland, R. A., The Human Body in Equipment Design, Harvard University Press, Cambridge, Massachusetts, 1966, pp. 253-75.

17. "Lunar Surface Mobility Systems Comparison and Evaluation (MOBEV)," Final Report, Volume II, Bendix Report No. BSR-1428, Bendix Aerospace Systems Division, Ann Arbor, Michigan, Nov. 1966.

18. "Proposal for Research on a Small Scale Lunar Surface Personnel Transporter Employing the Hopping Mode," Dept. of Aeronautics and Astronautics, Proposal No. 18-67, Stanford University, Stanford, California, Aug. 1967.

19. Cannon, R., "Basic Response Relations for Reaction-Wheel Attitude Control," ARS Journal, 32, 1962, pp. 61-74.

20. Havill, J. R. and Ratcliff, J. W., "A Twin-Gyro Attitude Control System for Space Vehicles," NASA Technical Note D-2419, Aug. 1964.

21. Davis, L. P., "Optimization of Control Moment Gyroscope Design," presented at Saturn V/Apollo and Beyond Symposium of the American Astronautical Society, Huntsville, Alabama, June 1967.

22. Goldstein, H., Classical Mechanics, Addison-Wesley, Reading, Massachusetts, 1950, pp. 10-18, 215-18.

23. "Flight Test of a One Man Flying Vehicle, Volume II – Final Report, Mission Application Studies," Bell Aerosystems Report No. 2330-950002, Textron's Bell Aerosystems Company, Buffalo, New York, July 1967.

24. Davids, N. and Mehta, P., "Computer Analysis Methods in Dynamics as Applied to Stress Waves and Spherical Cavities," Engineering Research Bulletin B-92, Pennsylvania State University, University

Park, Pennsylvania, May 1965.

25. ter Haar, D., Elements of Hamiltonian Mechanics, 2nd ed., North-Holland, Amsterdam, 1964, pp. 25-37, 95-6.

26. "System/360 Scientific Subroutine Package (360A-CM-03X) Version II Programmer's Manual," H20-0205-2, International Business Machines Corp., White Plains, N.Y., 1967, pp. 118-28, 178-85.

27. "Mathematical Computer Programs, a Compilation," NASA SP-5069, 1966, p. 22.

28. Hildebrand, F. B., Methods of Applied Mathematics, Prentice-Hall, Englewood Cliffs, New Jersey, 1952, Ch. 1.

29. Whittaker, E. T., A Treatise on the Analytical Dynamics of Particles and Rigid Bodies, 4th ed., Cambridge, London, 1937, pp. 34-40.

30. Hildebrand, F. B., Introduction to Numerical Analysis, McGraw-Hill, New York, 1956, pp. 64-69, 82.

31. "IBM System/360 FORTRAN IV Language," C28-6515-4, International Business Machines Corp., White Plains, N.Y., 1966.